(12)

DNA 4210F

EARTH PENETRATOR DESIGN STUDY PROGRAM SUBSCALE BALLISTIC PENETRATION TESTS

Avco Corporation
Avco Systems Division
201 Lowell Street
Wilmington, Massachusetts 01887

January 1977

Final Report for Period 6 May 1976—30 November 1976

CONTRACT No. DNA 001-76-C-0057

APPROVED FOR PUBLIC RELEASE;
DISTRIBUTION UNLIMITED.

THIS WORK SPONSORED BY THE DEFENSE NUCLEAR AGENCY UNDER RDT&E RMSS CODES B342076462 L41AAXYX96604 AND B342076464 N99QAXAC31801 H2590D.

Prepared for
Director
DEFENSE NUCLEAR AGENCY
Washington, D. C. 20305

Destroy this report when it is no longer needed. Do not return to sender.

UNCLASSIFIED

SECURITY CLASSIFICATION OF THIS PAGE (When Data Entered)

REPORT DOCUMENTATION PAGE

READ INSTRUCTIONS BEFORE COMPLETING FORM

1. REPORT NUMBER: DNA 4210F	2. GOVT ACCESSION NO.
3. RECIPIENT'S CATALOG NUMBER	
4. TITLE (and Subtitle): EARTH PENETRATOR DESIGN STUDY PROGRAM SUBSCALE BALLISTIC PENETRATION TESTS.	5. TYPE OF REPORT & PERIOD COVERED: Final Report, [redacted] 6 May [redacted]–30 Nov 76
	6. PERFORMING ORG. REPORT NUMBER: AVSD-0371-76-RR
7. AUTHOR(s): P. S. Soderstrom	8. CONTRACT OR GRANT NUMBER(s): DNA 001-76-C-0057
9. PERFORMING ORGANIZATION NAME AND ADDRESS: Avco Corporation, Avco Systems Division, 201 Lowell Street, Wilmington, Massachusetts 01887	10. PROGRAM ELEMENT, PROJECT, TASK AREA & WORK UNIT NUMBERS: NWET Subtasks L41AAXYX966-04 N99QAXAC318-01
11. CONTROLLING OFFICE NAME AND ADDRESS: Director, Defense Nuclear Agency, Washington, D.C. 20305	12. REPORT DATE: Jan [redacted] 1977
	13. NUMBER OF PAGES: 84 (12) 77 p.
14. MONITORING AGENCY NAME & ADDRESS (if different from Controlling Office)	15. SECURITY CLASS (of this report): UNCLASSIFIED
	15a. DECLASSIFICATION/DOWNGRADING SCHEDULE

16. DISTRIBUTION STATEMENT (of this Report)

Approved for public release; distribution unlimited.

17. DISTRIBUTION STATEMENT (of the abstract entered in Block 20, if different from Report)

18. SUPPLEMENTARY NOTES

This work sponsored by the Defense Nuclear Agency under RDT&E RMSS Codes B342076462 L41AAXYX96604 and B342076464 N99QAXAC31801 H2590D.

19. KEY WORDS (Continue on reverse side if necessary and identify by block number)

Subscale Penetration Tests	Ogive Earth Penetrator
Ballistic Penetration Tests	Single Stepped Tier Earth Penetrator
Penetration Trajectory Data	Conical Earth Penetrator

20. ABSTRACT (Continue on reverse side if necessary and identify by block number)

A series of 24 penetration tests were performed at various combinations of angle of attack and obliquity using three different models. Ogive, single stepped tier and conical tipped scale models were used to penetrate through concrete into a sand media. All tests were performed at 1000 ft/s. Copper balls were used to measure the peak deceleration for each test. Grids were used to monitor the penetrator trajectory and change of velocity through the sand media.

DD FORM 1 JAN 73 1473 EDITION OF 1 NOV 65 IS OBSOLETE

UNCLASSIFIED

SECURITY CLASSIFICATION OF THIS PAGE (When Data Entered)

404784

20. ABSTRACT (Continued)

Test results including velocity, angle of attack, obliquity, crater size, copper ball deformation, trajectory and change of velocity in sand media are reported. Variations in performance as a function of tip configurations are discussed. The results provide an extensive and significant addition to the understanding of the interaction between earth penetrators and representative target media.

PREFACE

A series of 24 subscale penetration tests were performed to investigate the variation of performance as a function of tip configuration. Ogive, single stepped tier and conical tipped subscale projectiles were fired through a concrete target into a sand media at various angles of attack and obliquity. The results of these successful tests may be used to refine predictive techniques concerning the performance of earth penetrators in typical target media.

The Program was conducted under Contract DNA001-C-76-0057-P00001 for the Defense Nuclear Agency. This work was administered under the direction of Lt. R. Nibe.

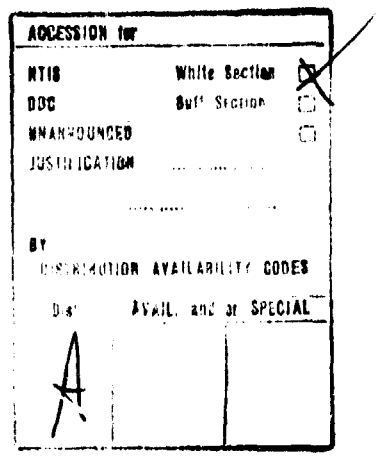

CONTENTS

ILLUSTRATIONS

ILLUSTRATIONS (Cont'd)

ILLUSTRATIONS (Concl'd)

TABLES

1.0 INTRODUCTION

A major factor in earth penetrator (EP) performance is the tip configuration. A program was initiated to determine the relative penetration performance of three different tip configurations. Full scale earth penetrators were designed with ogive, single stepped tier (SST) and conical tips. The total weight, c.g. location, and tip geometry was defined for each configuration. One twelfth scale models were designed to duplicate each of the important design parameters as closely as possible. These subscale model designs included provisions for a copper ball passive accelerometer.

Subscale EP models were fabricated and tested. A total of 24 tests were performed at various combinations of angle of attack and obliquity for each of the three model configurations. Tests were conducted at 1000 ft/s impact velocity through concrete into a sand media. EP model performance was monitored and compared.

The primary purpose of these tests was to determine relative "g" loads and trajectory performance for three realistic design configurations under typical operational conditions. It was further intended that the test results should provide a data base which could be used to predict future EP performance with regard to "g" loading and trajectory performance. This type of information is needed to ensure that EP designs can be evolved which can be realistically expected to achieve program objectives.

This report documents the subscale EP model test hardware, instrumentation, procedures, results and data trends. Detailed analysis of the data to develop and refine predictive computer trajectory codes is beyond the scope of this activity. However, it is recommended that detailed analysis of the test data be undertaken as a part of a future program to maximize data utility and to increase understanding of earth penetrator phenomenology.

2.0 TEST HARDWARE

Tests were conducted with subscale EP models fabricated to the three configurations shown in Figures 1 through 3. These represent 1/12 scale models of full scale penetrator design. Full scale designs were developed for each of the three candidate configurations; ogive, SST and conical tip designs. Each design realistically considered EP geometry, internal components, mass and c.g. The models were developed by scaling the total mass of the full scale design and the relative c.g. location into the models in a representative fashion. The design included the passive copper ball accelerometers. The three EP models are shown in Figure 4 together with the passive accelerometer assembly. An exploded detail of the passive accelerometer assembly is shown in Figure 5. The test model weights and c.g.'s are compared with the theoretical 1/12 scale model values in Table 1. As may be seen the models were very close to the desired values in all cases.

The test models were machined from maraging steel and heat treated to a hardness of approximately 50 on the Rockwell C scale. This is equivalent to an ultimate strength in excess of 255,000 lb/in^2.

The copper ball passive accelerometer design was based on work performed as reported in References 1 and 2. These reports were prepared by Mr. Val DeVost of the Naval Ordnance Laboratory, White Oak, Maryland. Mr. DeVost was of great assistance during this program, providing insight into the design and fabrication of these devices. He further identified a source and quality assurance procedure for the copper balls. NOL copper ball passive accelerometers (MOD 10-200,000 g) were used in all tests. The passive accelerometer assemblies including the copper balls were obtained from Halpro, Inc., Rockville, Maryland. These assemblies were made in accordance with Halpro Drawing No. 2425615. Copper balls were 0.1553 inch in diameter and were quality controlled to a tolerance of plus 0.0002 inch minus zero inches.

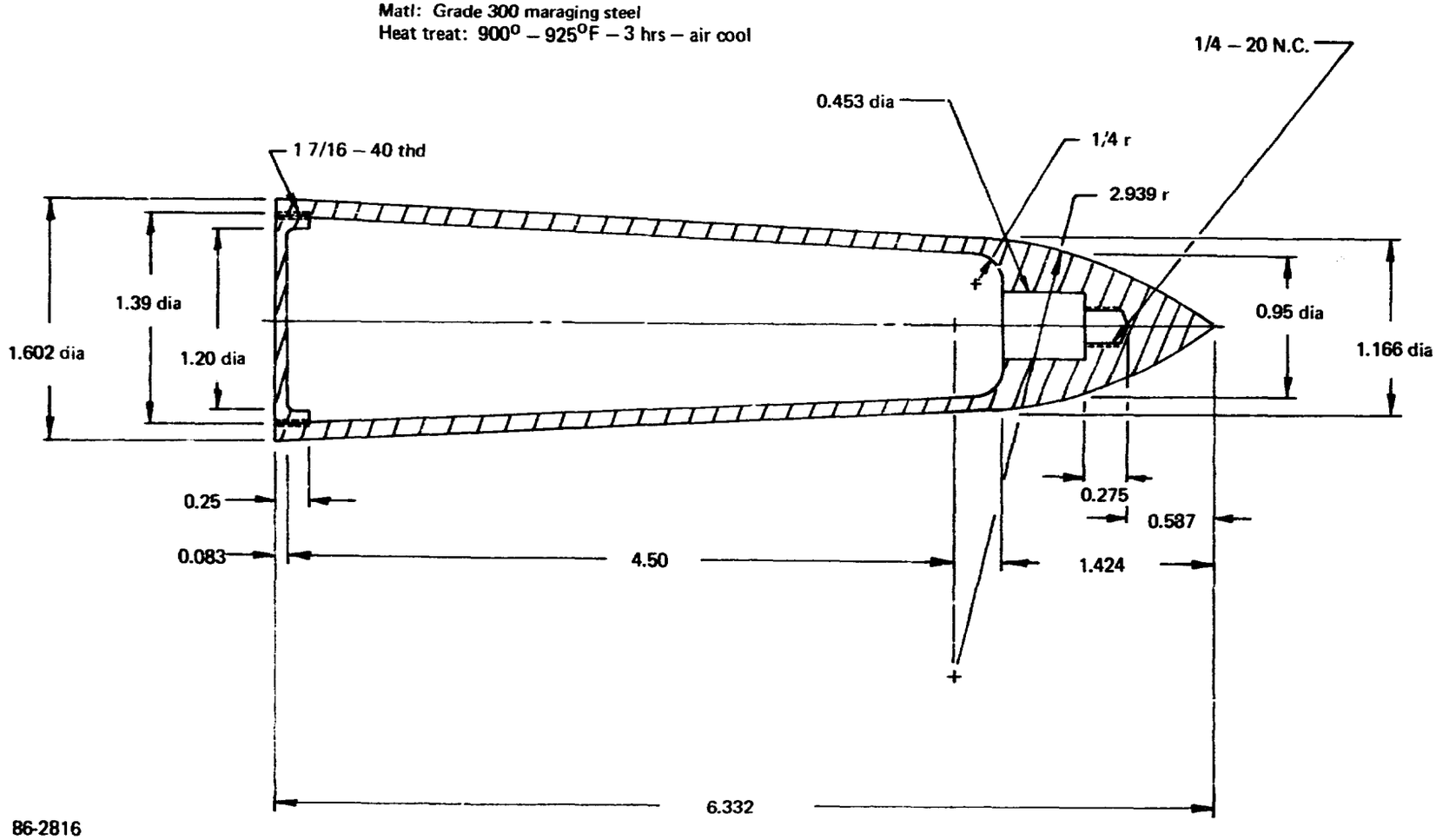

Figure 1 SUBSCALE PROJECTILE DESIGN – OGIVE

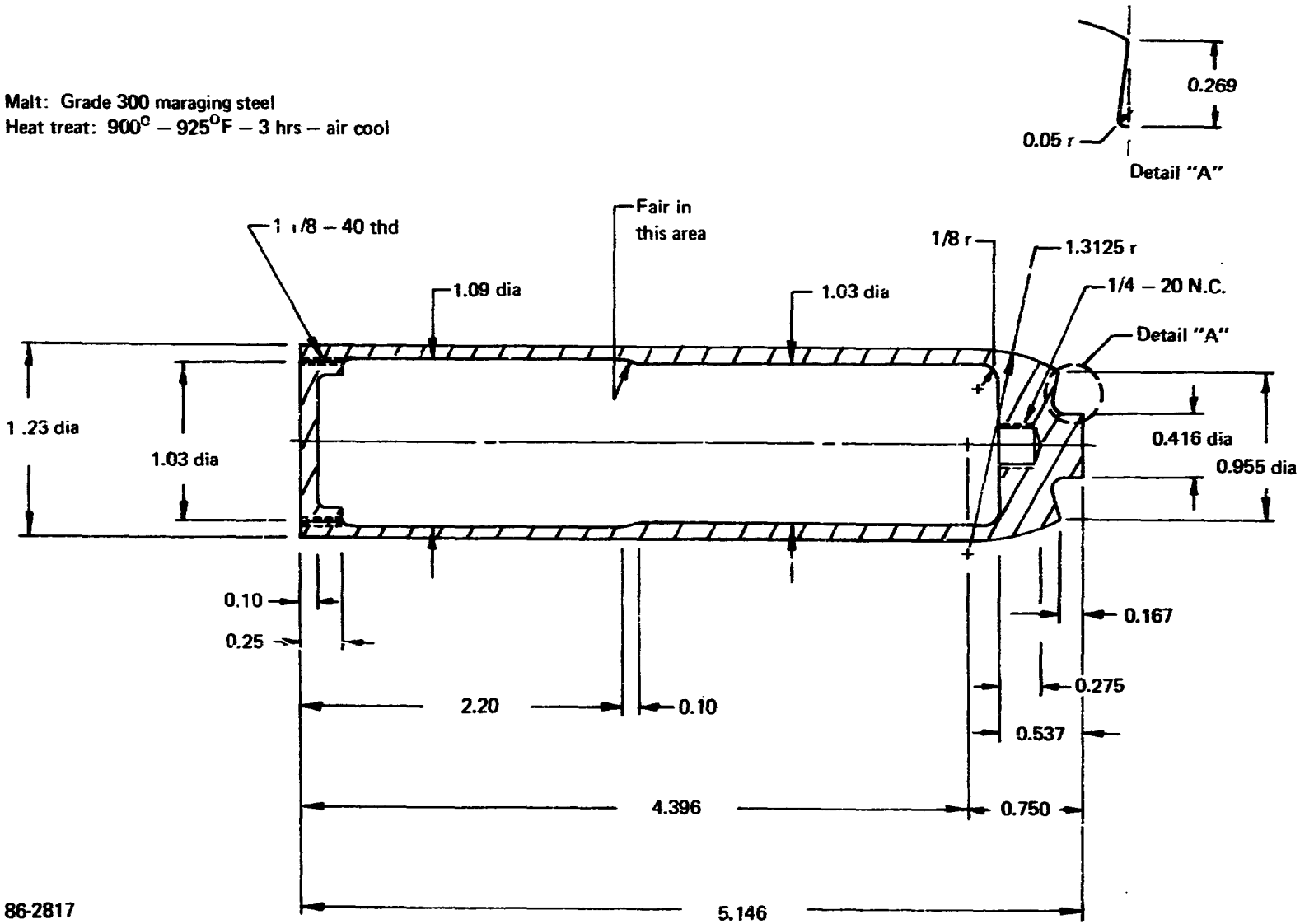

Figure 2 SUBSCALE PROJECTILE DESIGN – SST

Matl: Grade 300 maraging steel
Heat treat: 900° – 925°F – 3 hrs – air cool

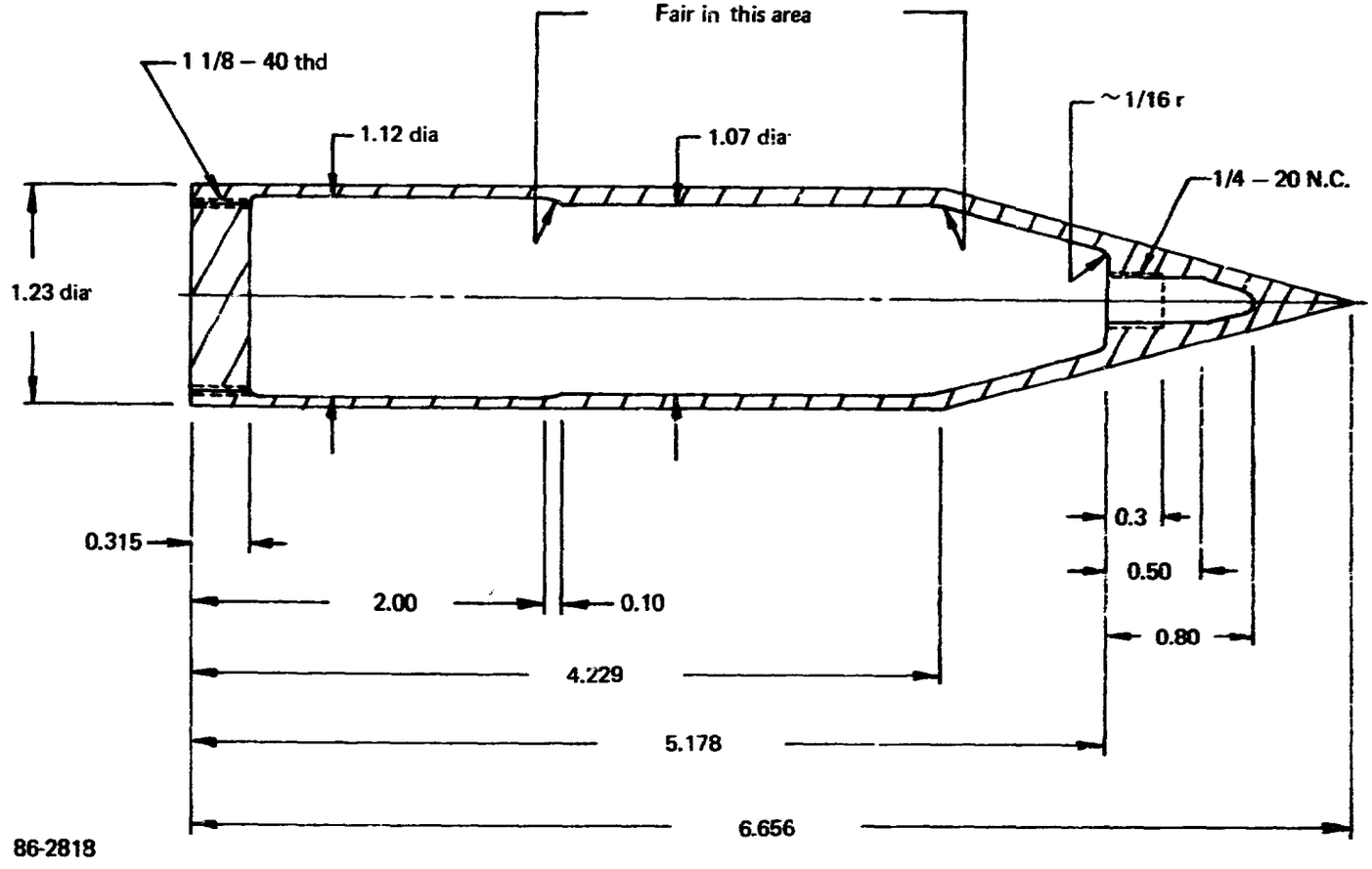

Figure 3 SUBSCALE PROJECTILE DESIGN – CONICAL

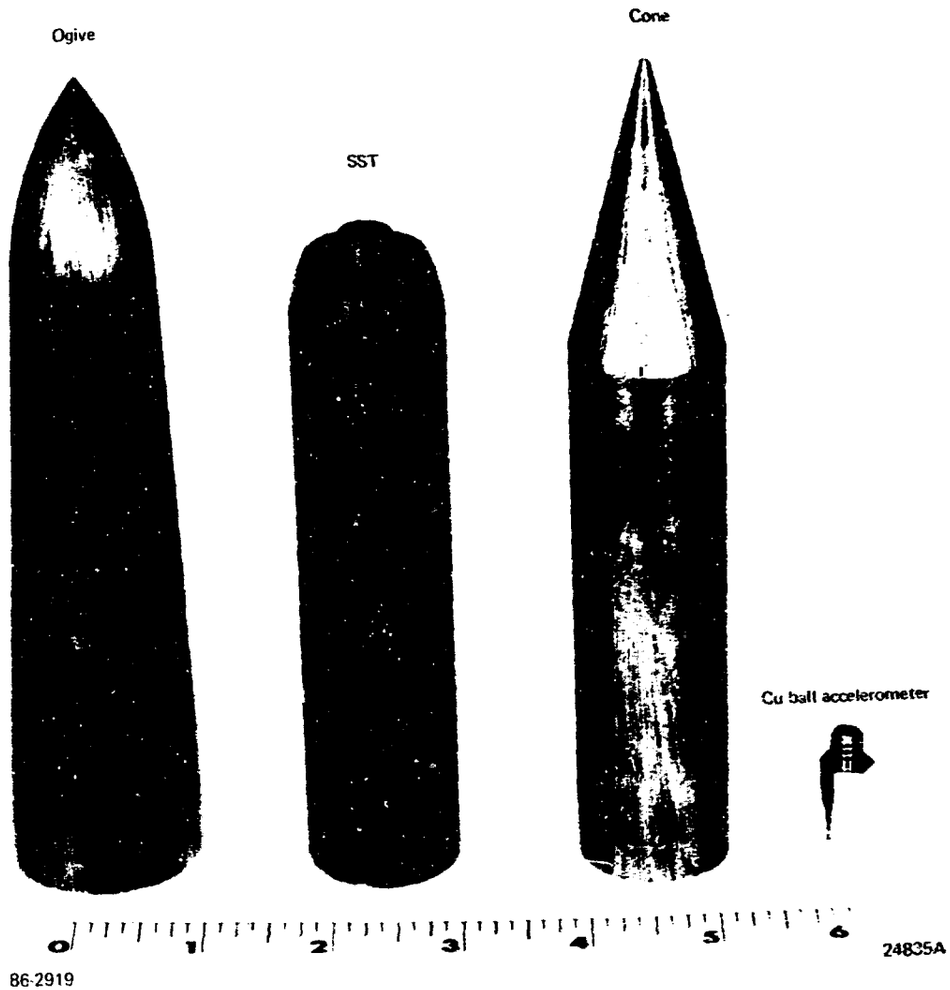

Figure 4 PROJECTILES AND ACCELEROMETER

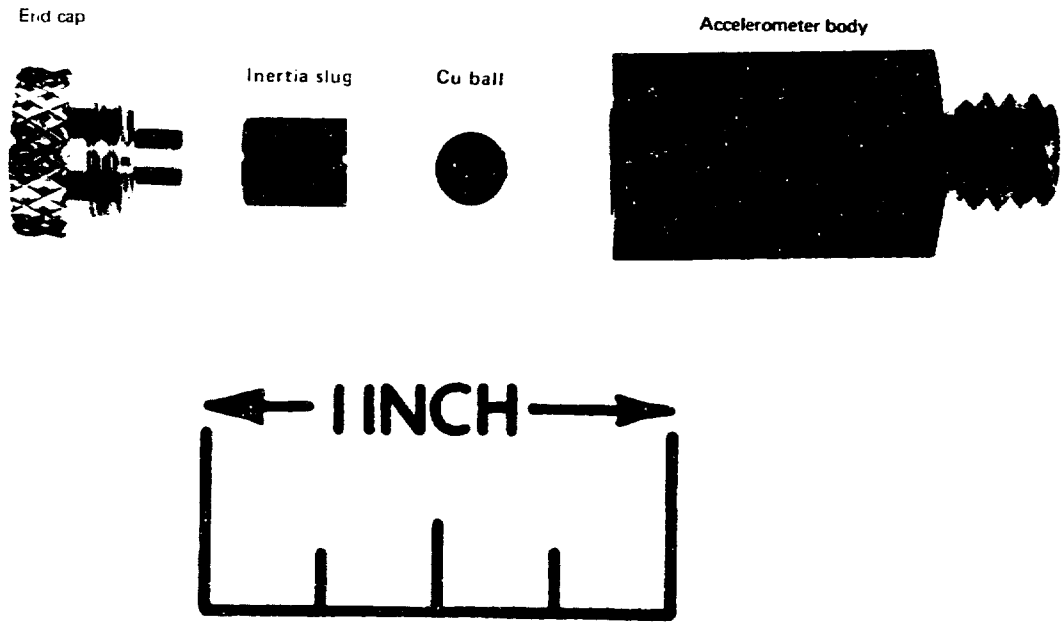

Figure 5 PASSIVE ACCELEROMETER PARTS

TABLE 1. COMPARISON OF TEST MODEL WEIGHTS AND C.G.'S WITH DESIRED VALUES

	Ogive		SST		Cone	
	Weight (gms)	C.G. % from tip	Weight (gms)	C.G. % from tip	Weight (gms)	C.G. % from tip
Actual test models	243	55	274	45.6	377	57.9
Theorectrical 1/12 scale models	247	57.28	276	45	358	57.95
Ratio actual to theorectical %	98.4	96.0	99.3	101.3	105.3	99.9

All tests were performed using a 2.9 inch diameter smooth bore launcher to accelerate the EP scale model to a nominal 1000 ft/s velocity. It was necessary to use sabots to support the projectiles to accommodate the difference between the EP diameters and the launcher diameter and to provide for angle of attack orientation where necessary. A sabot drawing is shown in Figure 6. The sabot and disc were fabricated from a 3-inch diameter polyethelene rod. The disc and base support configuration were varied to accommodate the desired angles of attack (i.e., 0, 2-1/2 or 5 degrees).

Figure 7 shows a typical sabot with an SST model installed. The saw cuts, 90 degrees apart, are typical for all sabots and are needed to accommodate separation of the EP model from the sabot after launch.

The target consisted of a three-foot square concrete slab backed by a box full of sand. The concrete had a nominal thickness of one inch which represented a 12-inch thick full scale concrete slab. The concrete was made with a sand aggregate. The concrete had a compressive strength of approximately 5000 lb/in^2 seven days after pouring using a high early strength cement.

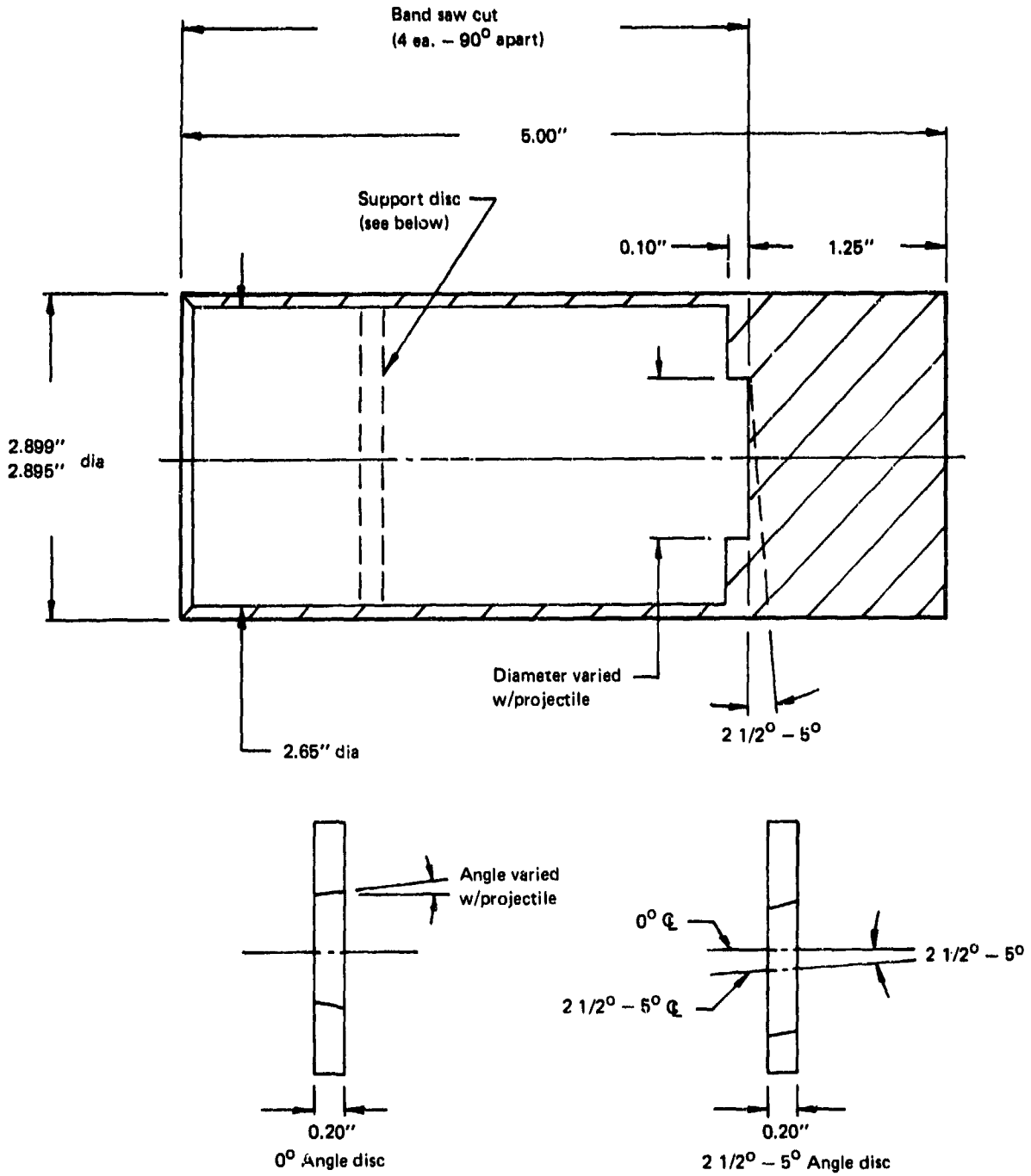

Figure 6 PROJECTILE SABOTS AND SUPPORT DISCS

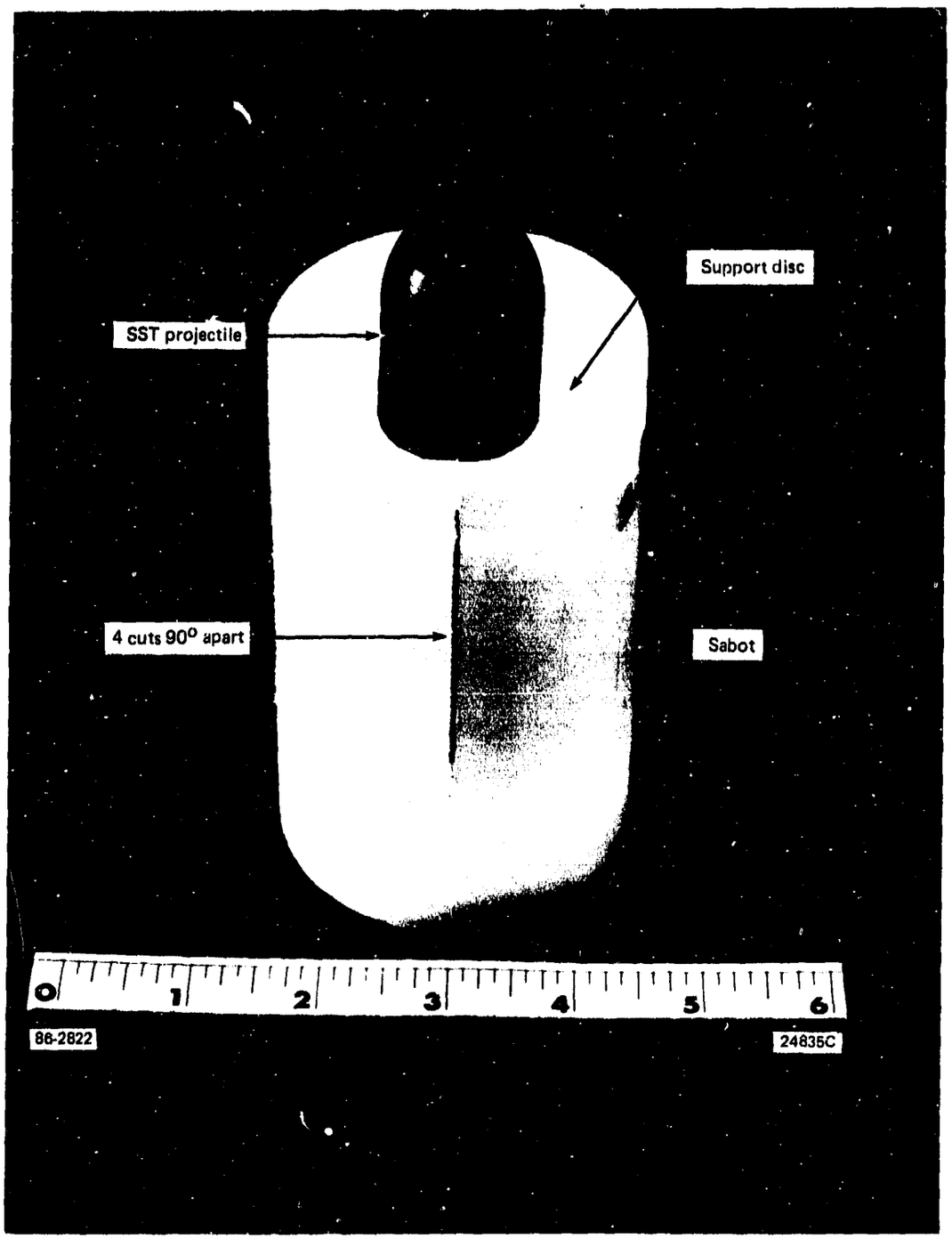

Figure 7 SST PROJECTILE IN SABOT

3.0 INSTRUMENTATION

The instrumentation used on all 24 tests consisted of high speed cameras to observe the projectile flight up to and including hitting the concrete slab and "make circuit" velocity grids to monitor velocity through the sand media. The passive accelerometers described under test hardware were used on each test to measure peak deceleration "g's". One mil of copper ball deformation equals approximately 22,600 g's up to 200,000 g's according to the Reference 1 data.

Two high speed Fastax cameras were located 90 degrees apart to observe the free flight of the EP model from a side view and from a top view. The cameras were operated at approximately 6000 frames per second and were used to measure EP model angle of attack and velocity. All sabots were oriented so that the angle of attack could be observed by the side view camera with EP nosetip up/tail down orientation. However, due to slight sabot roll during launch it was possible to observe some angle of attack orientation in the top camera.

The actual test angle of attack was of course the resultant of the angles observed in the top and side cameras. It was possible to measure angles to within ±0.5 degree using the Fastax camera filming technique. Velocity at impact into the concrete was also determined by analyzing the Fastax film data. The velocity data is accurate to within 5 percent or approximately plus or minus 50 ft/s.

EP model trajectory and velocity after concrete target penetration was determined with make-circuit velocity grids on the face of the concrete target and in the sand media behind the target. Three make-circuit grids were located in the sand media for each test. Each make-circuit in the sand consisted of two layers of aluminum screen (1 x 1 ft square) insulated with posterboard material. The concrete target face make-circuit (T_o) consisted of two layers of aluminum foil insulated with a layer of 5 mil mylar. EP model trajectory was

determined from the location of the holes in the grids and velocity was determined from the time interval and distance between grids. All grid circuit closing times were recorded on magnetic tape and playback was onto an oscilloscope.

4.0 TEST PROCEDURE

The test setup used for each of the 24 tests is shown in Figure 8. Each test was performed in the same manner as described below.

Make-circuits were positioned in the sand box as shown in Figure 9. Sand was put into the box to the depth shown in Figure 9. A concrete target was located in front of the sand box positioned to the obliquity desired for the particular test. A make-circuit was placed on the front surface of the concrete target to act as a T_o circuit. All make-circuits were connected to a magnetic tape recorder. Sabot peeler and deflection plates were located at the front of the EP model launcher (gun barrel). The hole in the peeler plate was smaller than the sabot, but, larger than the EP model. The peeler plate would retard the sabot while permitting the EP model to pass through. However, the sabot was still in line with the model such that it would impact the concrete target immediately after the EP model, making it impossible to evaluate model cratering effects. Therefore, a deflector plate was used to kick the peeled sabot to one side causing it to impact a steel plate located to the right of the concrete target.

The passive accelerometer was assembled after selecting and measuring a copper ball. The passive accelerometer was assembled into the EP model and the aft model cover screwed in place. The EP model was then placed in a sabot selected to produce the desired angle of attack. The sabot EP assembly was located so the aft end of the sabot was flush with the aft end of the gun barrel. The EP model tip was oriented upward such that the angle would be seen in the side view camera for all angle of attack tests. A powder charge of 10 grams FFG black powder and 90 grams 4895 powder, as determined by calibration tests, was placed in the breech along with a S-94 electric squib. The breech was assembled to the gun barrel.

The two fastax cameras were loaded with film and the firing circuit connected.

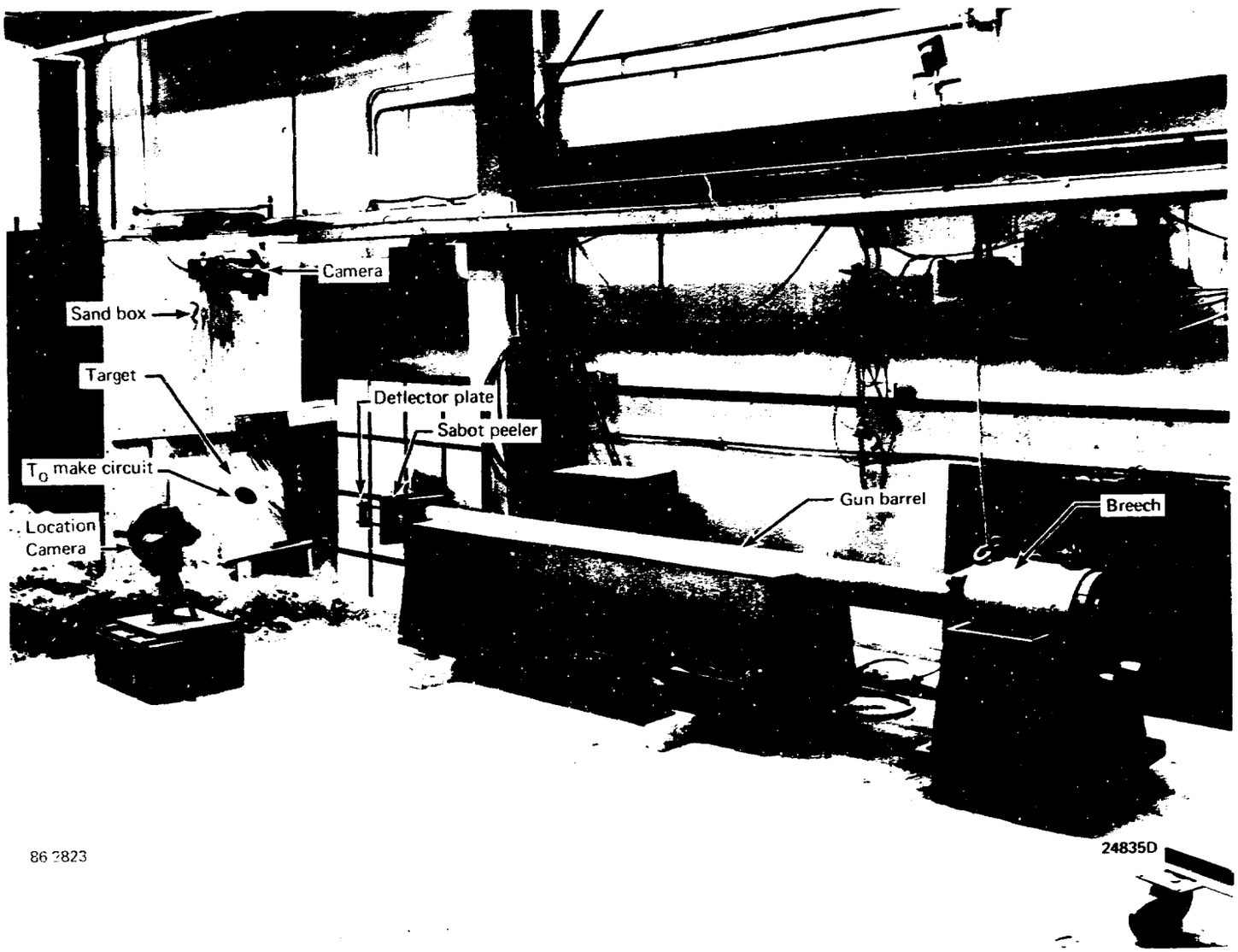

Figure 8 S/S PENETRATION TEST SETUP

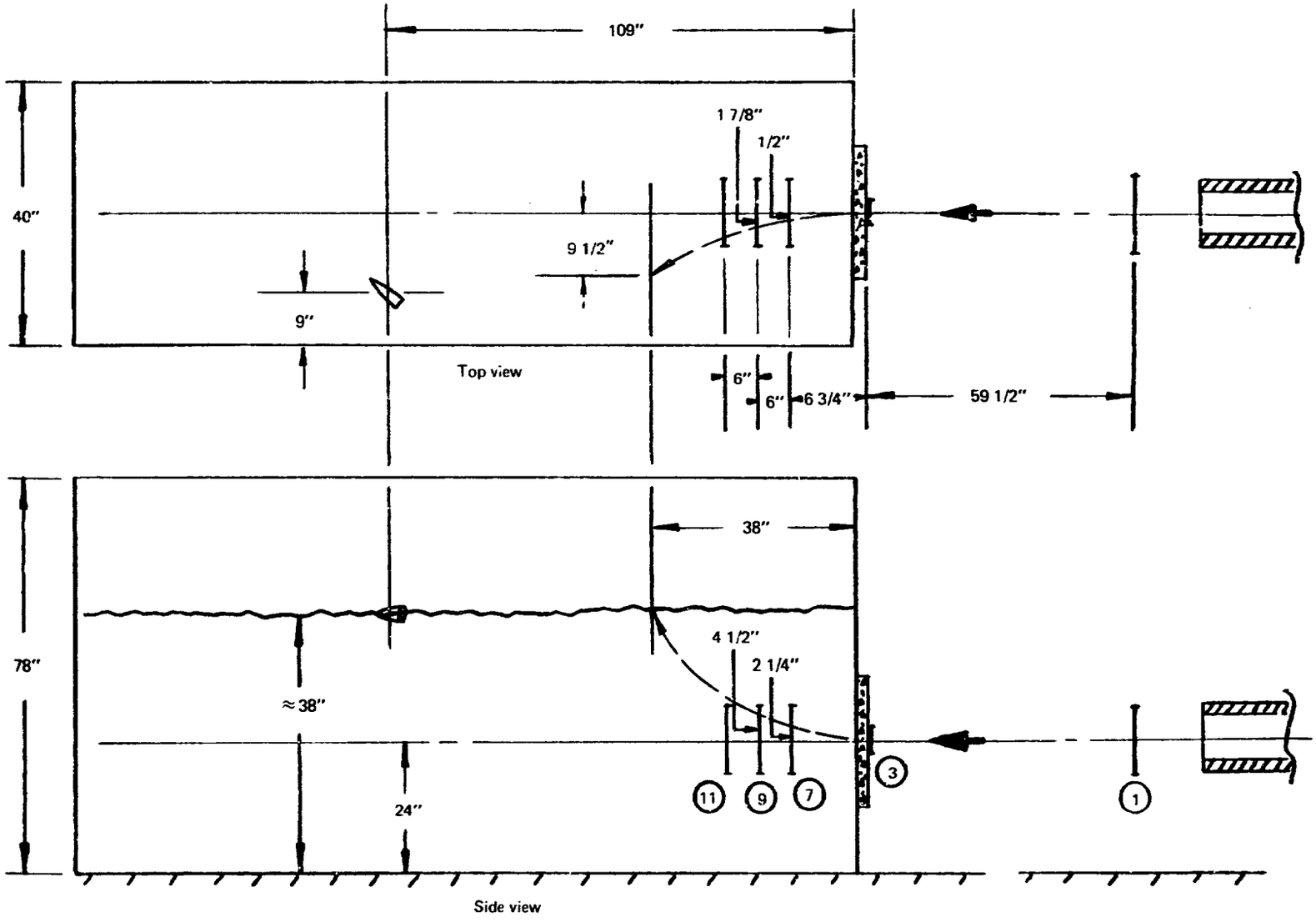

Figure 9 SUBSCALE OGIVE PENETRATION TEST 1, $\gamma = 0^{o}$, $\alpha = 5^{o}$

The cameras were started prior to firing the EP model so that the desired film speed of 6000 frames per second could be achieved. The tape recorders were started and the S-94 squib initiated causing the EP model to be launched. The gun to concrete target distance varied from prior test to test because of different target obliquities, but was nominally 52 inches.

At the conclusion of testing the EP model was recovered from the sand box with the final location noted. The location of holes in the velocity grids were used to provide trajectory data through the sand media. The tape recorder velocity grid data was played back through oscilloscopes to provide a measure of elapsed time from penetration of one grid to the next. Knowing the distance between grids permitted the calculation of EP model velocity through the sand media.

The Fastax film data was recovered, developed and analyzed to provide EP model velocity and angle of attack data. The concrete target crater was measured in detail for each test.

5.0 TEST RESULTS AND DISCUSSION

The test results are summarized in Table 2. Details of the EP model trajectory in the sand media and the target crater characteristics are presented for each test in Figures 9 through 52.

Table 2 shows the order in which the tests were performed, the EP model used for each test, the angle at which the concrete target media was set for each test, and the desired angle of attack. The measured angles of attack as observed from analysis of the side and top located Fastax camera films are listed. The resultant angle of attack was calculated from the side and top values. The resultant angle of attack is the angle of attack of the EP model when it hit the concrete target. The EP models were located nose up in the launcher so that angle of attack could be observed in the side camera. It is obvious from the data that the sabots rotated somewhat during transit of the launcher. The actual (resultant) angle of attack compares quite well with the desired angle of attack for all but Tests 19 and 21. The average difference between the desired and actual angle of attack was approximately one degree for the 22 tests, excluding Tests 19 and 21. The maximum deviation range for the 22 tests was -2.5 degrees and +3.0 degrees. If Tests 19 and 21 are included the average deviation per test increases to 1.4 degrees and the maximum difference increases to 6 degrees. The results of Tests 19 through 21 seem to be more representative of five degree angle of attack data than zero degree data and is not completely understood. It seems evident that sabot machining and assembly is very critical to achieving the desiged angle of attack and must be carefully controlled for each test.

The impact velocity data shown in Table 2 was obtained from analysis of the film data. The average velocity for the 24 tests was 977 ft/s with maximum deviations of +160 ft/s and -122 ft/s. The average velocity is quite close to the desired velocity of 1000 ft/s. The average velocities achieved for the ogive, SST and cone tip models

TABLE 2. SUMMARY OF EP MODEL PENETRATION TEST DATA

Test no.	EP model type	Target angle (deg)	Desired angle of attack (deg)	Resultant angle of attack (deg)	Side view angle of attack (deg)	Top view angle of attack (deg)	V_1 impact velocity (ft/s)	V_2 velocity T_0 MC_1 (ft/s)	V_3 velocity MC_1 MC_2 (ft/s)	V_4 velocity MC_2 MC_3 (ft/s)	Cu ball(4) deformation (mils)	Trajectory path	Target crater data
1	Ogive	0	5.0	7.6	6.5	4.0	933	672	462	(2)	4.7	See Fig. 9	(5)
2A	Ogive	0	0.0	1.3	1.3	(1)	926	707	520	438	0.9	See Fig. 10	See Fig. 11
3	SST	0	0.0	1.4	1.0	1.0	913	636	341	123	21.5	See Fig. 12	See Fig. 13
4	SST	0	5.0	5.0	5.0	0.0	900	617	301	143	16.3	See Fig. 14	See Fig. 15
5	Cone	0	0.0	0.0	(1)	0.0	990	725	430	248	1.3	See Fig. 16	See Fig. 17
6	Cone	0	5.0	7.7	6.3	4.5	926	650	(2)	(2)	1.8	See Fig. 18	See Fig. 19
7	Ogive	45	5.0	5.9	2.5	5.3	878	542	(2)	(2)	2.7	See Fig. 20	See Fig. 21
8	Ogive	45	0.0	0.0	0.0	0.0	898	629	(2)	(2)	4.6	See Fig. 22	See Fig. 23
9	SST	45	5.0	3.8	3.8	0.0	911	357	57	(2)	7.6	See Fig. 24	See Fig. 25
10	SST	45	0.0	0.5	0.0	0.5	947	375	70	(2)	(3)	See Fig. 26	See Fig. 27
11	Cone	45	5.0	2.5	1.5	2.0	935	653	(2)	(2)	5.8	See Fig. 28	(5)
12	Cone	45	0.0	1.3	1.0	0.8	900	518	(2)	(2)	5.1	See Fig. 29	See Fig. 30
13	Ogive	22.5	5.0	4.5	4.5	0.0	1033	714	286	(2)	4.1	See Fig. 31	See Fig. 32
14	Cone	22.5	5.0	5.0	5.0	0.0	1114	(2)	(2)	(2)	4.9	See Fig. 33	See Fig. 34
15	SST	22.5	5.0	8.0	0.0	8.0	978	(2)	(2)	(2)	8.1	See Fig. 35	See Fig. 36
16	Ogive	22.5	2.5	2.1	0.5	2.0	921	773	286	176	2.7	See Fig. 37	See Fig. 38
17	SST	22.5	2.5	2.3	2.3	0.0	1065	(3)	(2)	(2)	24.5	See Fig. 39	See Fig. 40
18	Cone	22.5	2.5	1.8	1.8	0.0	1060	(2)	(2)	(2)	4.6	See Fig. 41	See Fig. 42
19	Ogive	22.5	0.0	4.5	0.0	4.5	1160	677	375	(2)	3.8	See Fig. 43	See Fig. 44
20A	SST	22.5	0.0	2.5	2.0	1.5	960	333	84	(2)	12.8	See Fig. 45	See Fig. 46
21	Cone	22.5	0.0	6.0	1.0	6.0	955	(2)	(2)	(2)	2.9	See Fig. 47	See Fig. 48
22	Ogive	45	2.5	2.3	2.3	0.0	1052	779	510	361	4.5	See Fig. 49	See Fig. 50
23	SST	45	2.5	2.0	0.0	2.0	1124	523	89	(2)	11.9	See Fig. 51	(5)
24	Cone	45	2.5	2.0	2.0	0.0	970	(2)	(2)	(2)	4.3	See Fig. 52	(5)

Notes:
(1) Camera malfunctioned, no data.
(2) Projectile missed make-circuit grid due to trajectory through sand media.
(3) No data.
(4) Cu ball calibration - one mil deformation = 22,600 g's
Linear up to 200,000 g's.
(5) No crater data, concrete target broke up on removal from setup.

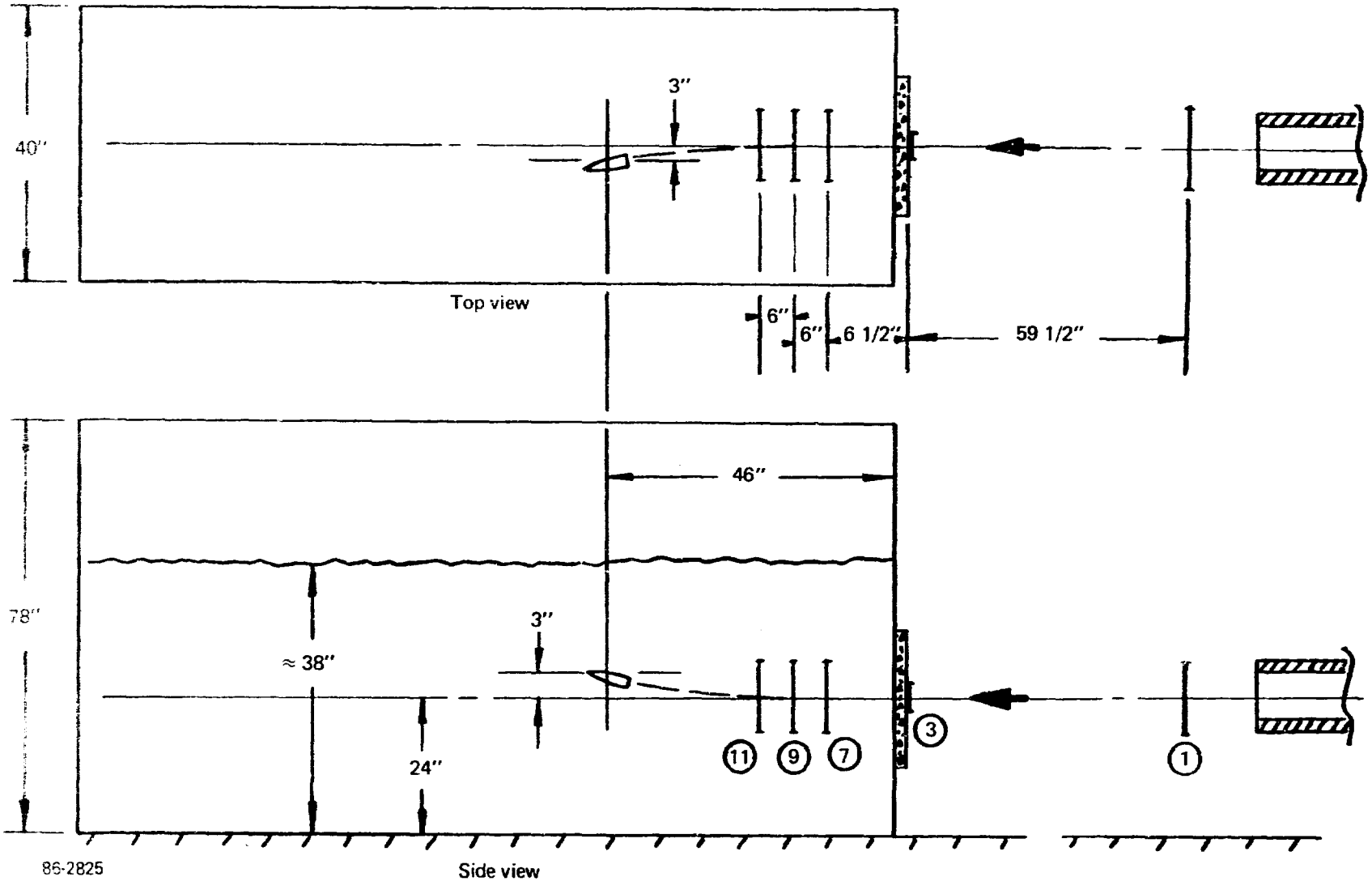

Figure 10 SUBSCALE OGIVE PENETRATION TEST 2A, $\gamma = 0^{o}$, $\alpha = 0^{o}$

Target no. 2A
1" thick

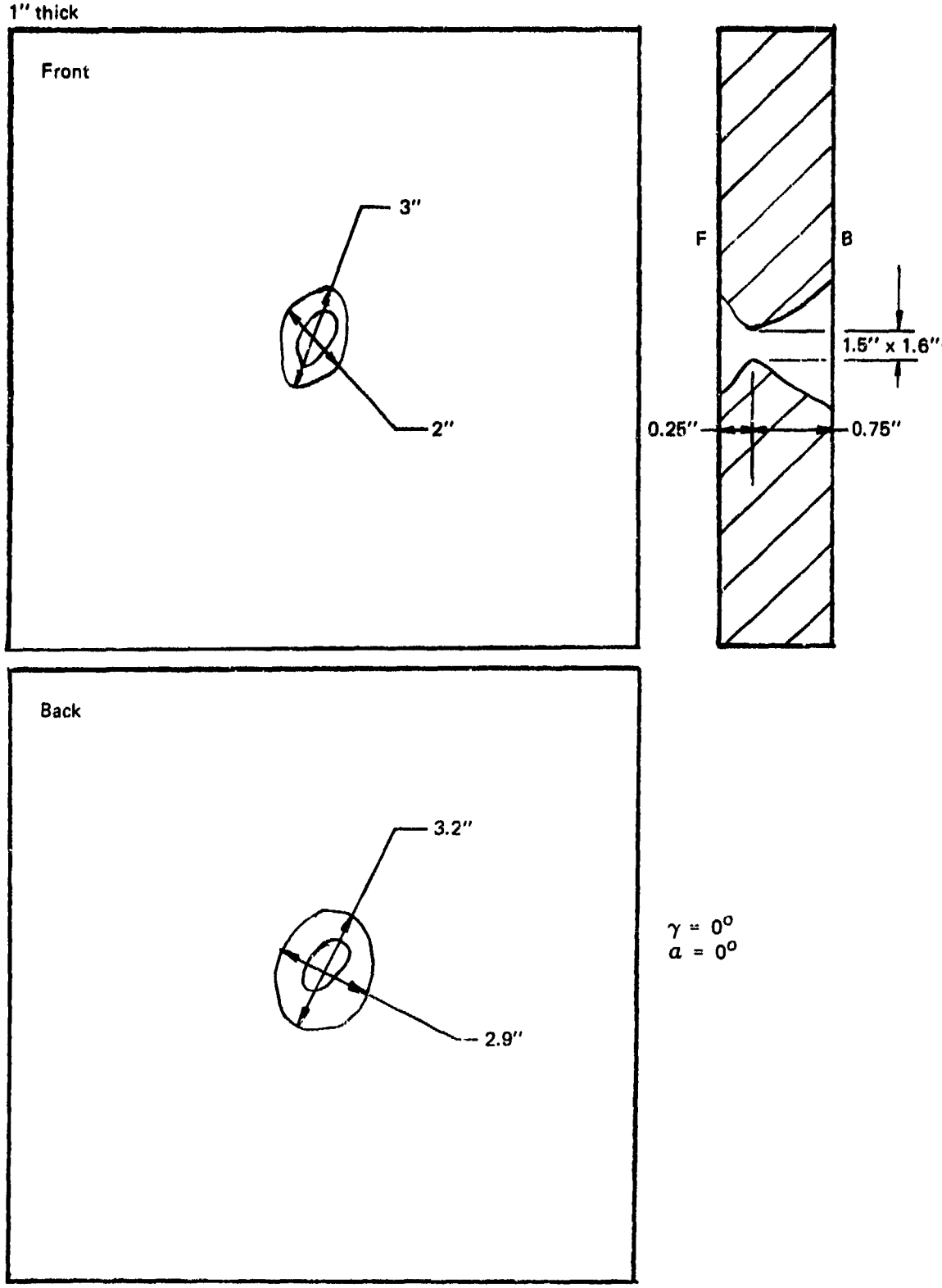

Figure 11 TEST 2A TARGET DATA – OGIVE PROJECTILE

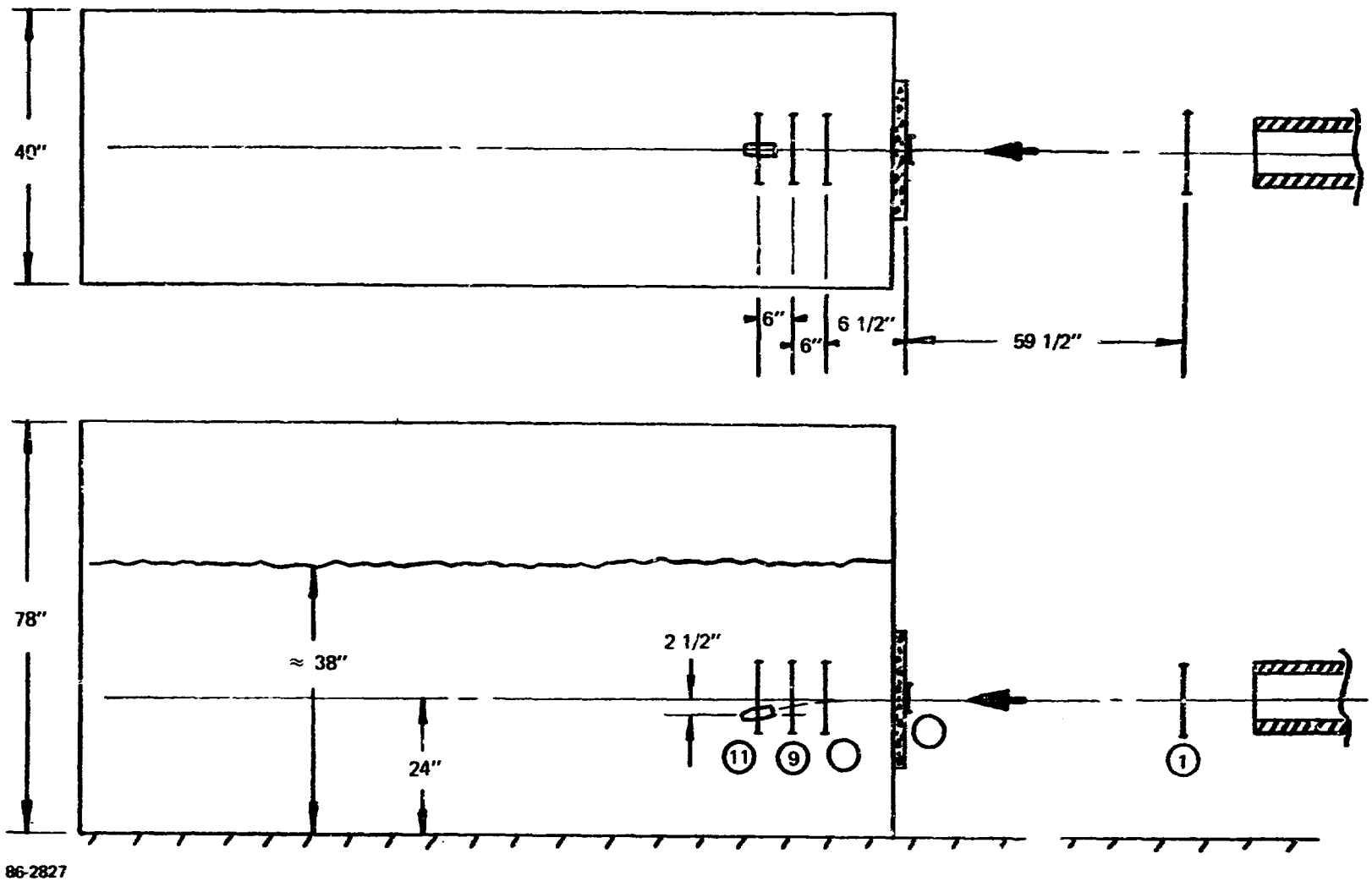

Figure 12 SUBSCALE SST PENETRATION TEST 3, $\gamma = 0^{o}$, $\alpha = 0^{o}$

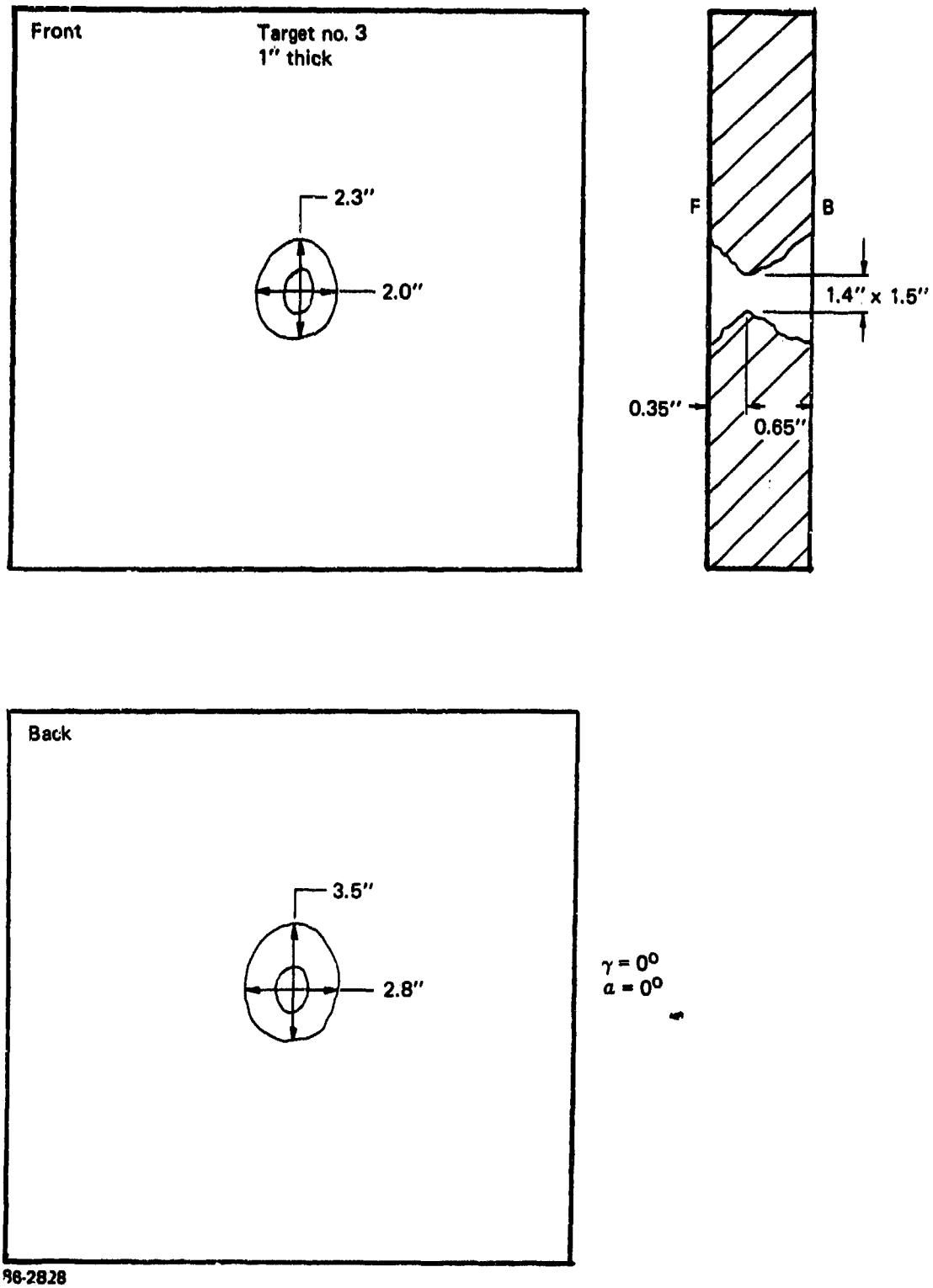

Figure 13 TEST 3 TARGET DATA – SST PROJECTILE

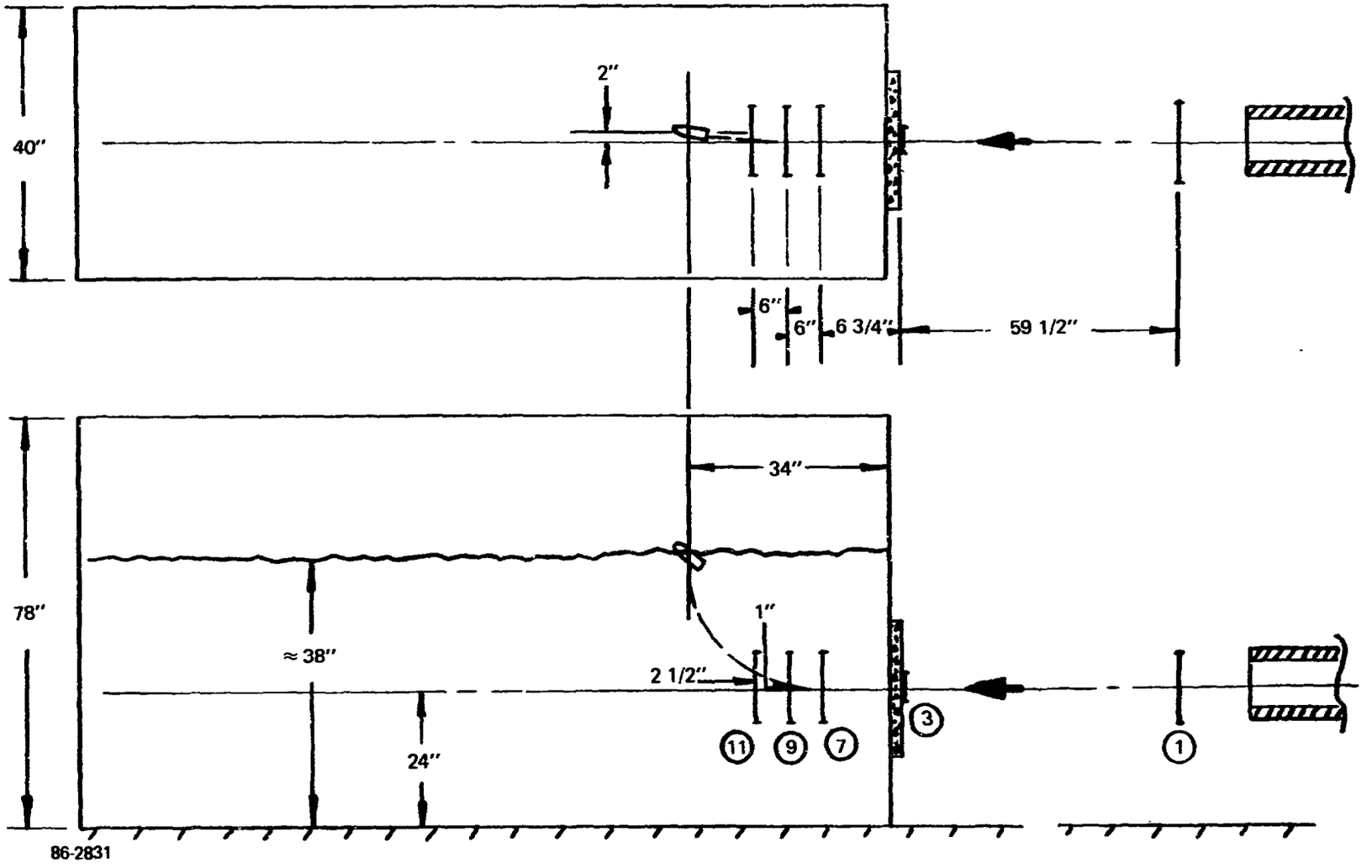

Figure 14 SUBSCALE SST PENETRATION TEST 4, $\gamma = 0^{o}$, $a = 5^{o}$

Target no. 4
1" thick – (1 3/32)

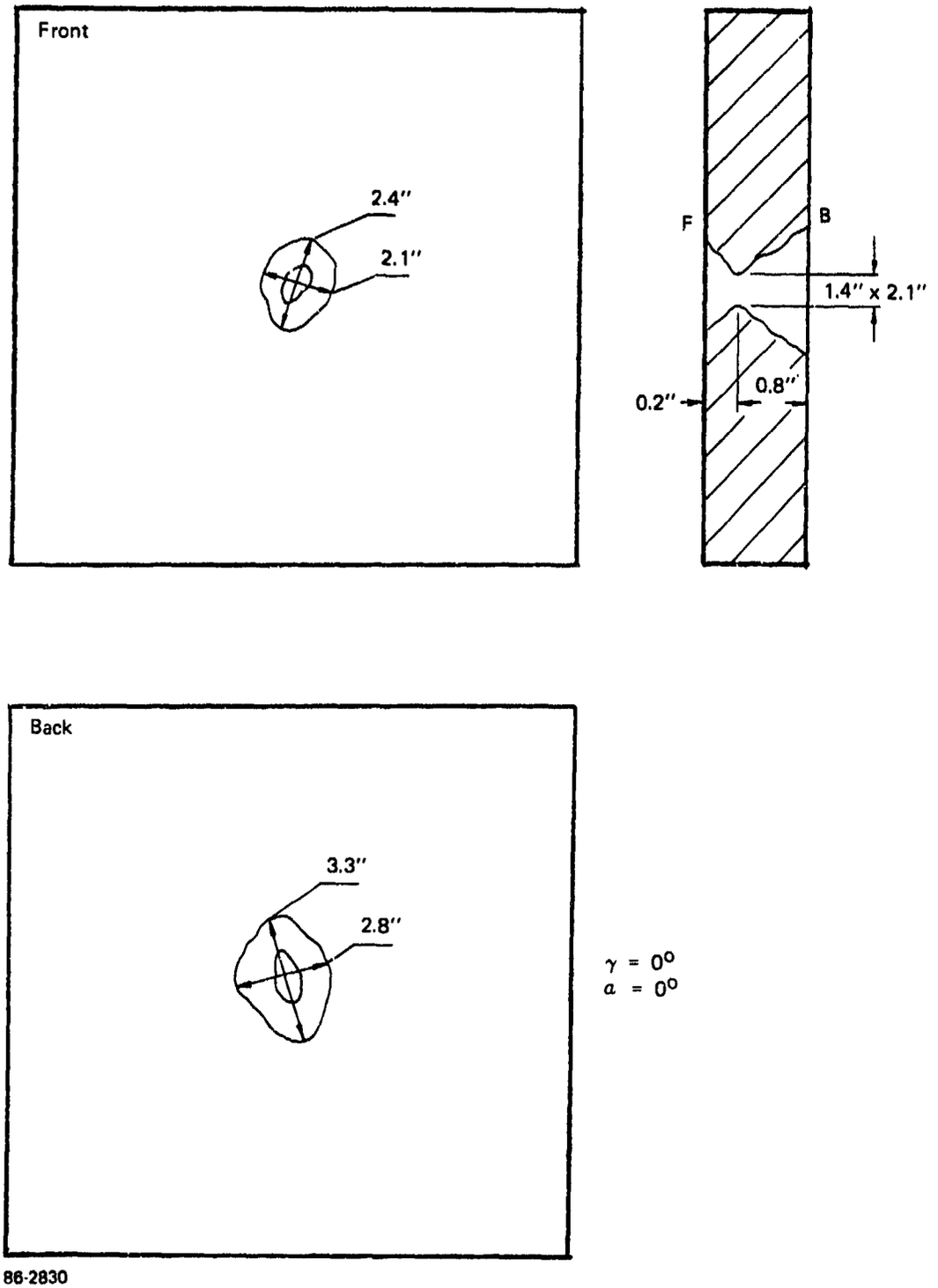

86-2830

Figure 15 TEST 4 TARGET DATA – SST PROJECTILE

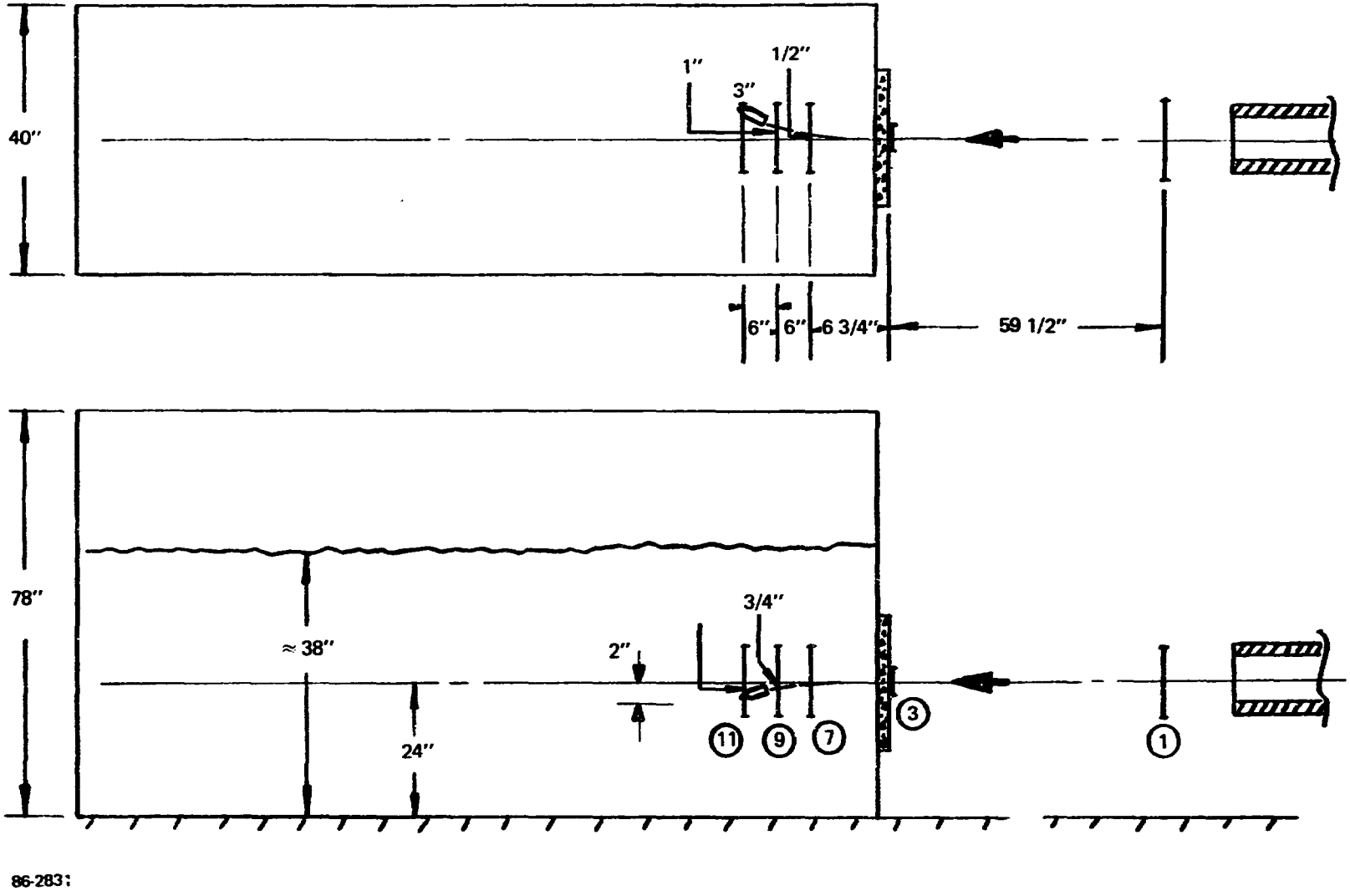

Figure 16 SUBSCALE CONE PENETRATION TEST 5, $\gamma = 0^{o}$, $\alpha = 0^{o}$

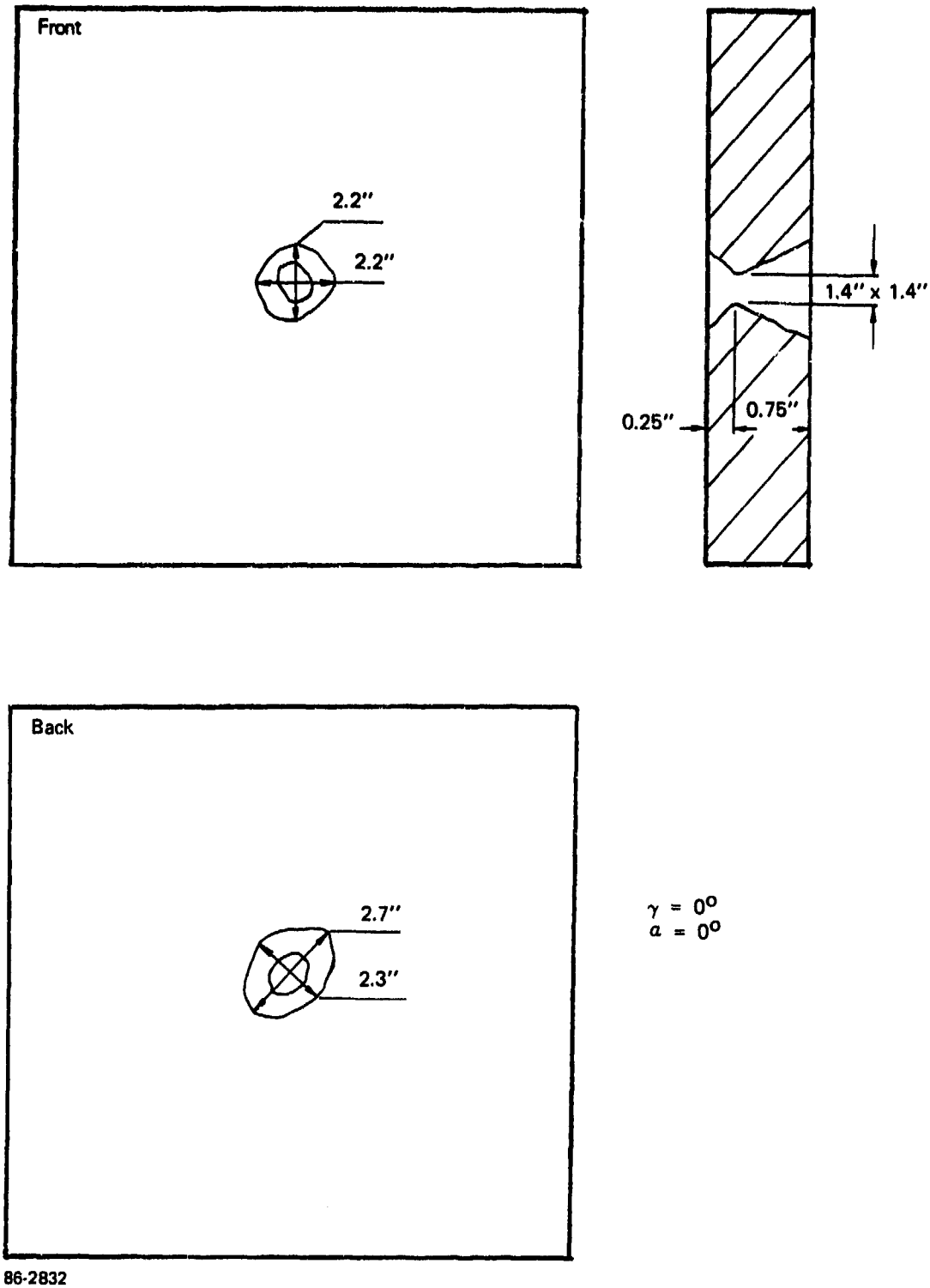

Figure 17 TEST 5 TARGET DATA – CONE PROJECTILE

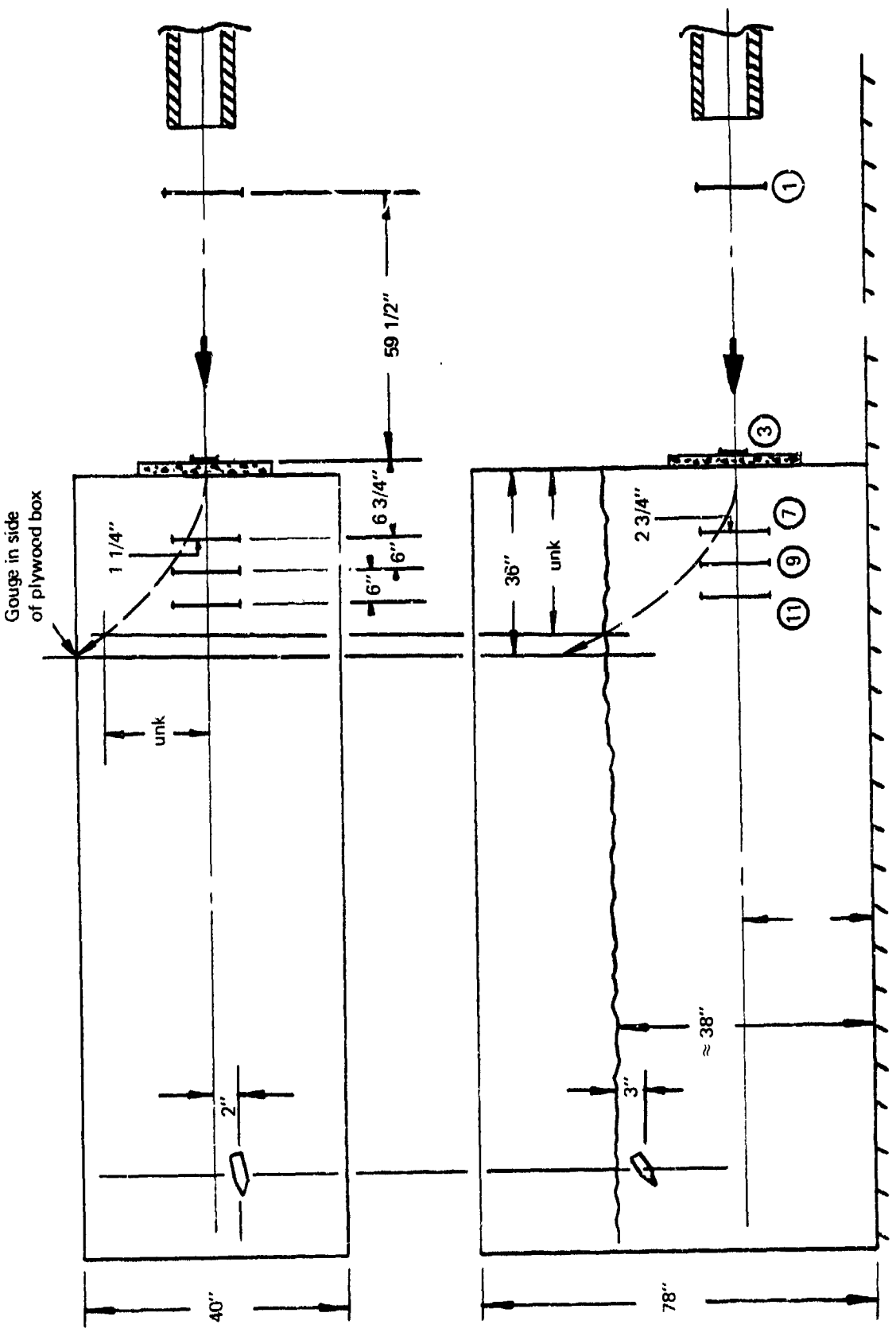

Figure 18 SUBSCALE CONE PENETRATION TEST 6, $\gamma = 0^{o}$, $a = 5^{o}$

Target no. 6
1" thick

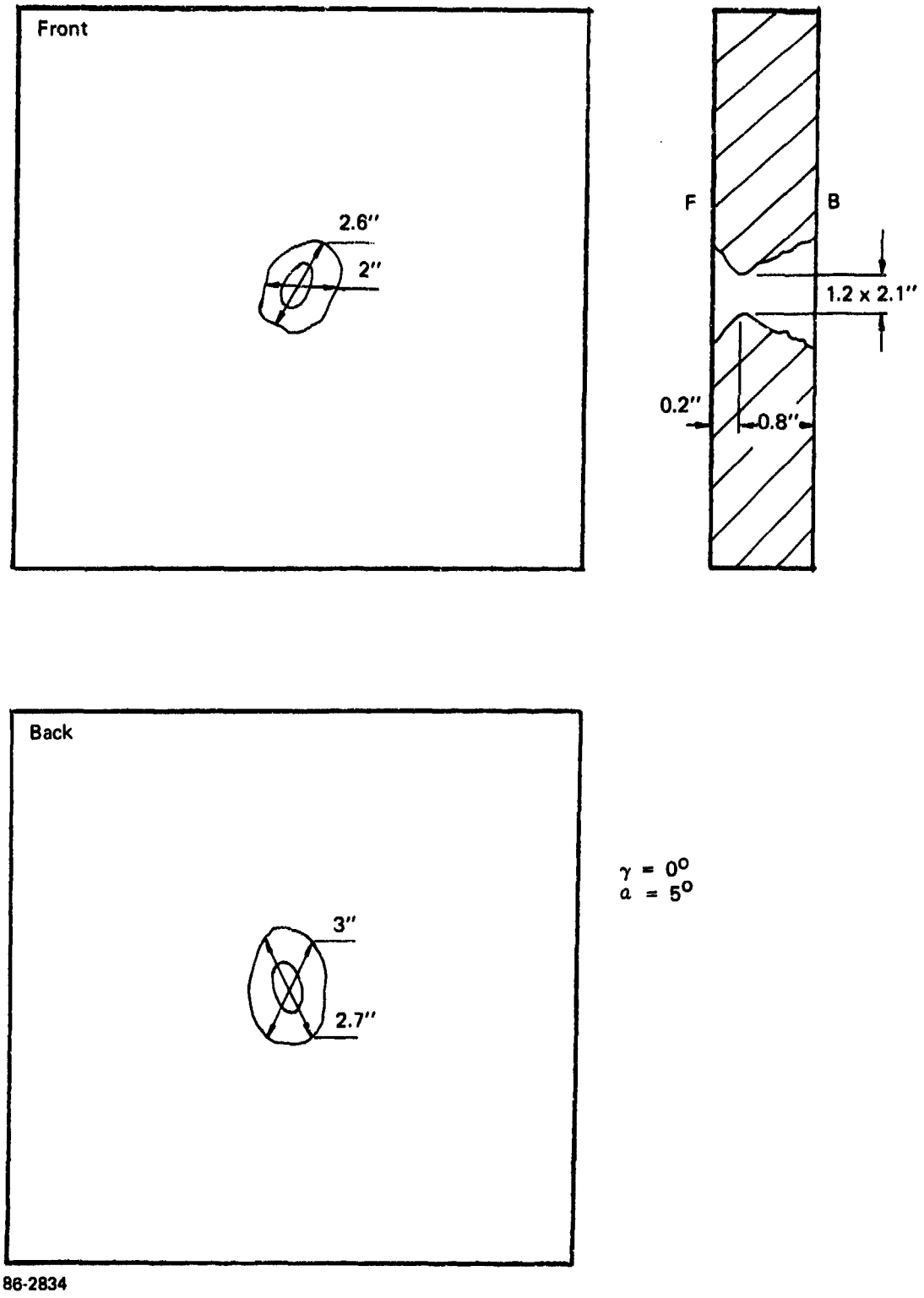

Figure 19 TEST 6 TARGET DATA – CONE PROJECTILE

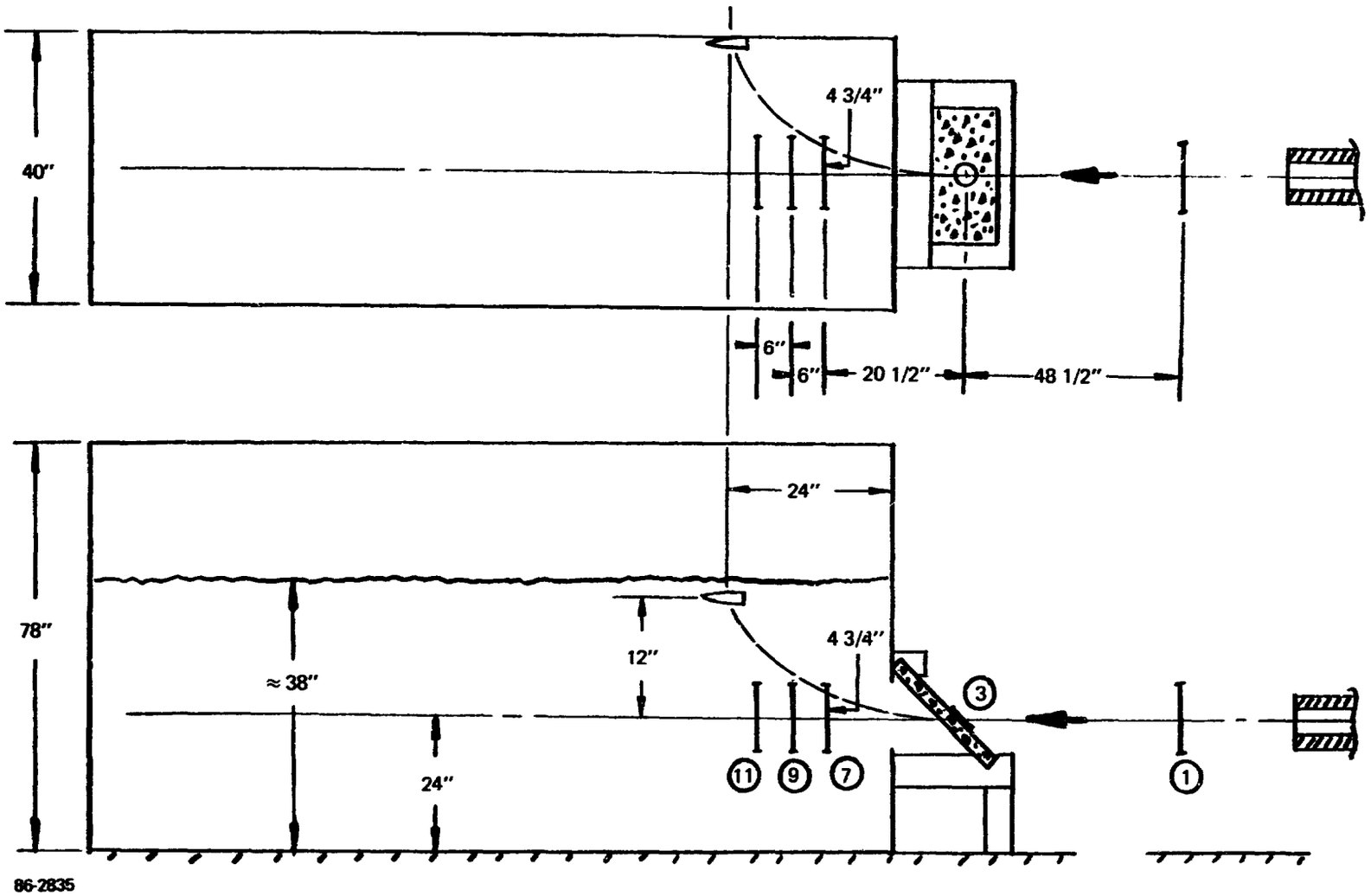

Figure 20 SUBSCALE OGIVE PENETRATION TEST 7, $\gamma = 45^{o}$, $\alpha = 5^{o}$

Target no. 7
1" thick

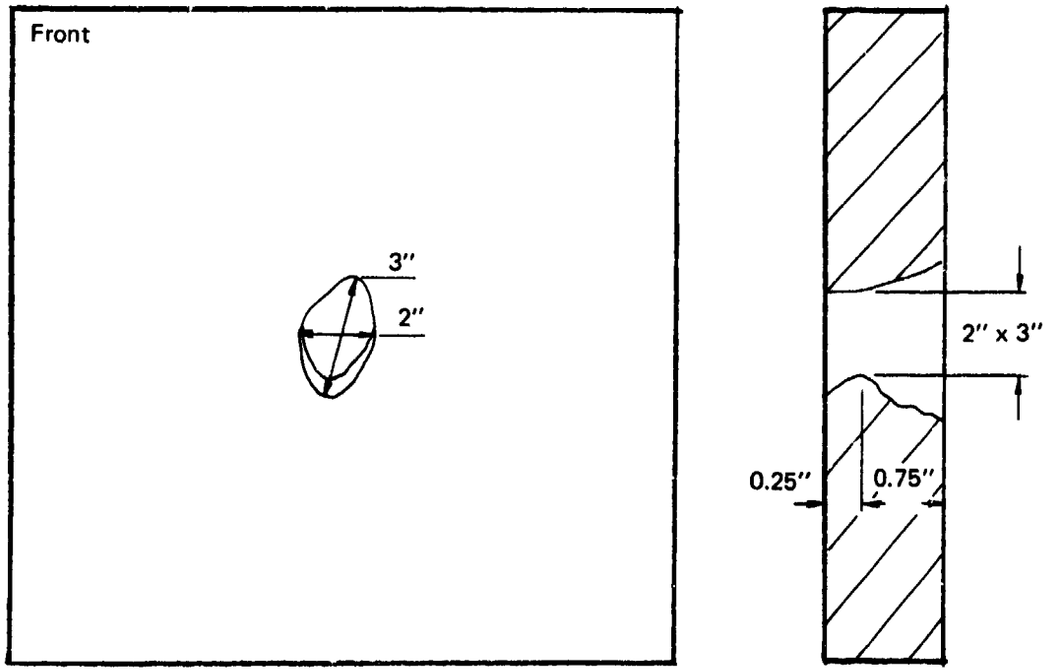

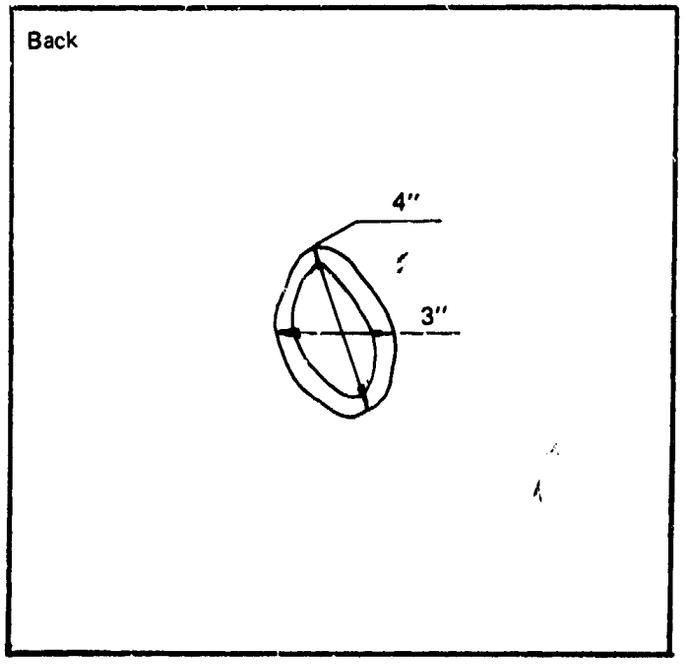

$\gamma = 0^{o}$
$a = 5^{o}$

86-2836

Figure 21 TEST 7 TARGET DATA – OGIVE PROJECTILE

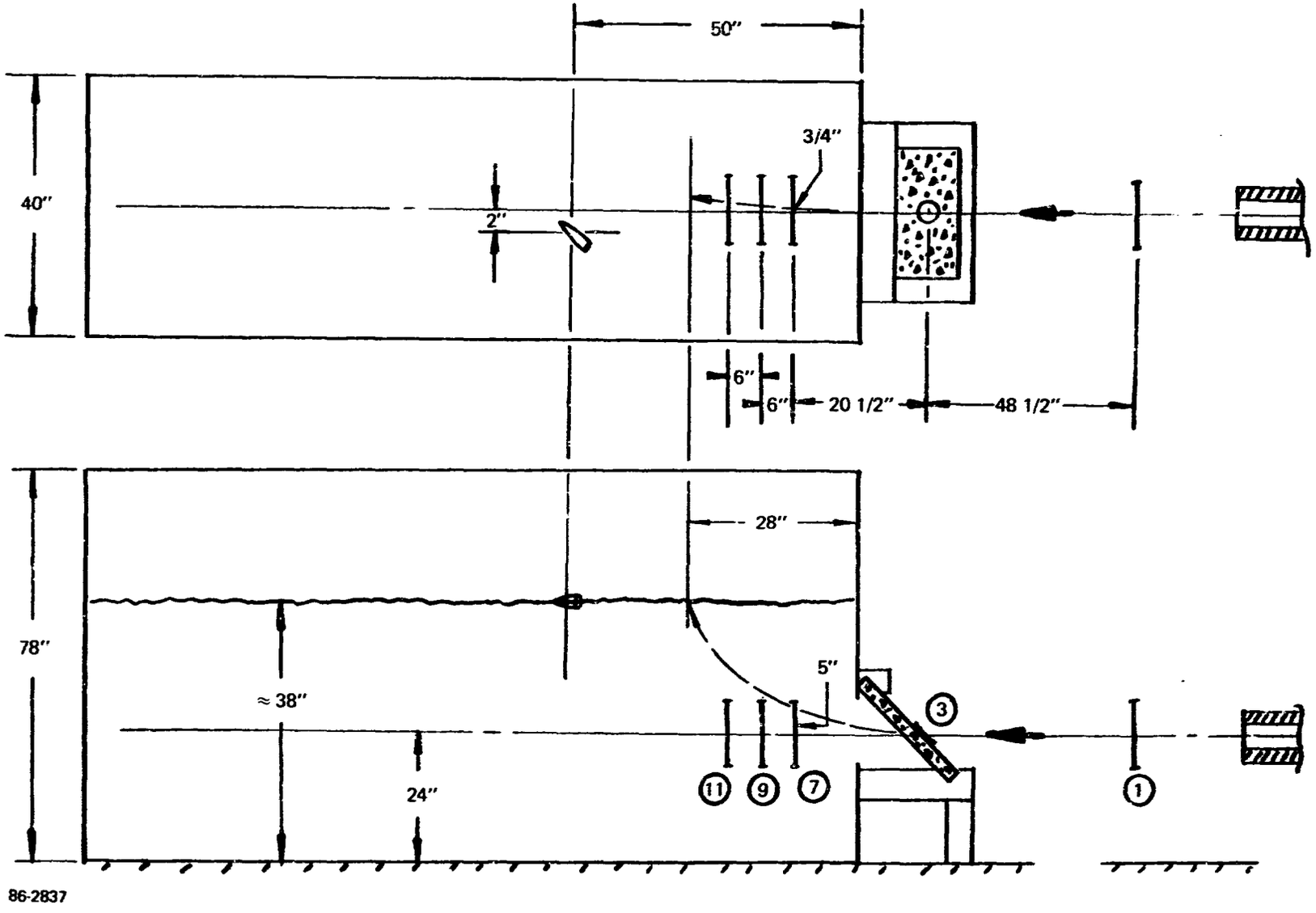

Figure 22 SUBSCALE OGIVE PENETRATION TEST 8, $\gamma = 45^{o}$, $\alpha = 0^{o}$

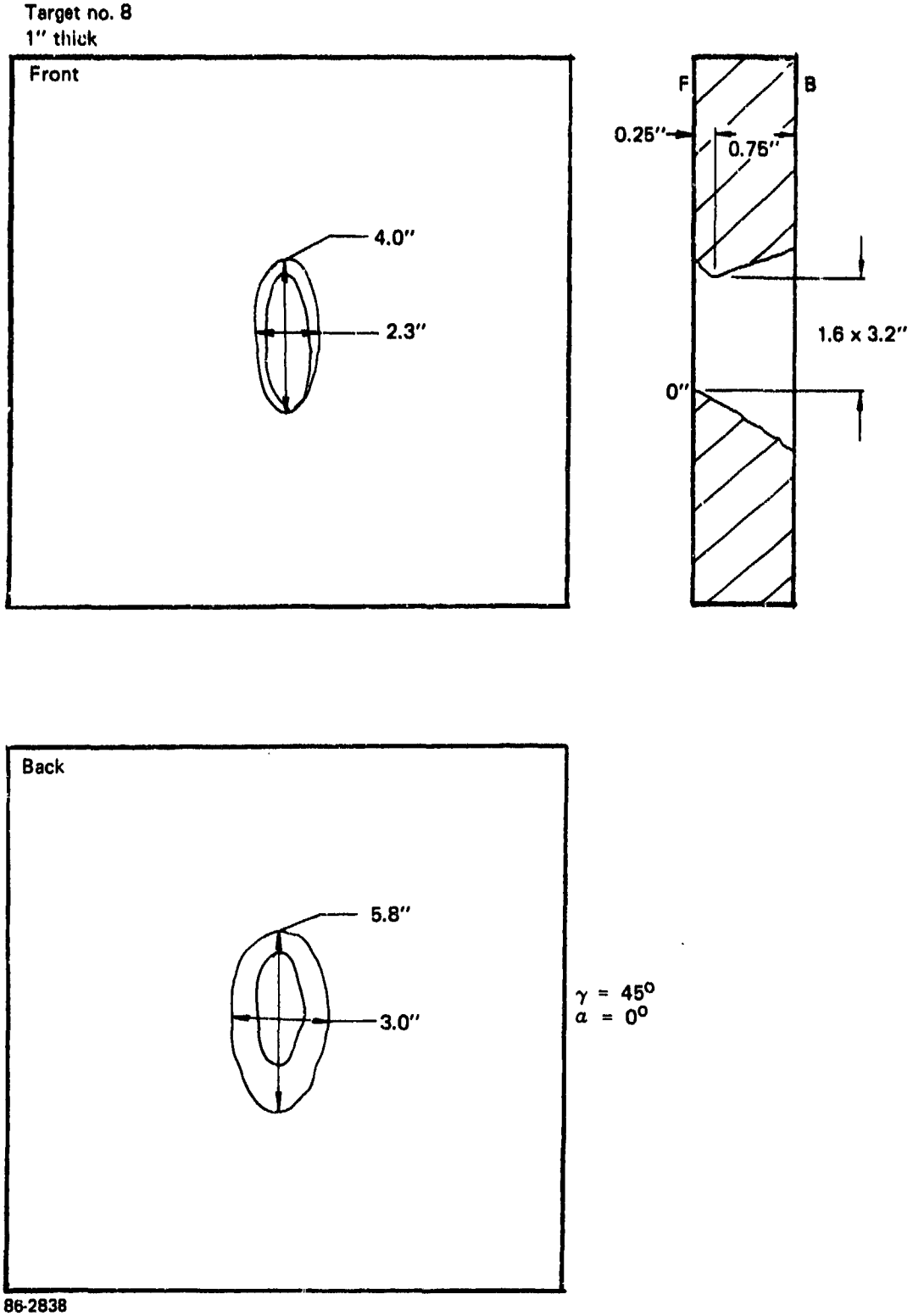

Figure 23 TEST 8 TARGET DATA – OGIVE PROJECTILE

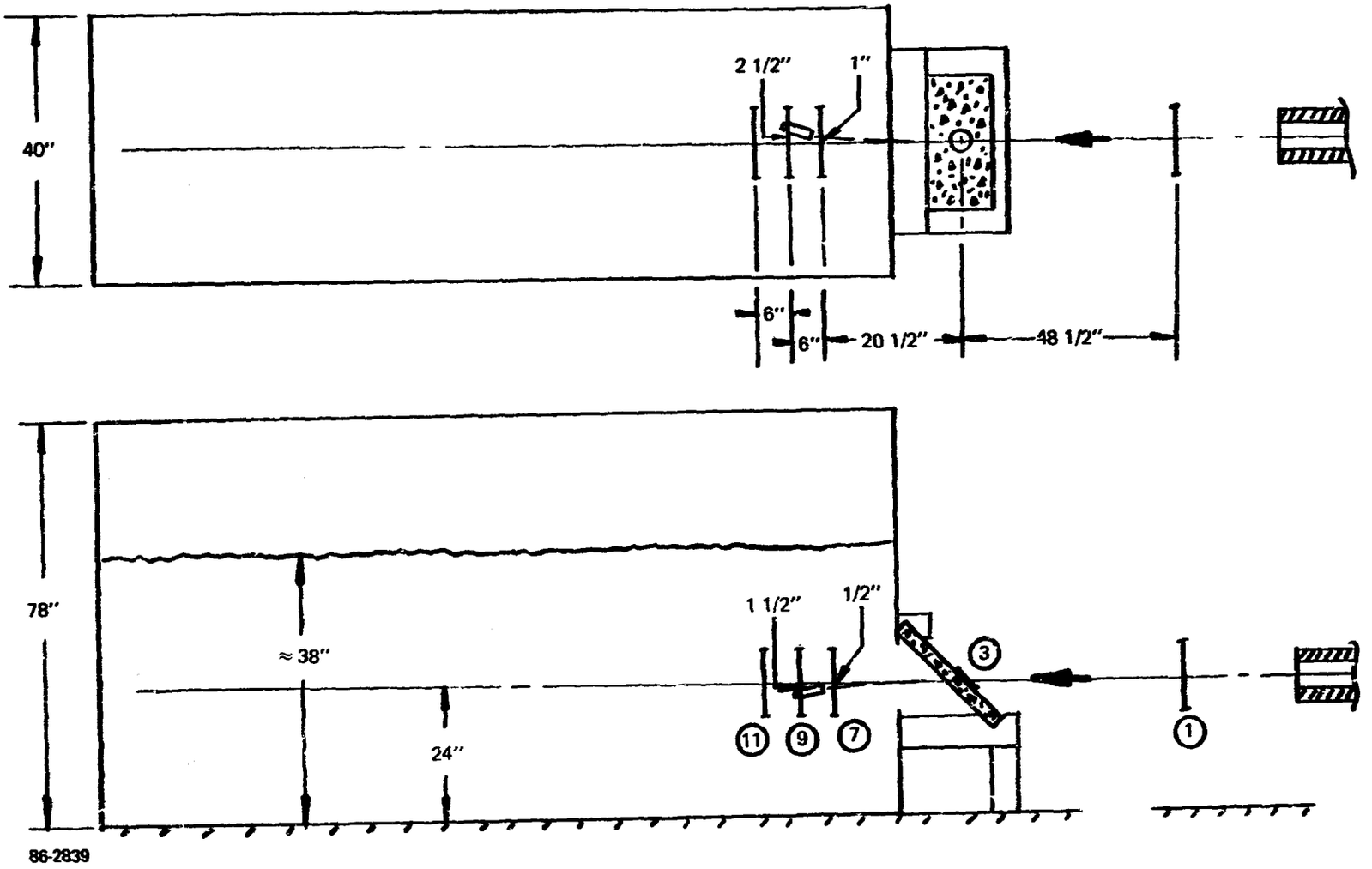

Figure 24 SUBSCALE SST PENETRATION TEST 9, $\gamma = 45^{o}$, $\alpha = 5^{o}$

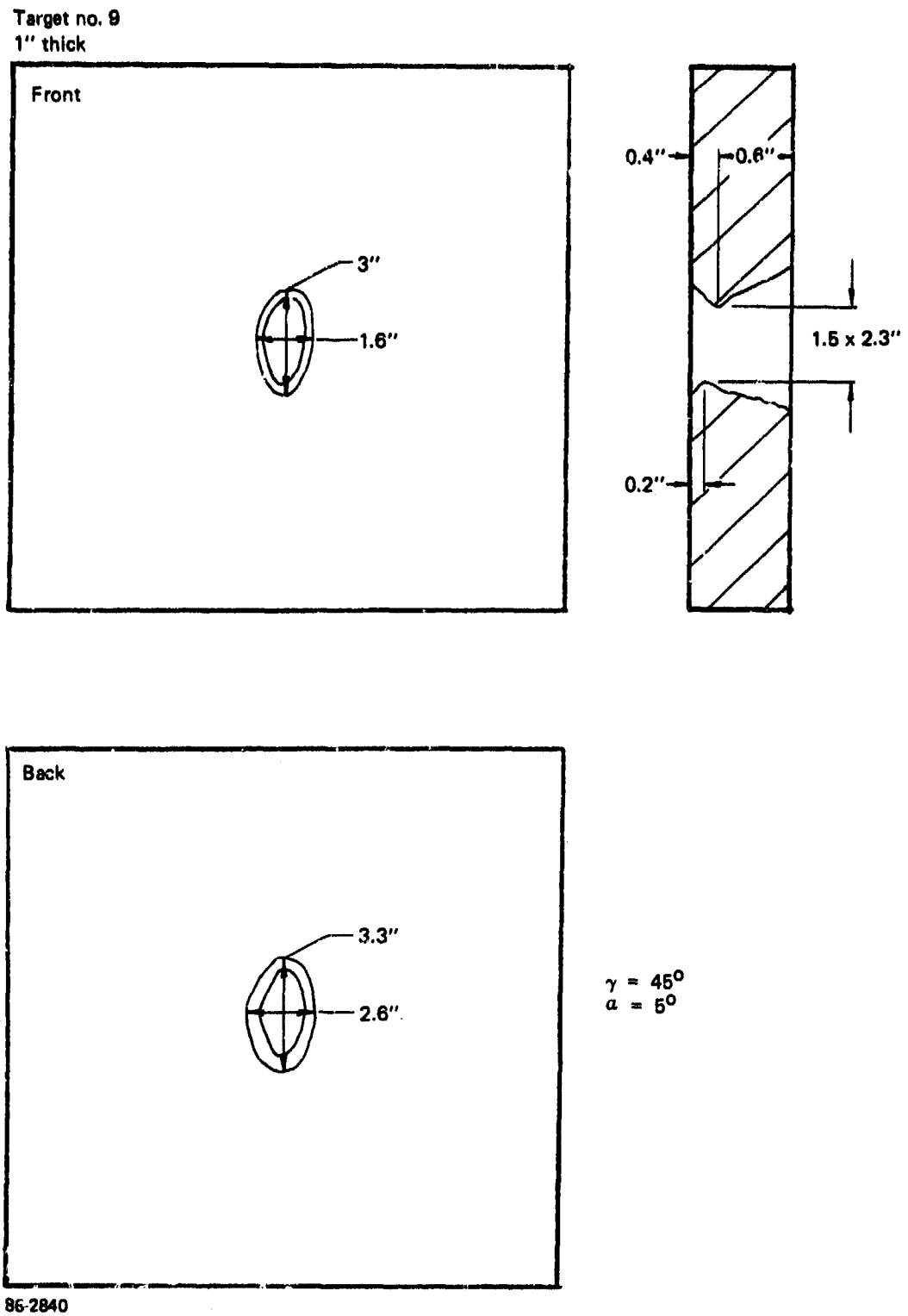

Figure 25 TEST 9 TARGET DATA – SST PROJECTILE

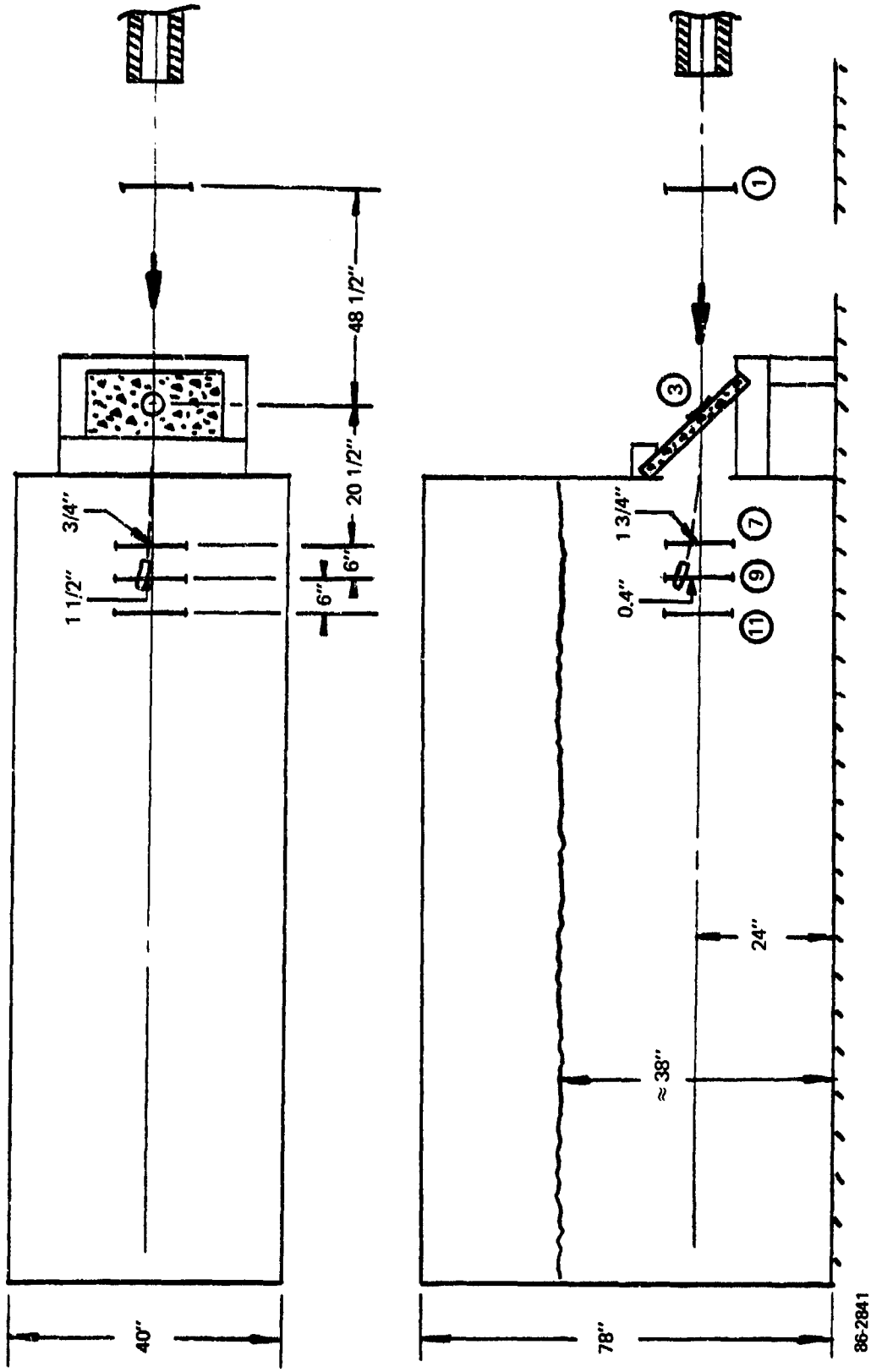

Figure 26 SUBSCALE SST PENETRATION TEST 10, $\gamma = 45^{o}$, $\alpha = 0^{o}$

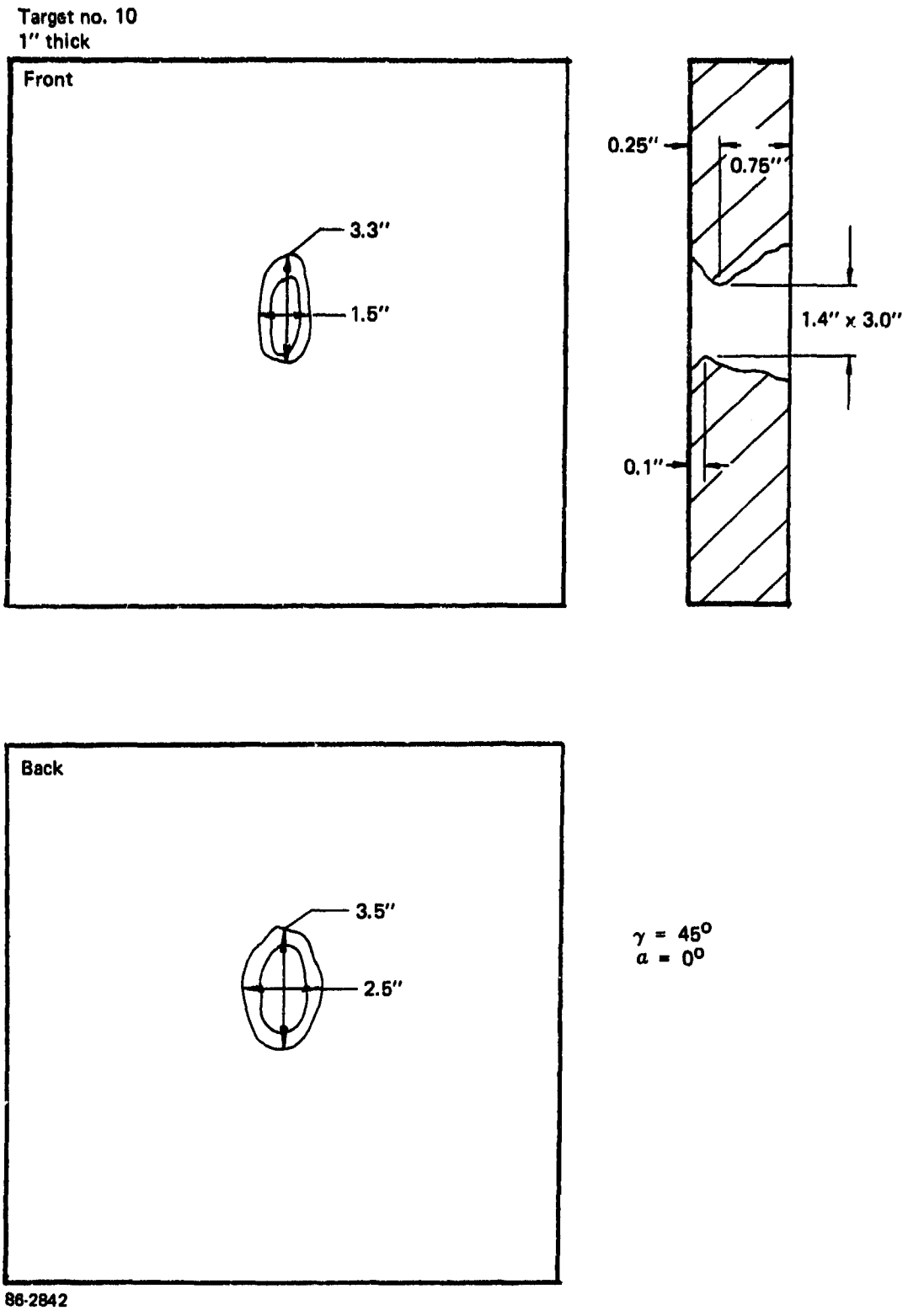

Figure 27 TEST 10 TARGET DATA – SST PROJECTILE

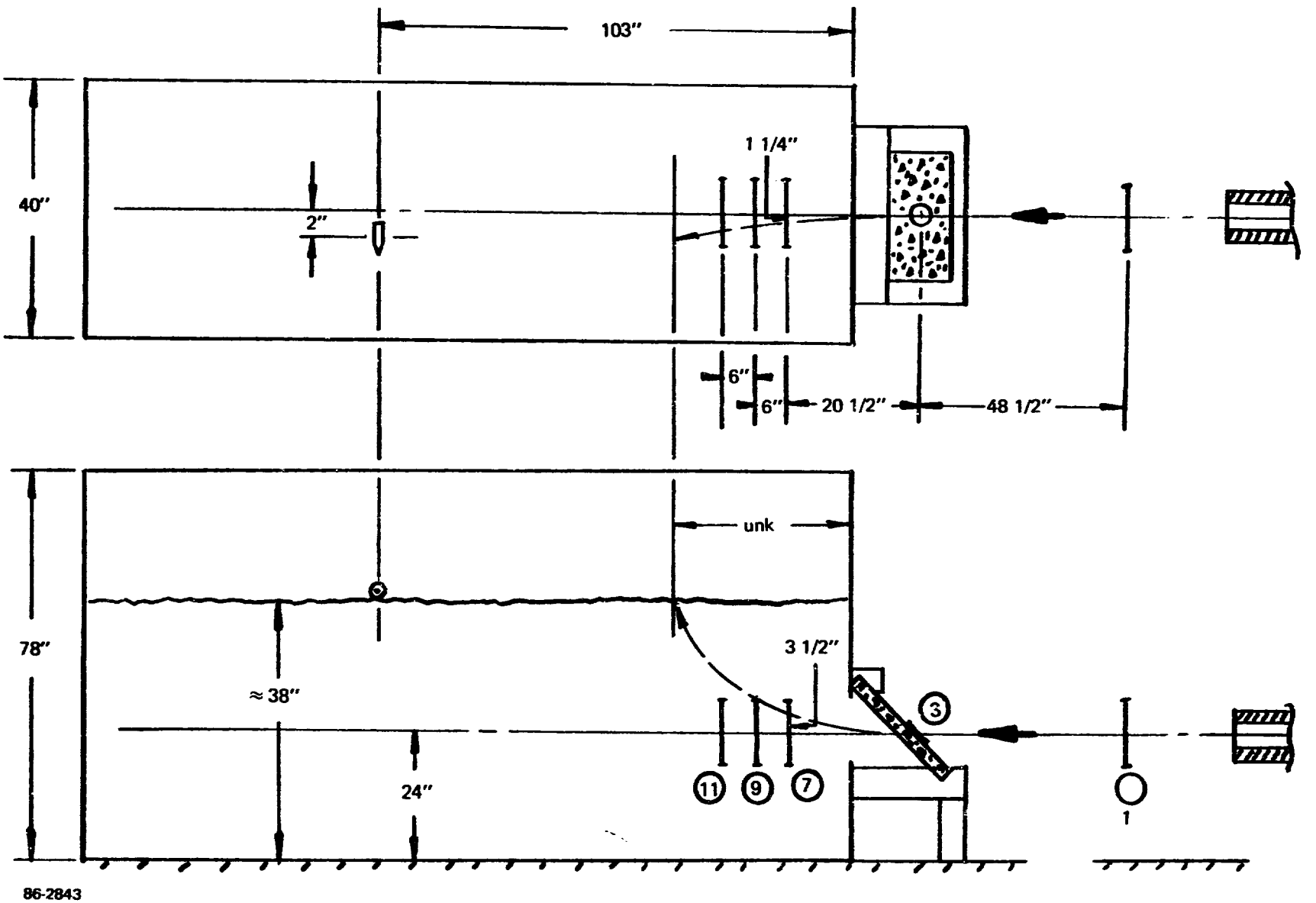

Figure 28 SUBSCALE CONE PENETRATION TEST 11, $\gamma = 45^{o}$, $\alpha = 5^{o}$

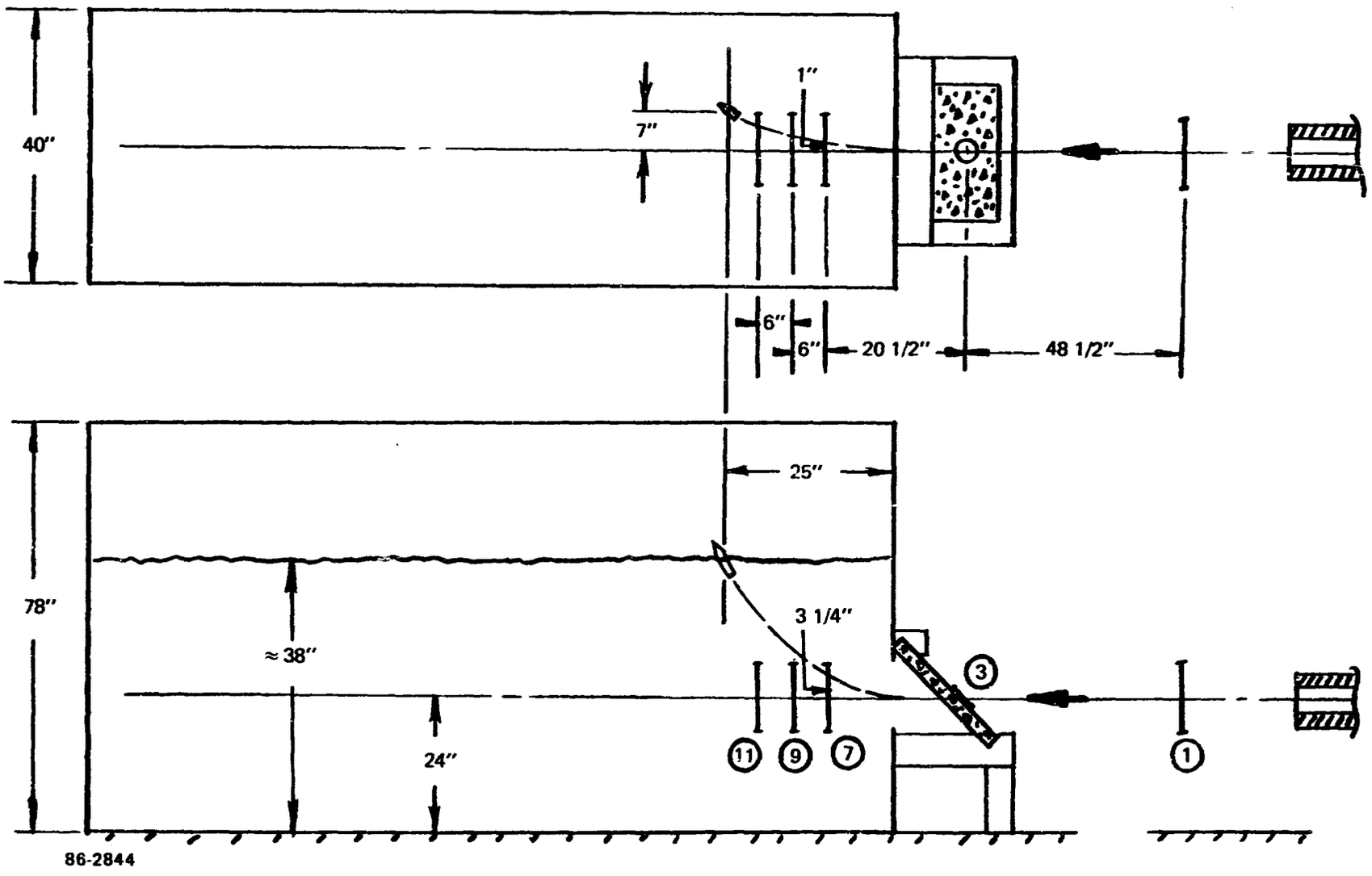

Figure 29 SUBSCALE CONE PENETRATION TEST 12, $\gamma = 45^{o}$, $\alpha = 0^{o}$

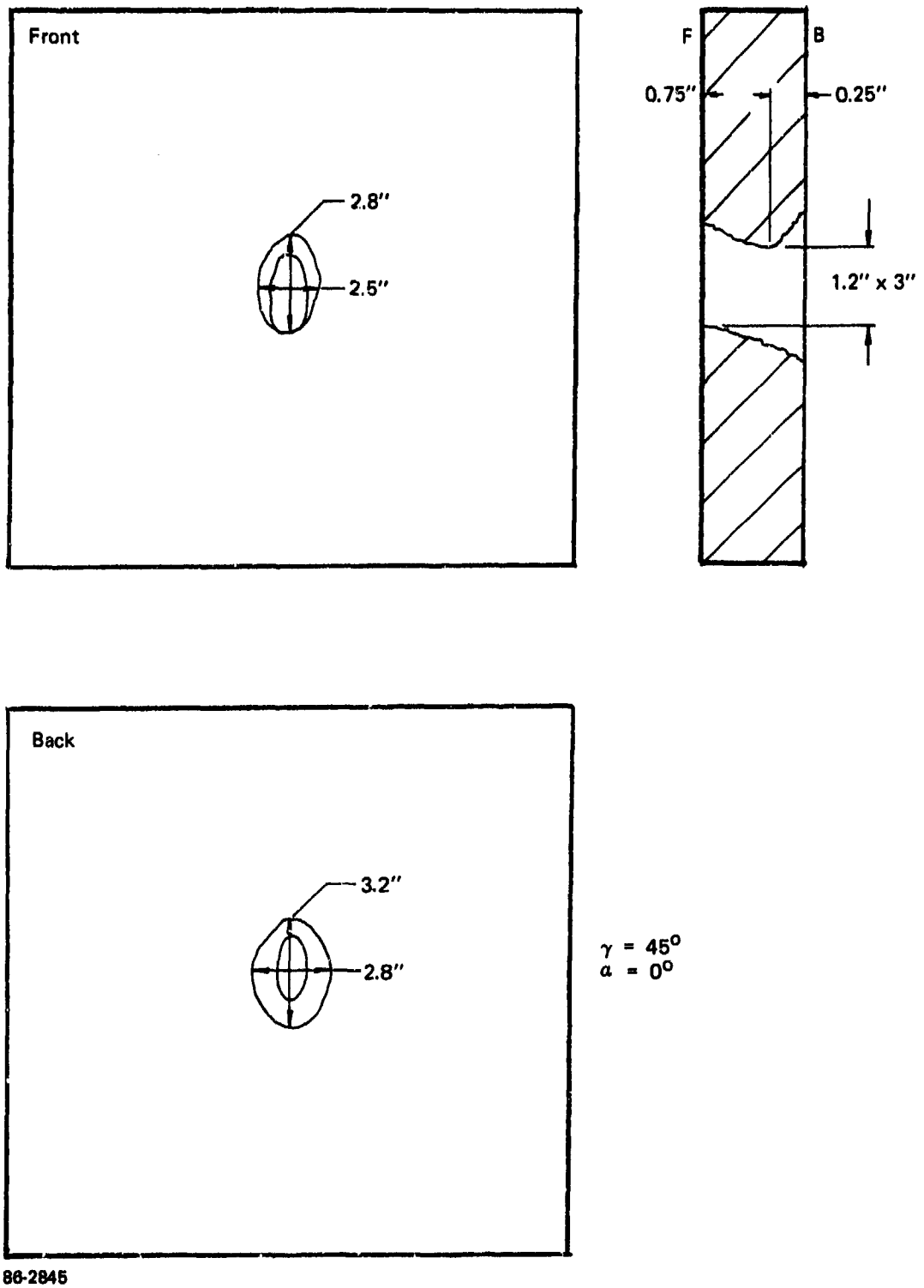

Figure 30 TEST 12 TARGET DATA – CONE PROJECTILE

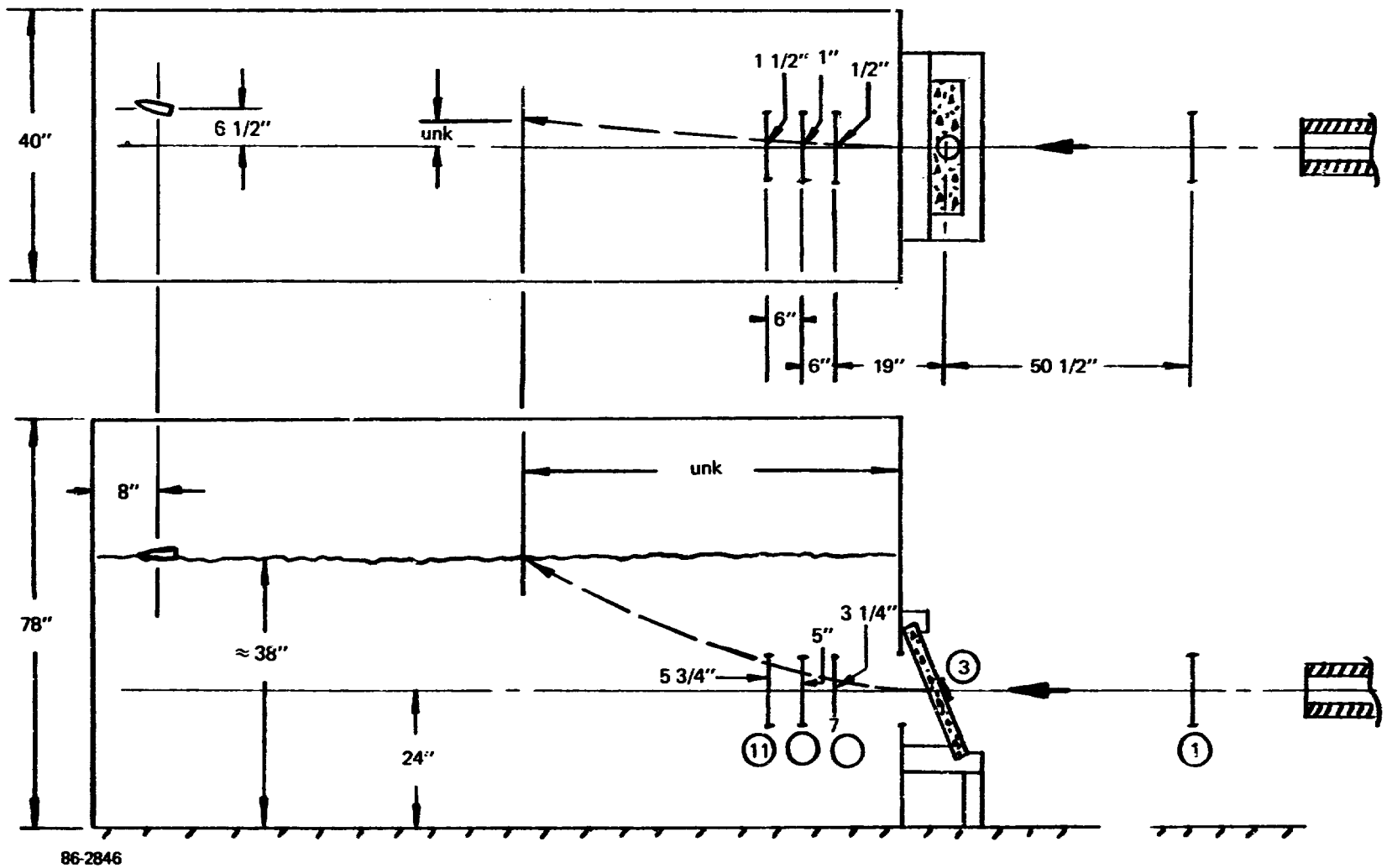

Figure 31 SUBSCALE OGIVE PENETRATION TEST 13, $\gamma = 22\text{-}1/2^{o}$, $\alpha = 5^{o}$

Target no. 13
1" thick

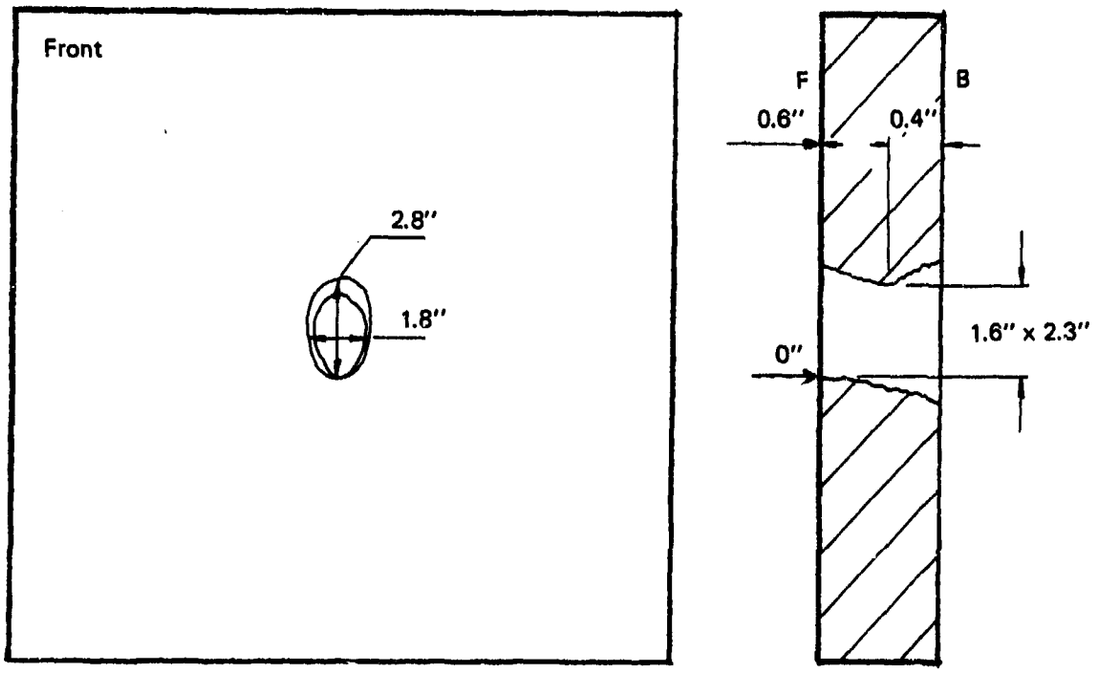

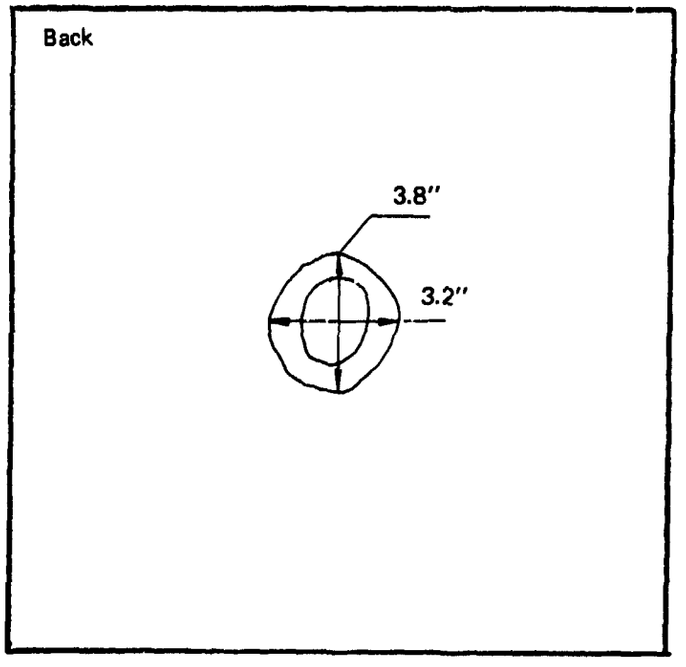

$\gamma = 22\ 1/2^{o}$
$a = 5^{o}$

86-2847

Figure 32 TEST 13 TARGET DATA

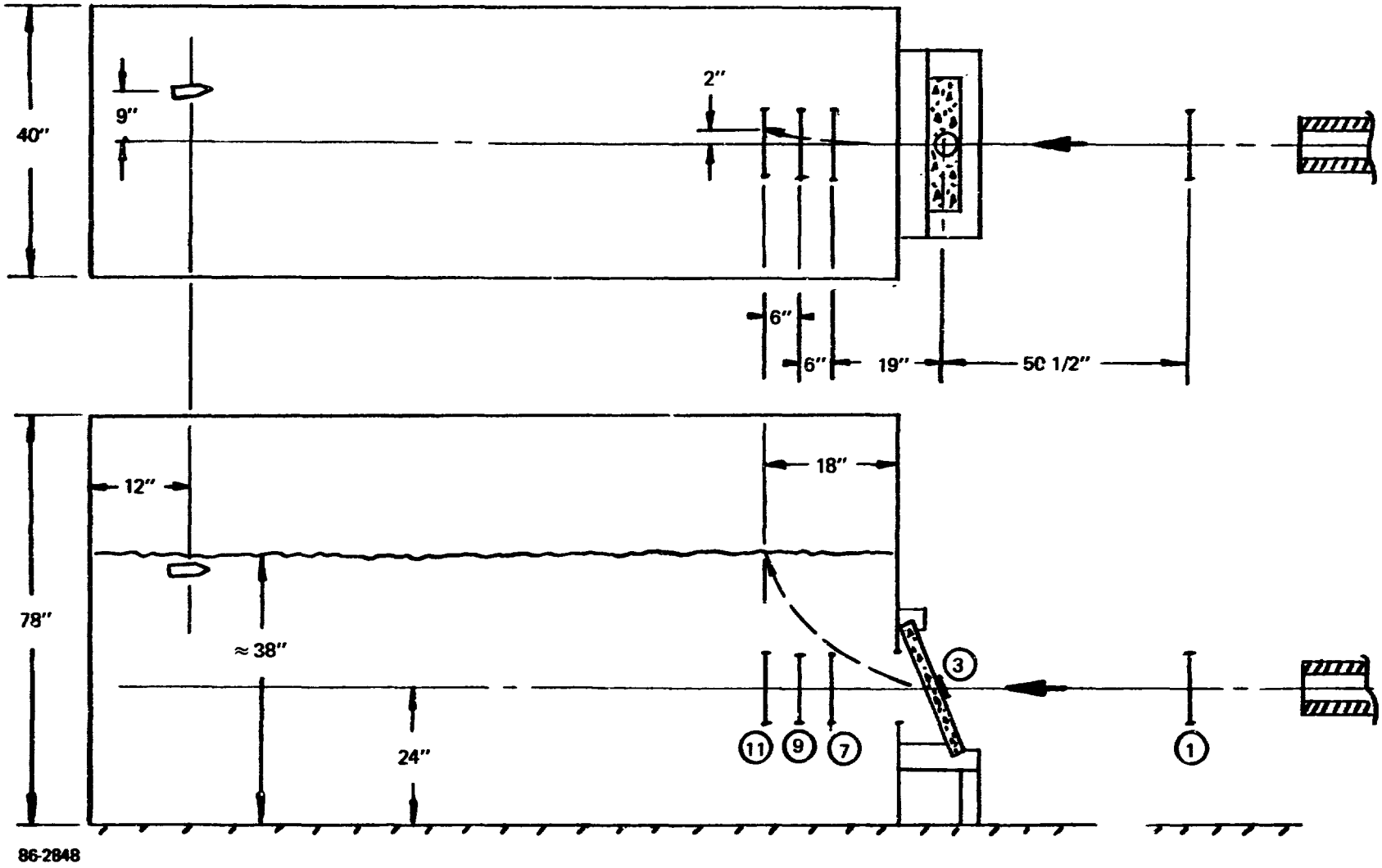

Figure 33 SUBSCALE CONE PENETRATION TEST 14, $\gamma = 22\text{-}1/2^{o}$, $\alpha = 5^{o}$

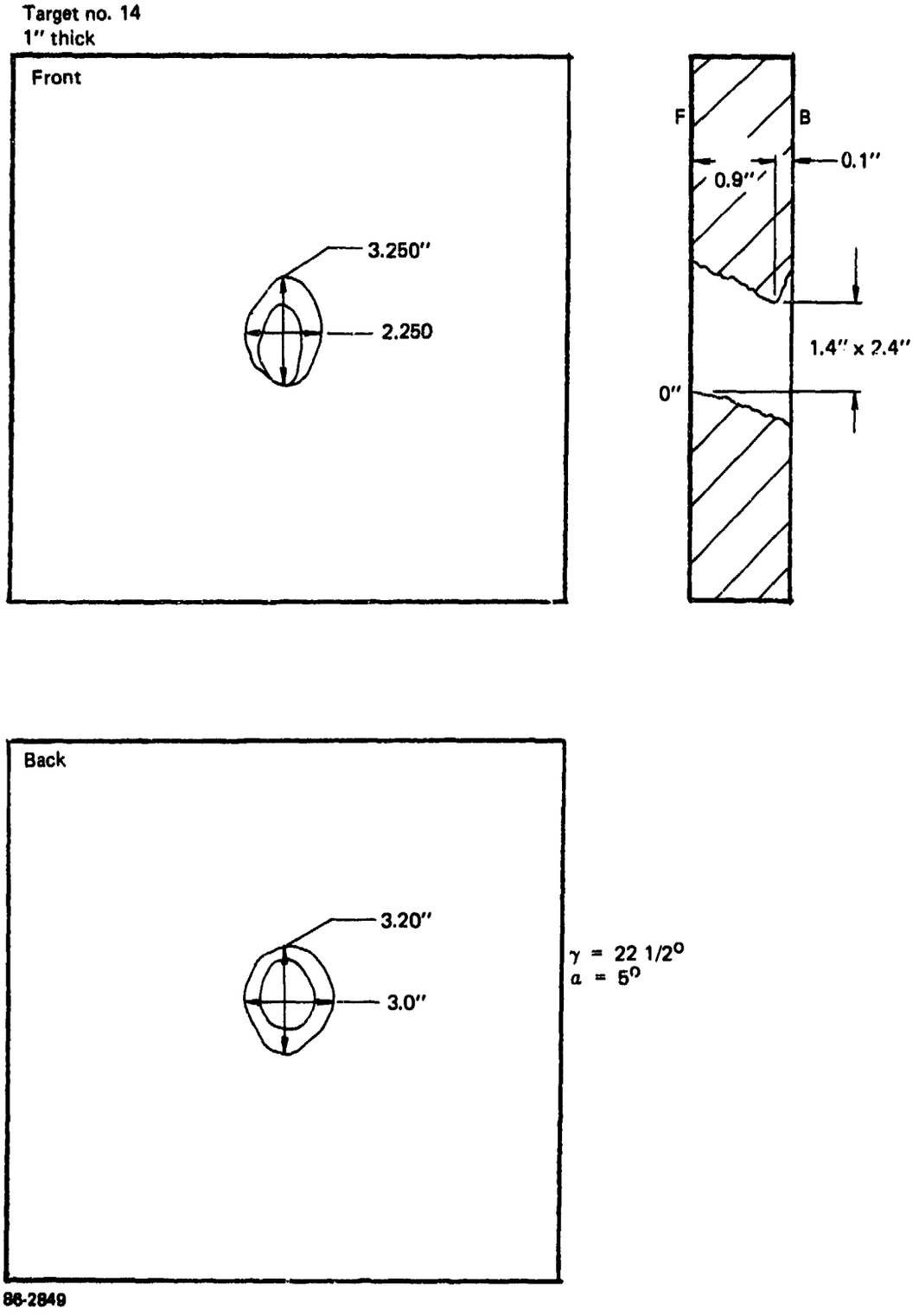

Figure 34 TEST 14 TARGET DATA – CONE PROJECTILE

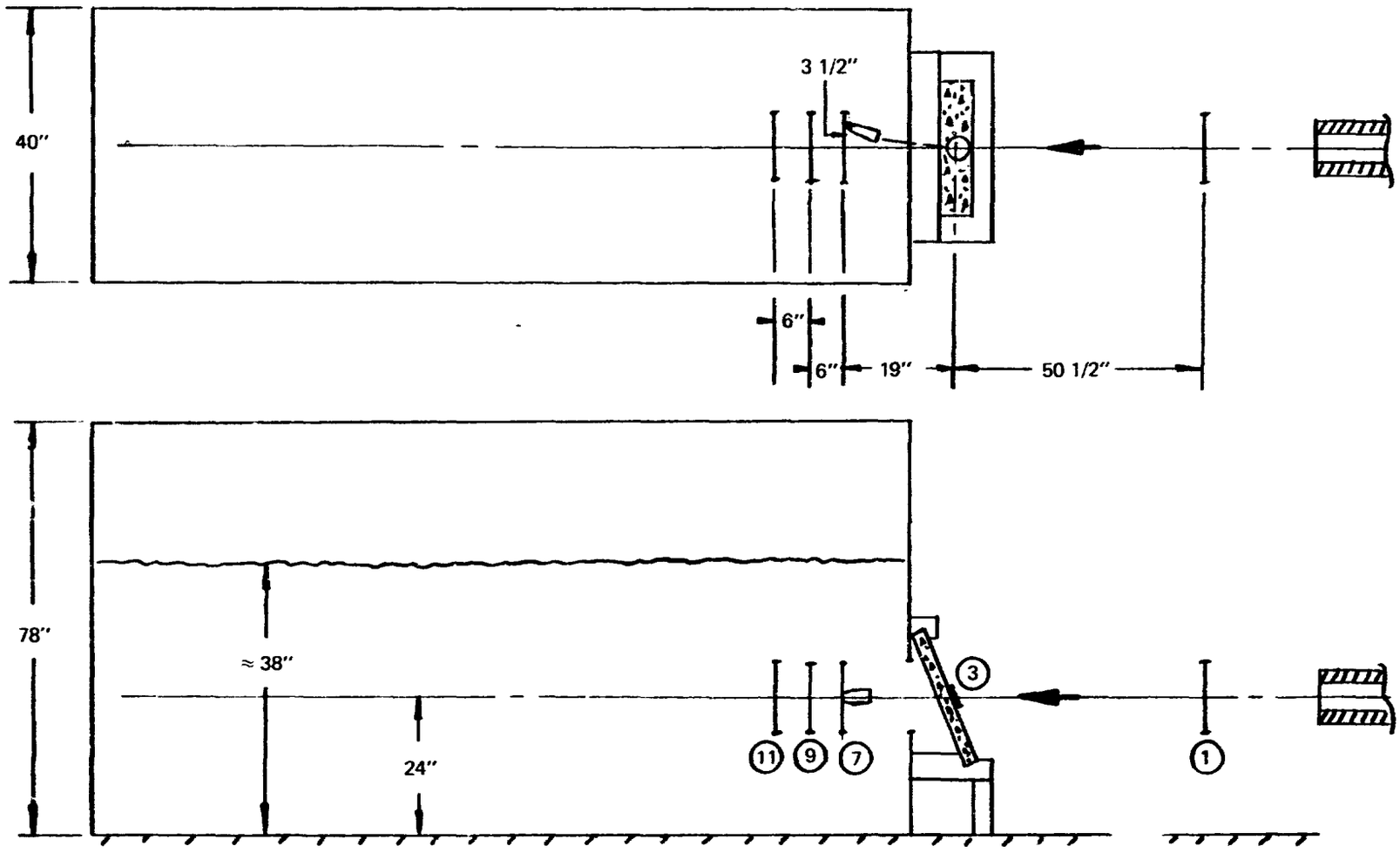

86-2850

Figure 35 SUBSCALE SST PENETRATION TEST 15, γ = 22-1/2°, α = 5°

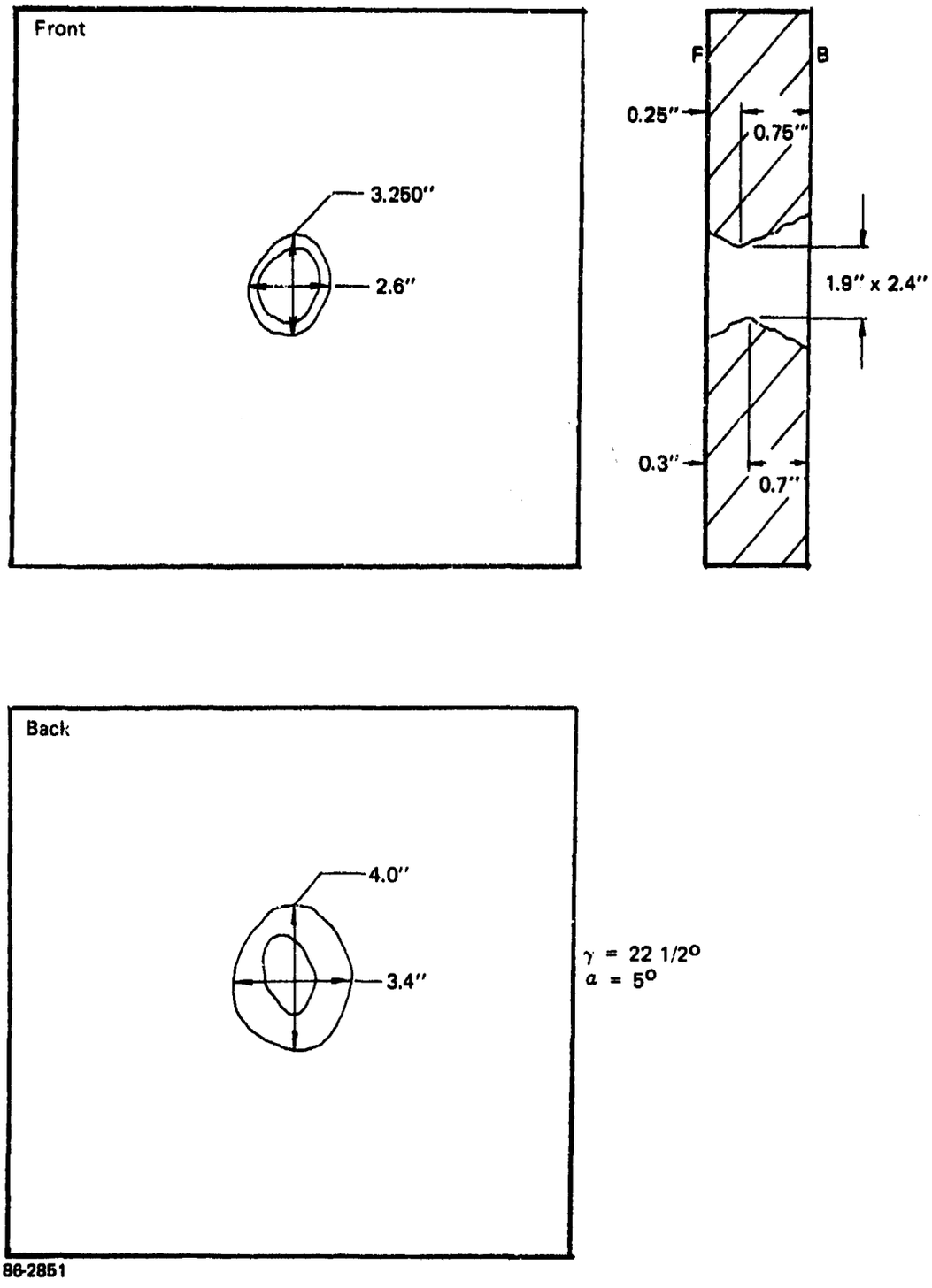

Figure 36 TEST 15 TARGET DATA – SST PROJECTILE

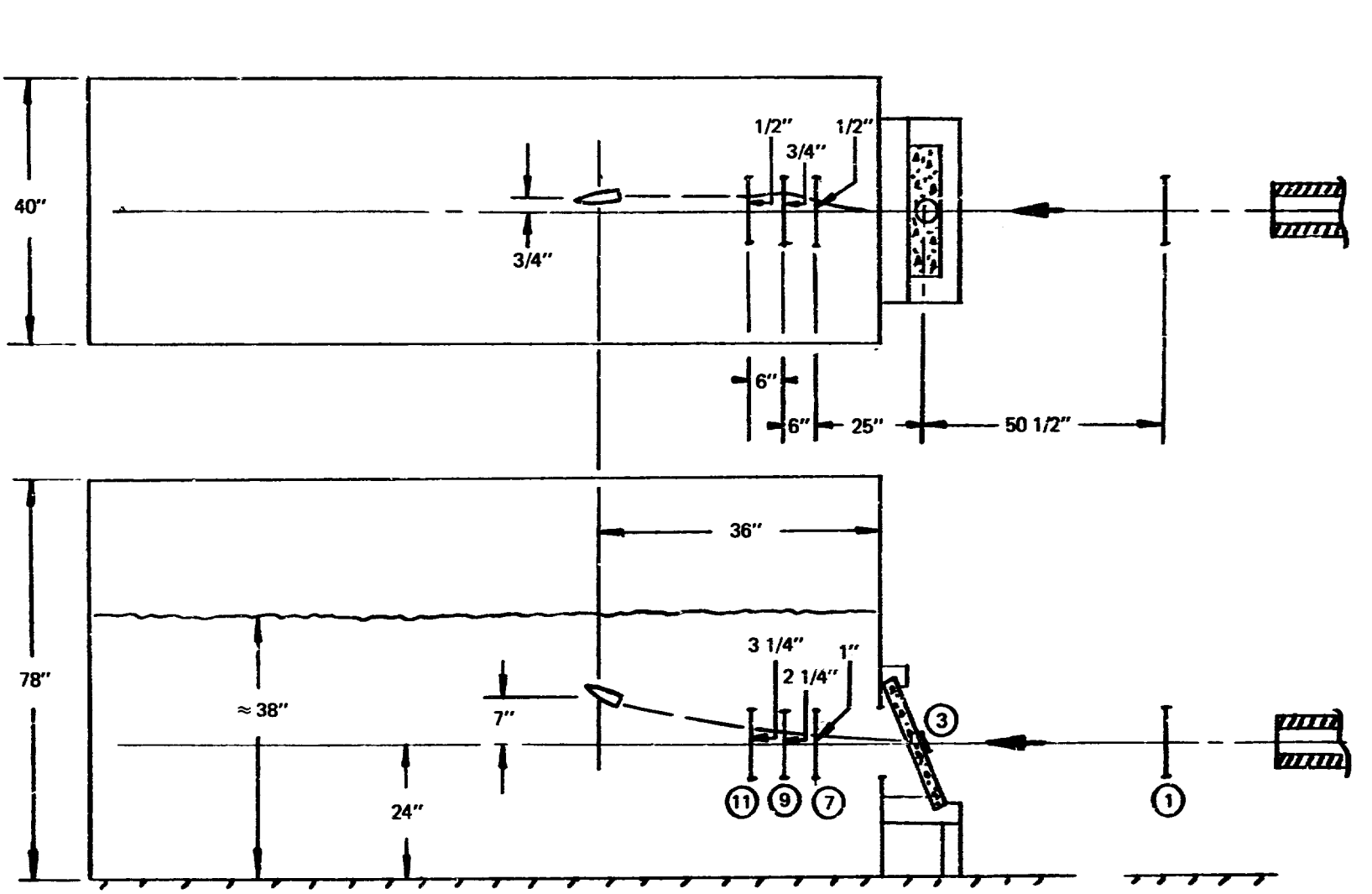

86-2852

Figure 37 SUBSCALE OGIVE PENETRATION TEST 16, γ = 22-1/2°, α = 2-1/2°

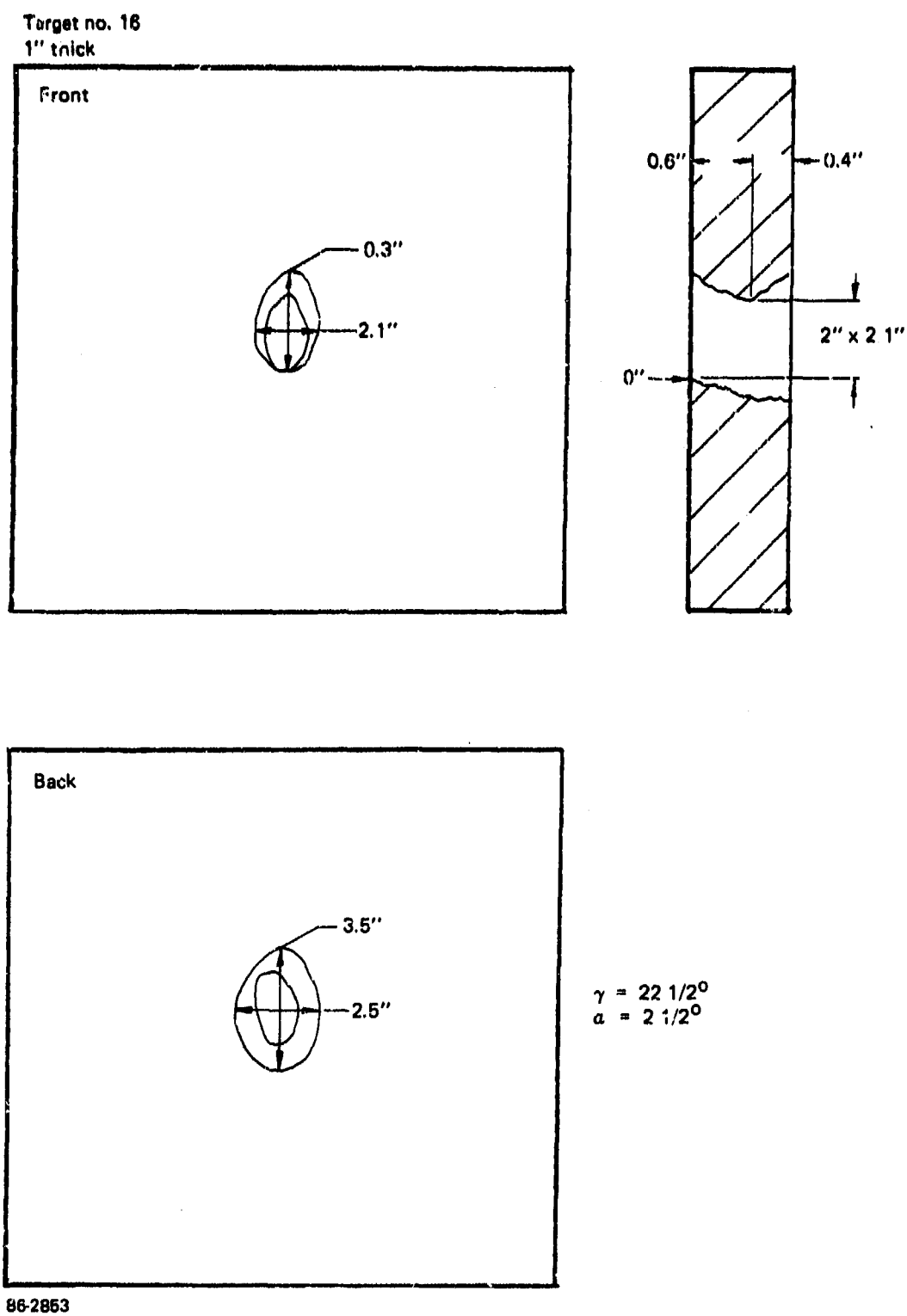

Figure 38 TEST 16 TARGET DATA – OGIVE PROJECTILE

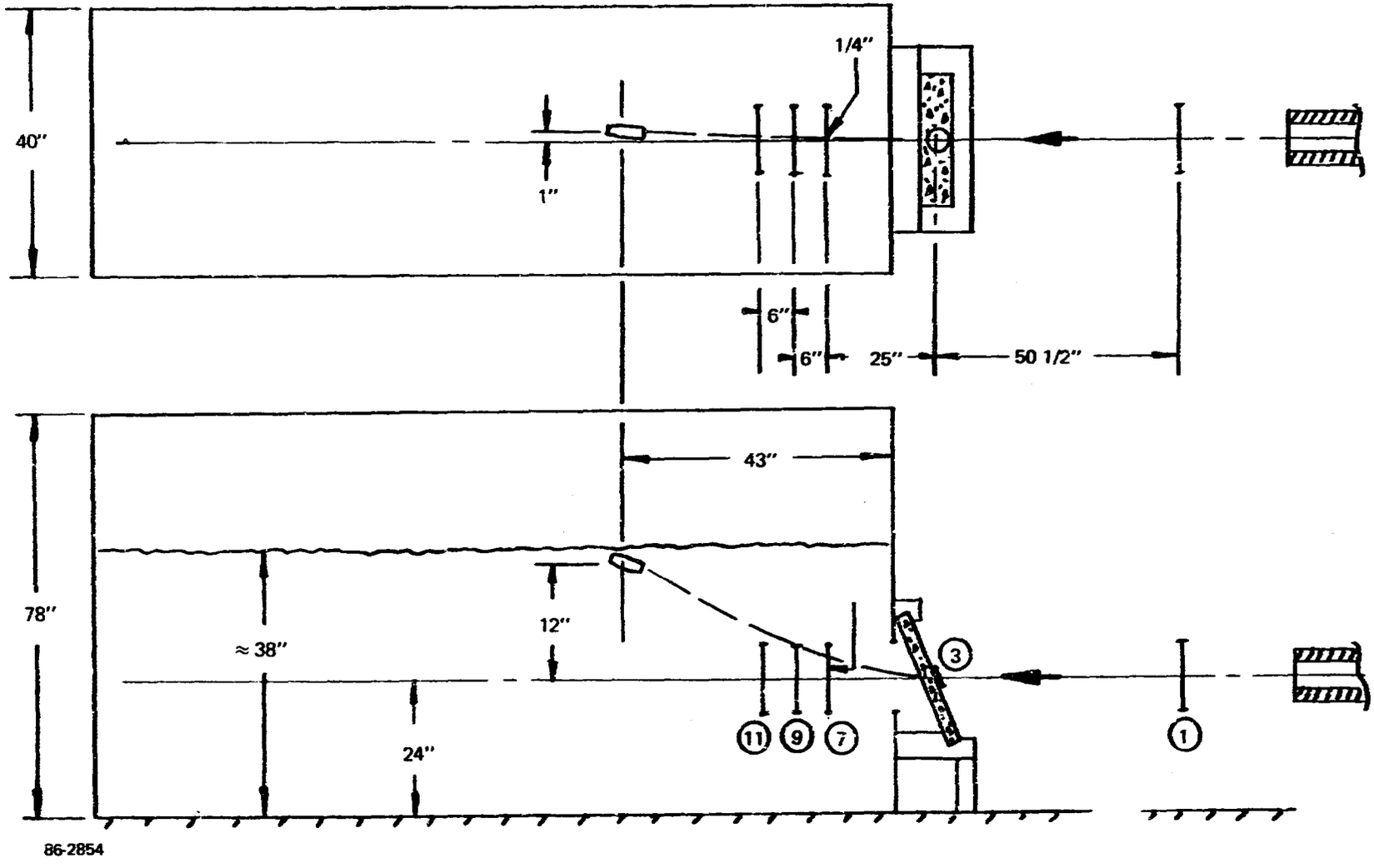

Figure 39 SUBSCALE SST PENETRATION TEST 17, $\gamma = 22\text{-}1/2^{o}$, $\alpha = 2\text{-}1/2^{o}$

Target no. 17
1" thick

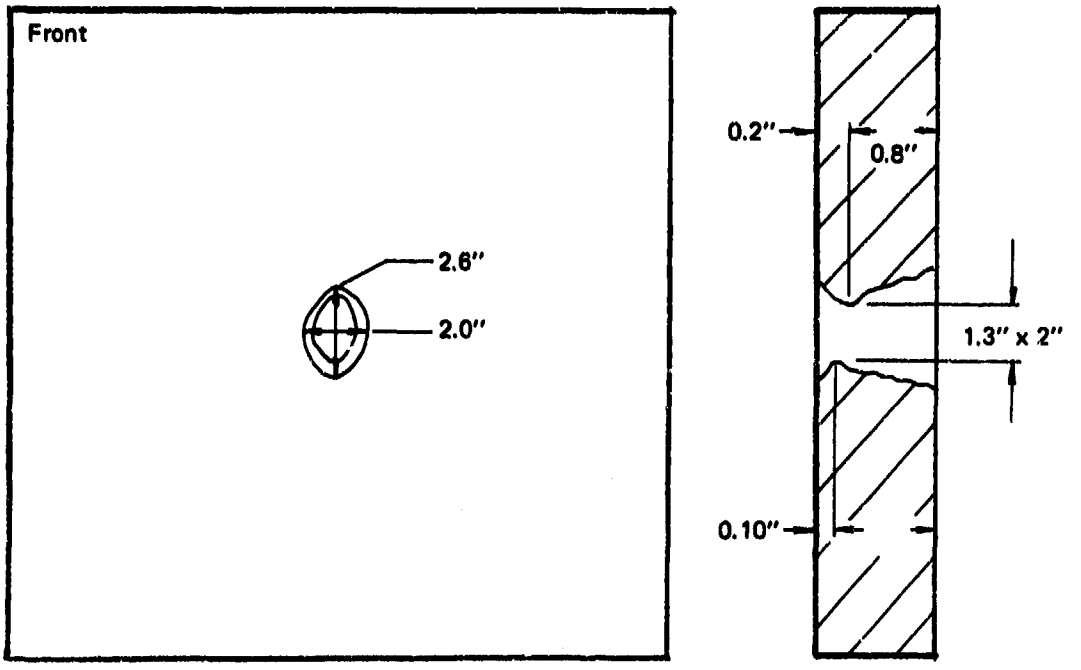

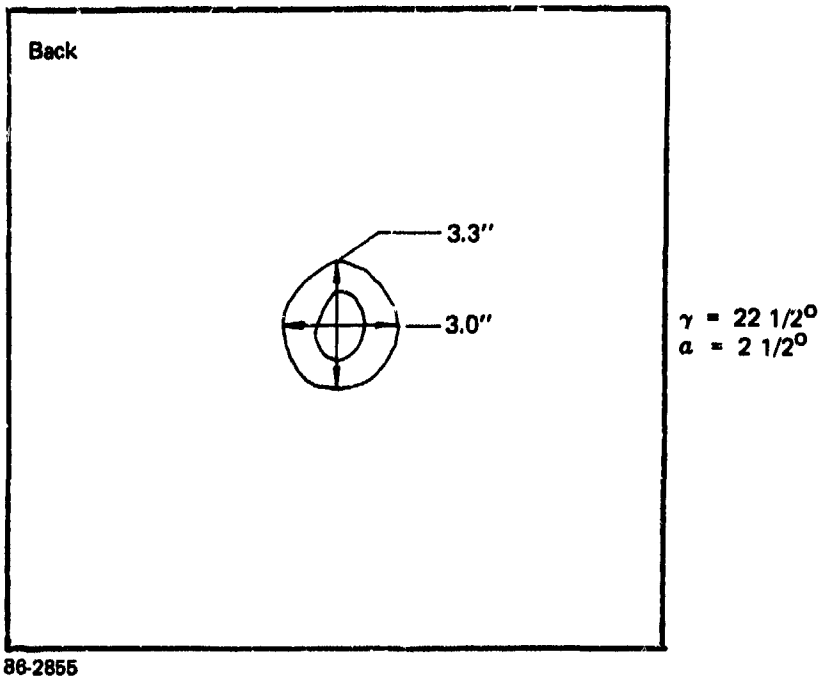

γ = 22 1/2°
α = 2 1/2°

86-2855

Figure 40 TEST 17 TARGET DATA – SST PROJECTILE

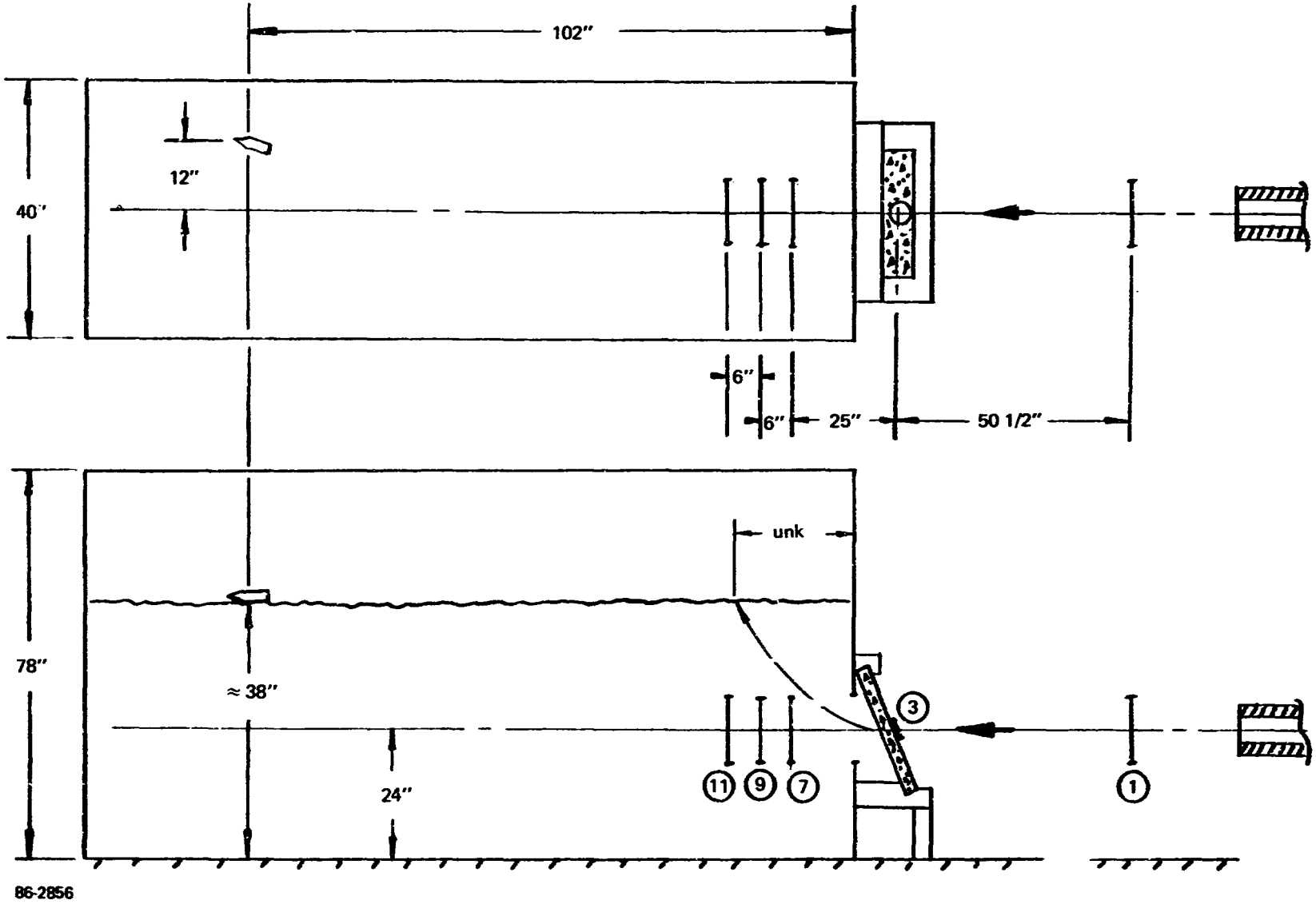

Figure 41 SUBSCALE CONE PENETRATION TEST 18, γ = 22-1/2°, α = 2-1/2°

Target no. 18
1" thick

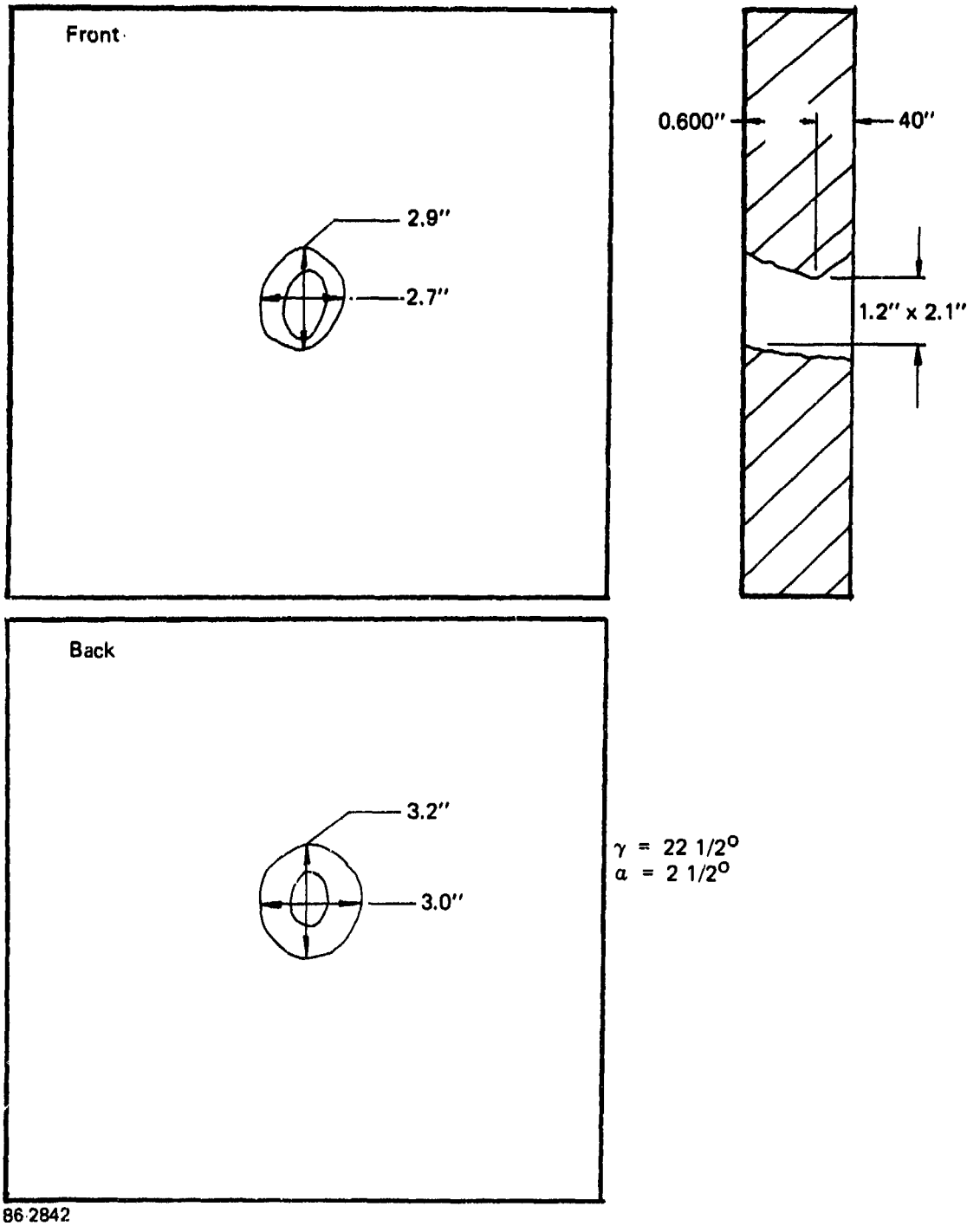

Figure 42 TEST 18 TARGET DATA – CONE PENETRATION

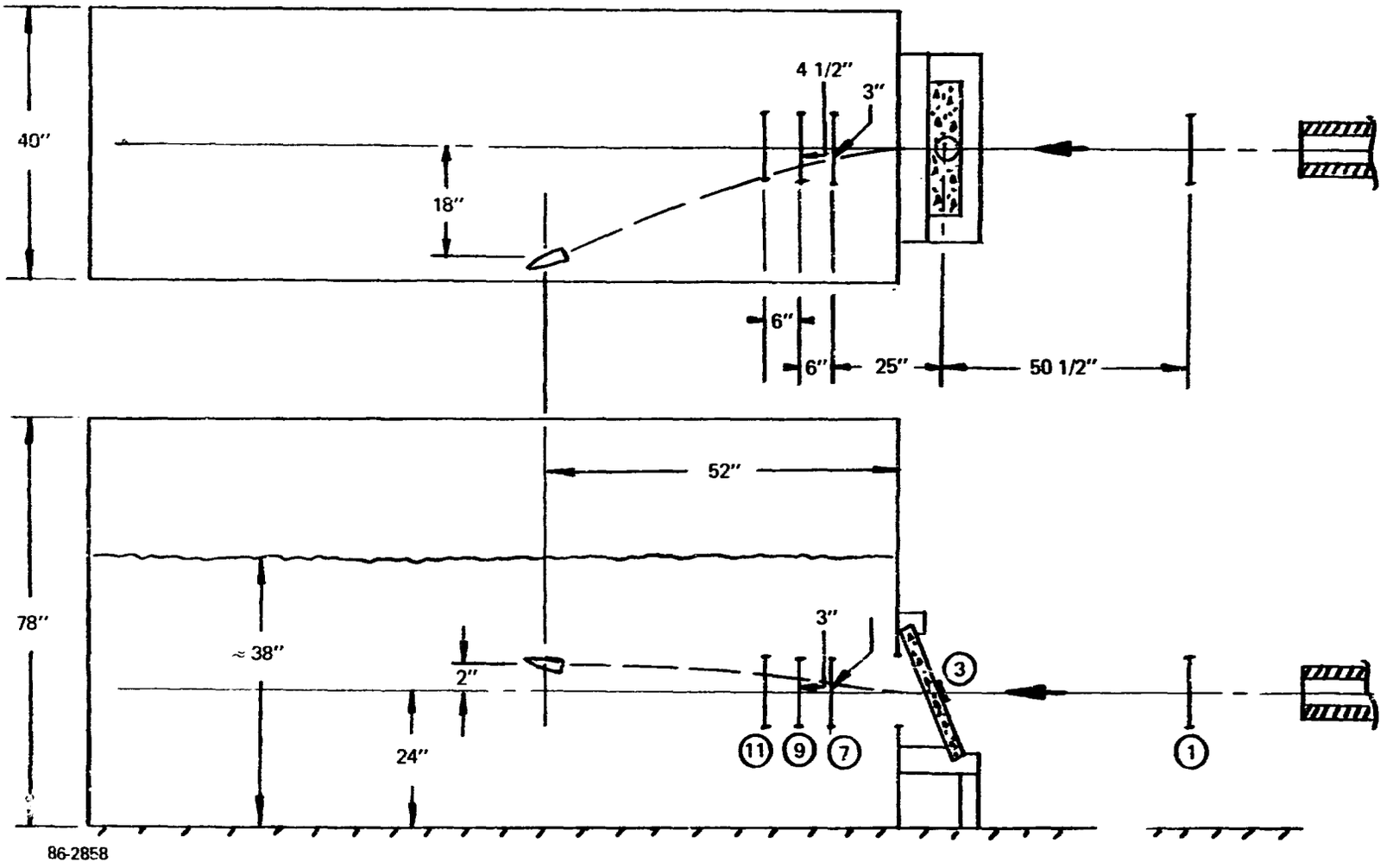

Figure 43 SUBSCALE OGIVE PENETRATION TEST 19, $\gamma = 22\text{-}1/2^{o}$, $\alpha = 0^{o}$

Target no. 19
1" thick

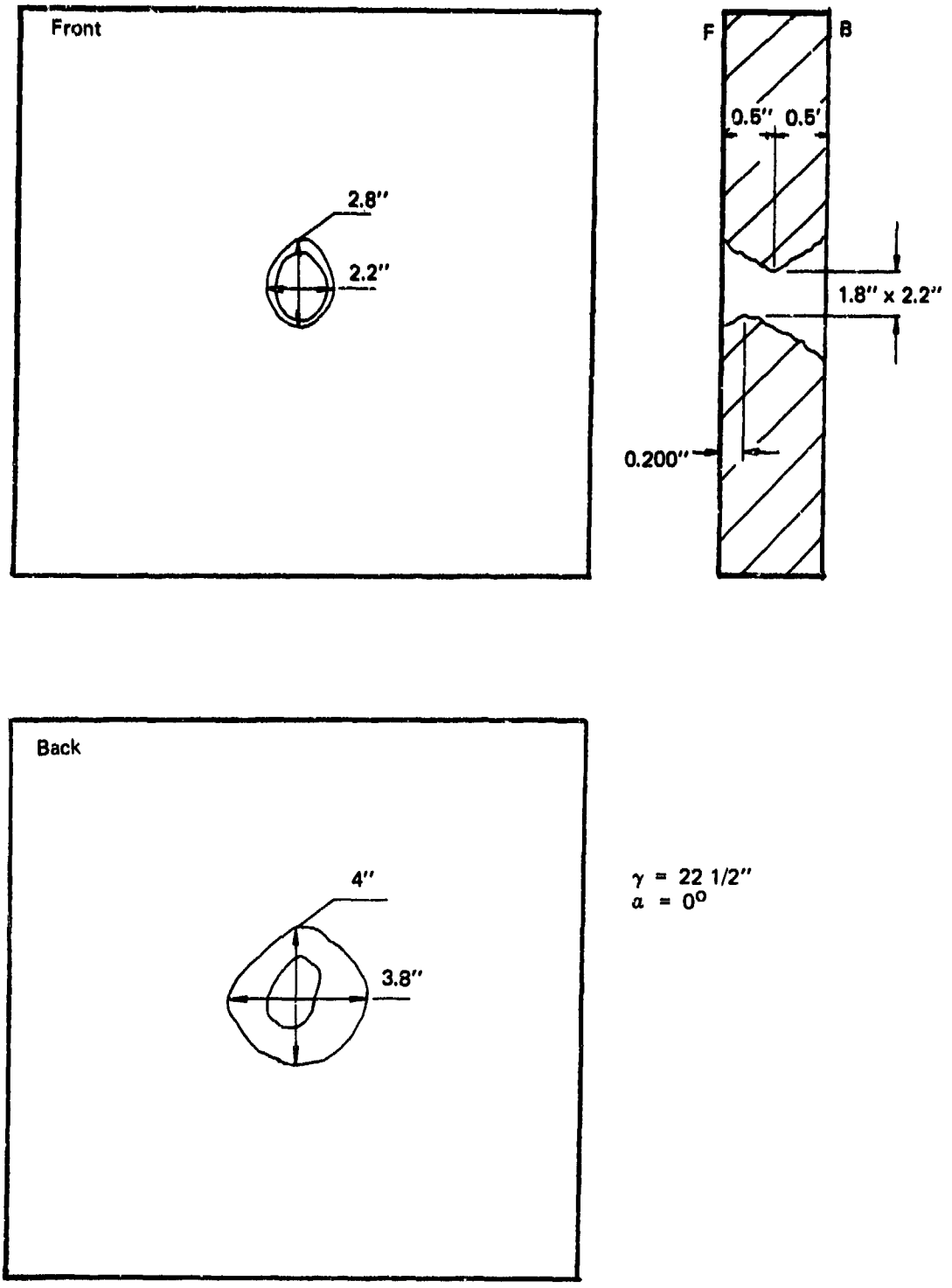

Figure 44 TEST 19 TARGET DATA – OGIVE PROJECTILE

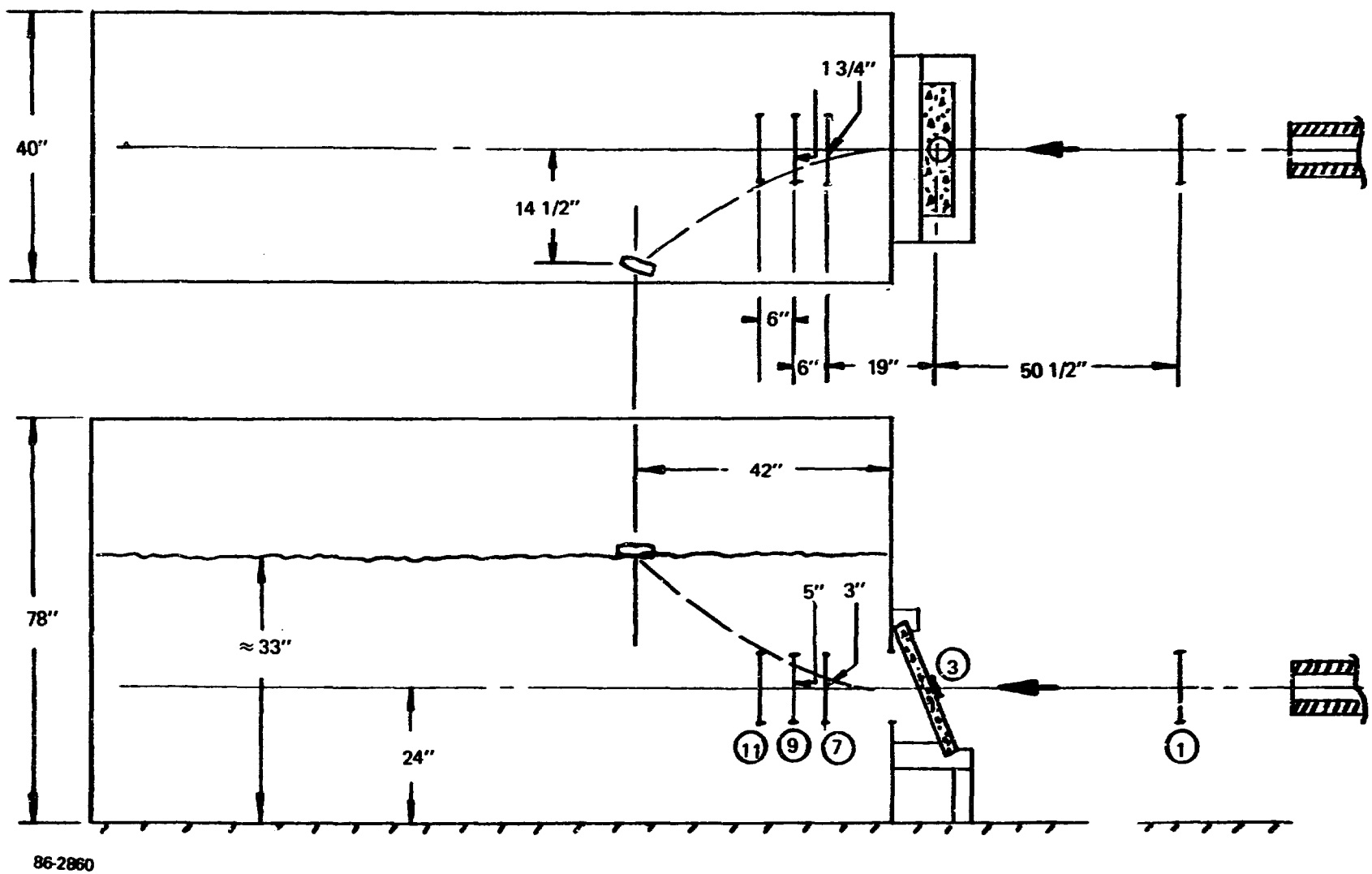

Figure 45 SUBSCALE SST PENETRATION TEST 20A, γ = 22-1/2^{o}, α 0^{o}

Target no. 20A
1" thick

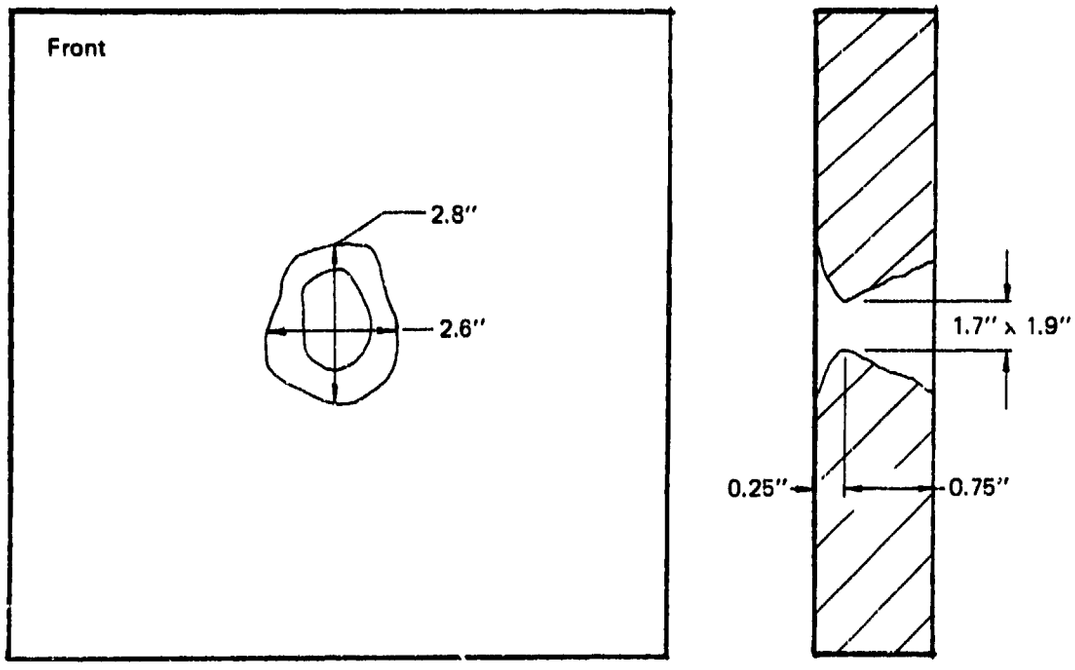

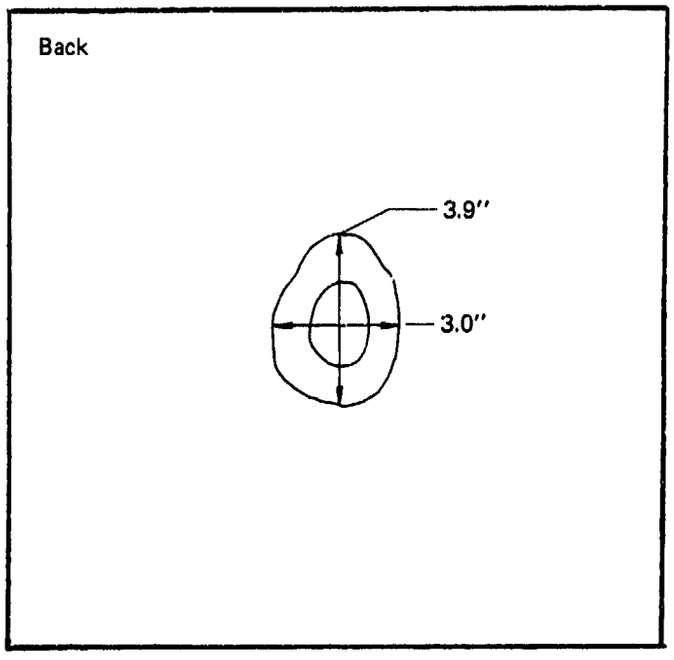

$\gamma = 22\ 1/2^{o}$
$a = 0^{o}$

86-2861

Figure 46 TEST 20A TARGET DATA – SST PROJECTILE

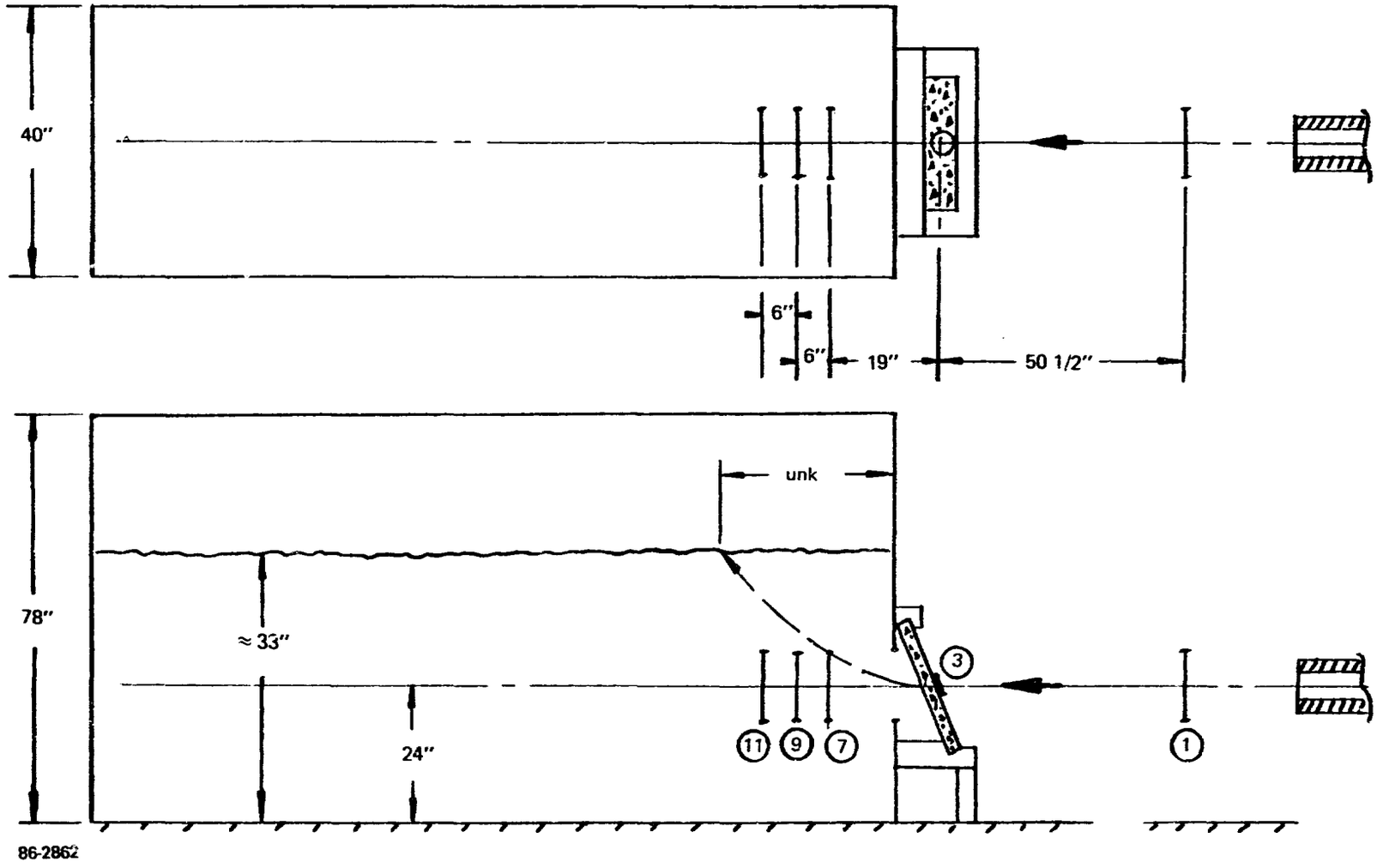

Figure 47 SUBSCALE CONE PENETRATION TEST 21, γ = 22-1/2°, α = 0°

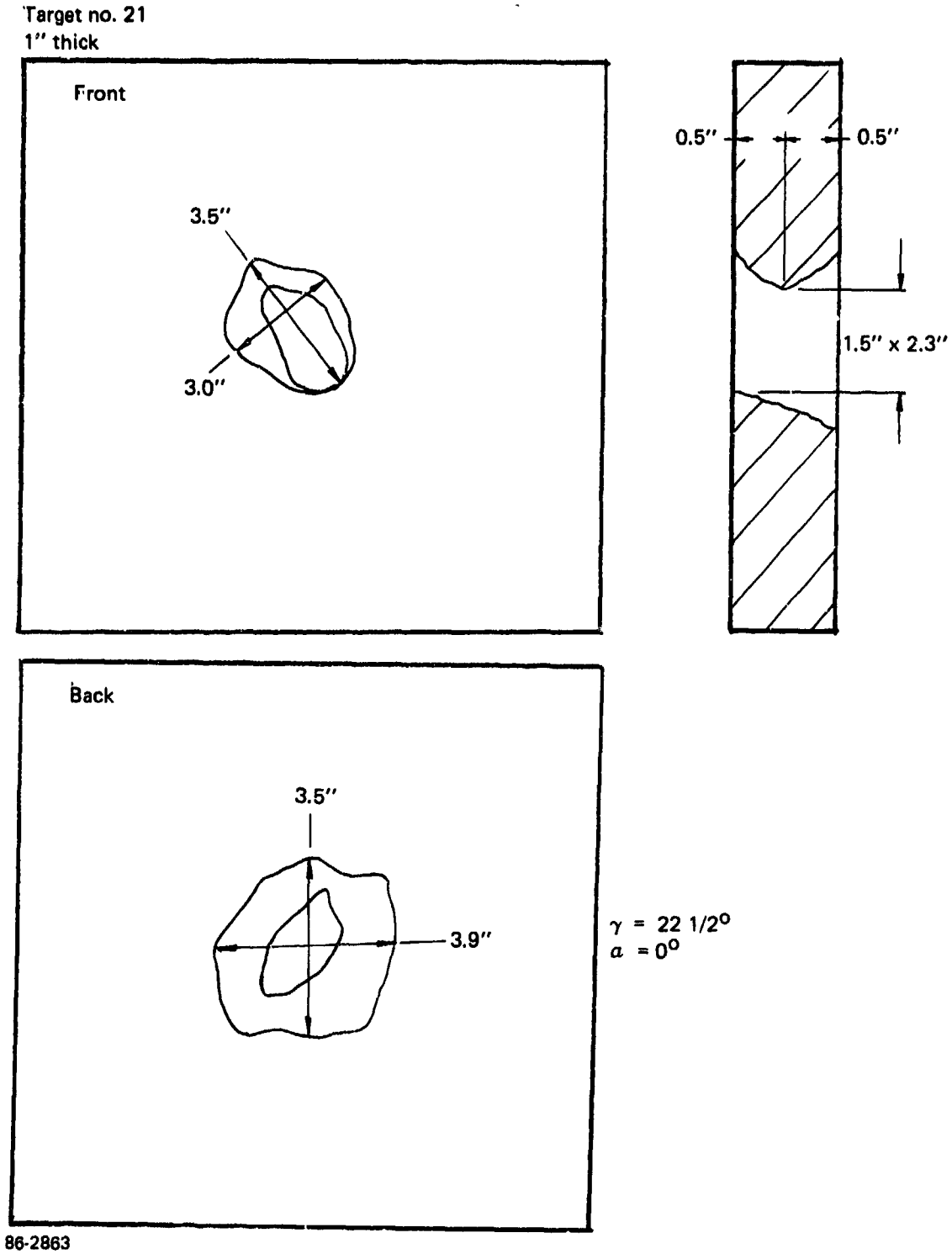

Figure 48 TEST 21 TARGET DATA – CONE PROJECTILE

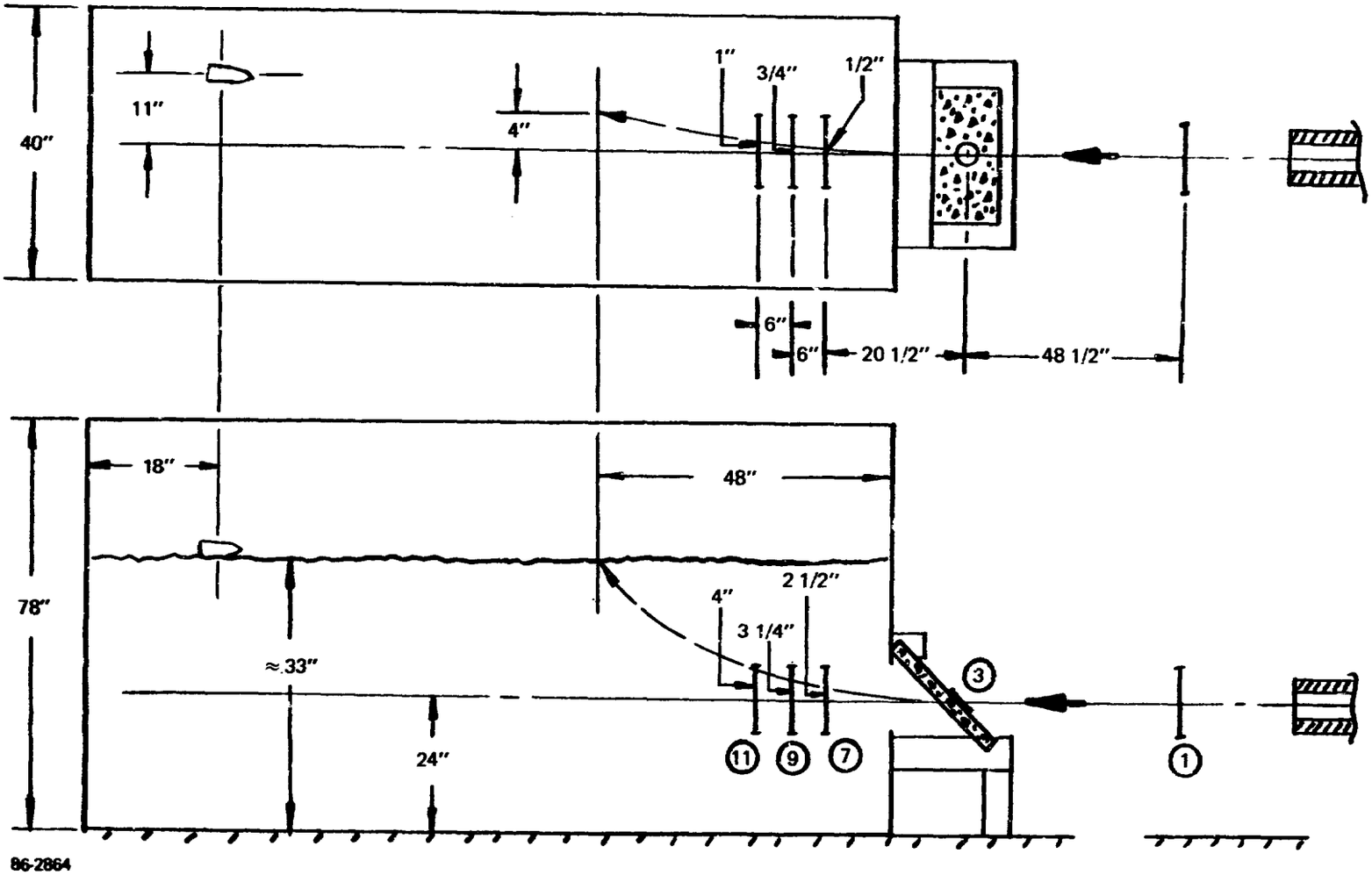

Figure 49 SUBSCALE OGIVE PENETRATION TEST 22, $\gamma = 45^{o}$, $\alpha = 2\text{-}1/2^{o}$

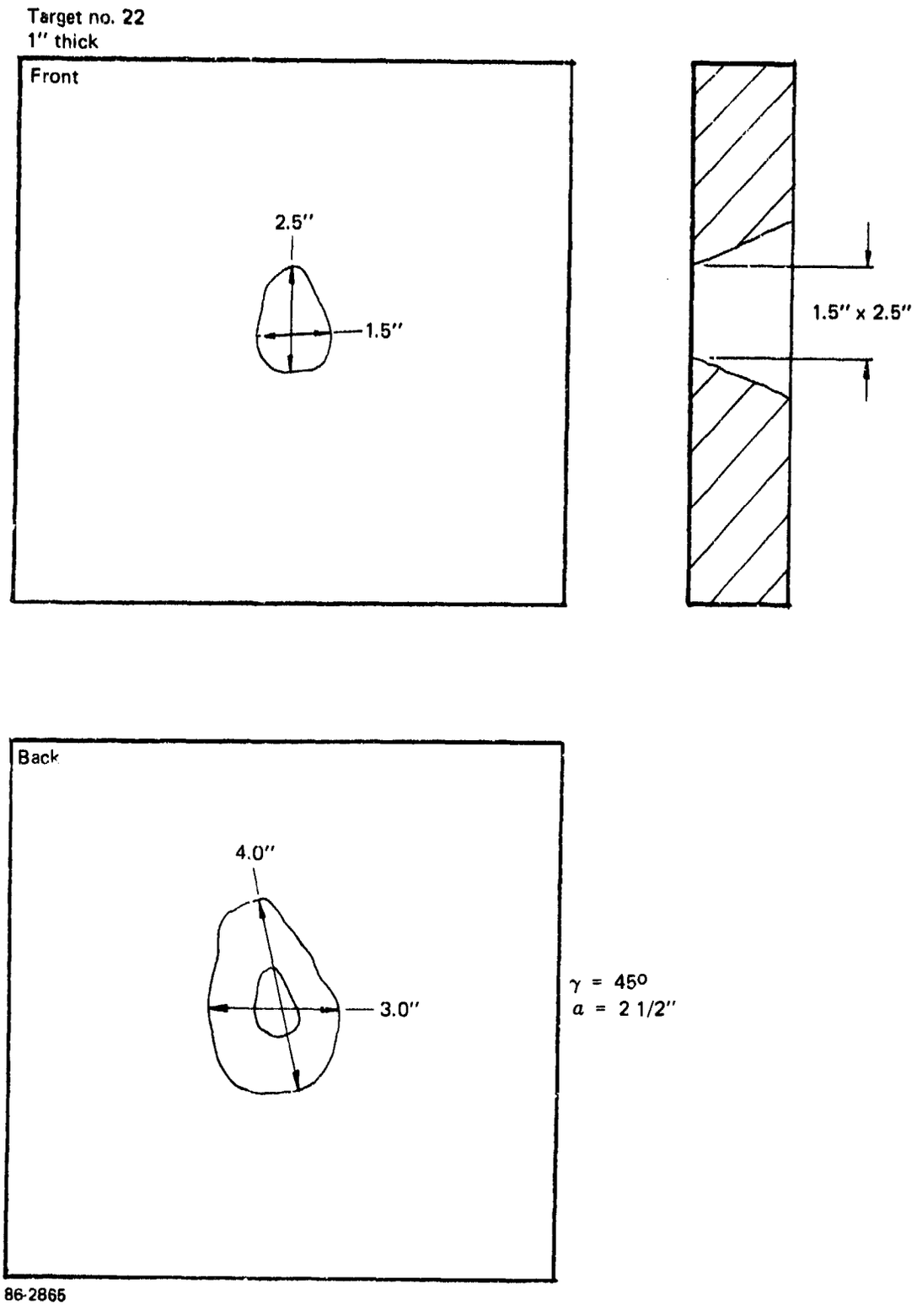

Figure 50 TEST 22 TARGET DATA – OGIVE PROJECTILE

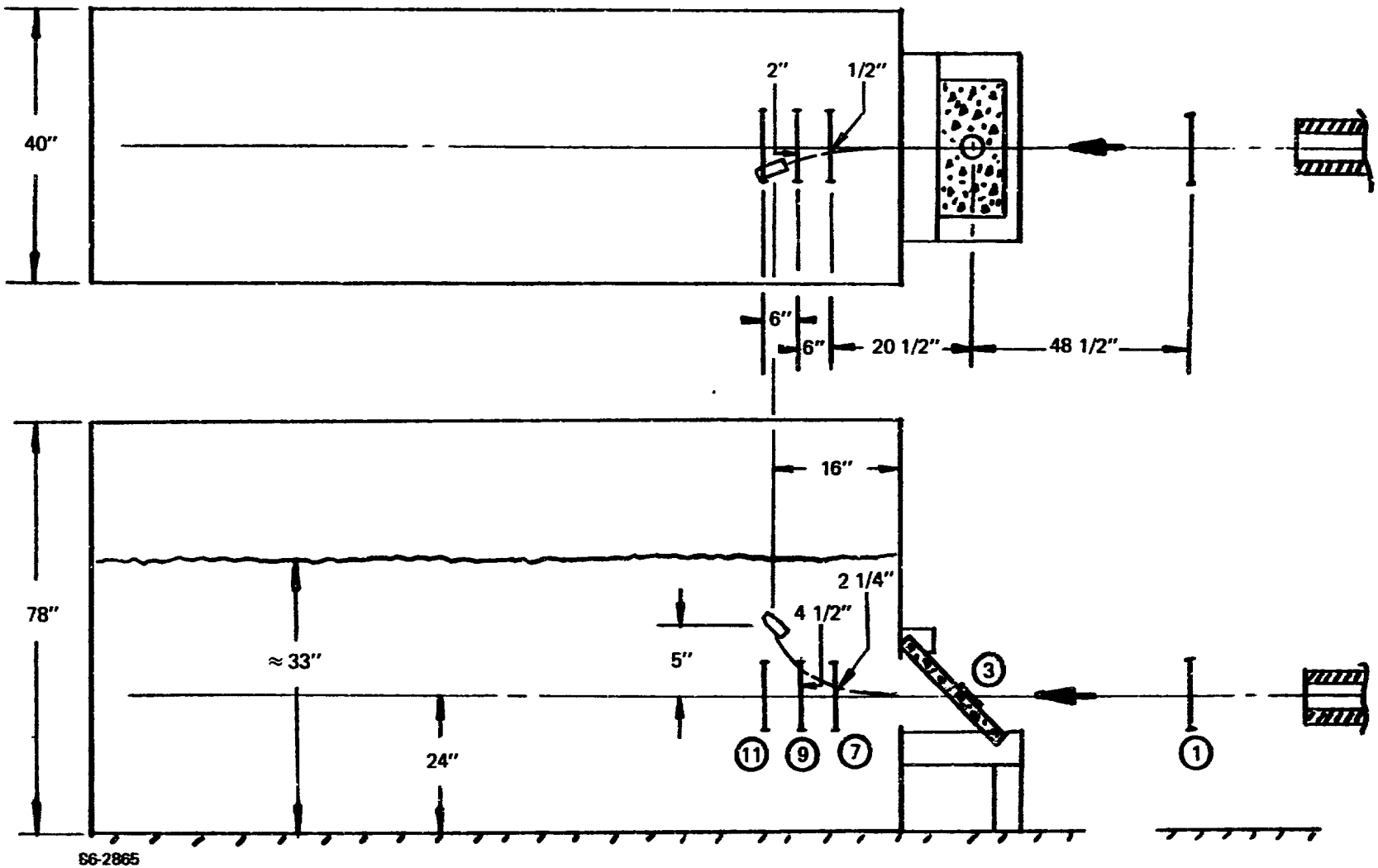

Figure 51 SUBSCALE SST PENETRATION TEST 23, $\gamma = 45^{o}$, $\alpha = 2\text{-}1/2^{o}$

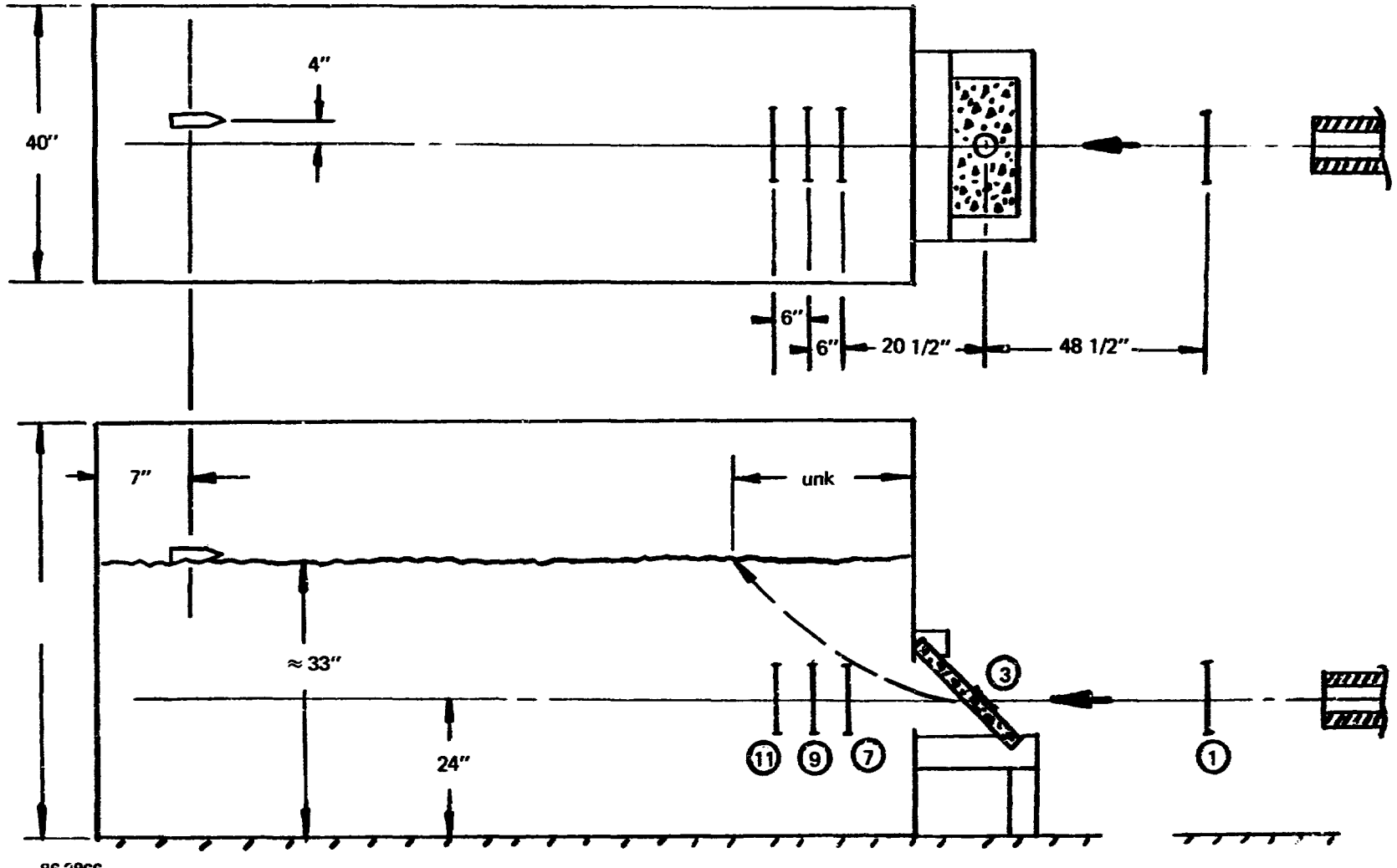

Figure 52 SUBSCALE CONE PENETRATION TEST 24, $\gamma = 45^{o}$, $\alpha = 2\text{-}1/2^{o}$

were 975, 974 and 981 ft/s, respectively. Thus, slight differences in launch weight due to the different configurations had little influence on launch velocity. The primary factor influencing launch velocity was probably the tolerances between the sabot and launcher barrel.

The copper ball deformation is listed for each test. These values are more indicative of relative performance than actual g measurement since many of the measurements are outside the linear range of the copper ball. Trajectory estimates through the sand media were made for each EP model. Concrete crater measurements were made on each concrete target except for four targets which broke up during removal from the test setup. These data are presented in Figures 9 through 52. Typical craters are shown in Figures 53 and 54. Because of the difficulty in comparing the many test variables and referring to a large number of figures, an attempt has been made to summarize the test results in tabular form. This summary is presented in Table 3.

The data in Table 3 is grouped by EP tip configuration, obliquity and angle of attack for ease of review. Test number, measured angle of attack and, copper ball deformation are taken from Table 2. Velocity loss is calculated by taking representative velocity values from Table 2 and dividing the change in velocity in the sand media by the distance over which the change of velocity occurred. This is done for changes in velocity over distances of 6.5 and 18.5 inches for the zero obliquity tests and for approximately 20 inches for the 22.5 degree and 45 degree obliquity cases. The stability factor shown in Table 3 is an attempt to quantify and simplify the trajectory data. Basically, the value is obtained by dividing the distance traveled in the sand media by the total deviation from the normal path. For Test 1, the EP traveled 38 inches in the sand and deviated a total of 23.5 inches before leaving the sand. The result of dividing 38 by 23.5 is 1.6, the stability factor. The higher the stability factor the more stable the trajectory. The fact that the Test 1 EP left the sand means that the stability factor was probably less than the 1.6 value shown. That is, had there been

Figure 53 CONCRETE TARGET, FRONT FACE

Figure 54 CONCRETE TARGET, BACK FACE

TABLE 3. DATA SUMMARY EP MODEL TEST RESULTS

		Ogive									SST									Cone								
					Velocity loss (ft/s/in.)			Crater size max. dimension (inches)						Velocity loss (ft/s/in.)			Crater size max. dimension (inches)						Velocity loss (ft/s/in.)			Crater size max. dimension (inches)		
Target angle (degrees)	Desired angle of attack (degrees)	Test number	Angle of attack measured (degrees)	Passive accel. deformation (mils)	At 6.5 inch depth	At 18 to 20 inch depth	Stability factor[3]	Entrance	Exit	Throat	Test number	Angle of attack measured (degrees)	Passive accel. deformation (mils)	At 6.5 inch depth	At 18 to 20 inch depth	Stability factor[3]	Entrance	Exit	Throat	Test number	Angle of attack measured (degrees)	Passive accel. deformation (mils)	At 6.5 inch depth	At 18 to 20 inch depth	Stability factor[3]	Entrance	Exit	Throat
0	0.0	2	1.3	0.9	24.7	23.2	7.7	3.0	3.2	1.6	3	1.4	21.5	39.8	41.7	7.4	2.3	3.5	1.5	5	0.0	1.3	39.3	39.6	3.8	2.2	2.7	1.4
0	5.0	1	7.6	4.7	38.6	36.9	1.6[4]	-	-	-	4	5.0	16.5	43.5	40.4	2.1	2.4	3.3	2.1	6	7.7	1.8	40.9	-	1.1[4]	2.6	3.0	2.1
22.5	0.0	19	4.5	3.8	-	19.3[1]	3.0	2.7	4.0	2.2	20A	2.5	12.8	-	33.0	2.1	2.8	3.9	1.9	21	6.0	2.9	-	-	(5)	3.5	3.9	2.3
22.5	2.5	16	2.1	2.7	-	20.5[2]	5.5	3.0	3.5	2.1	17	2.3	24.5	-	-	3.8	2.6	3.3	2.0	18	1.8	4.6	-	-	(5)	2.9	3.2	2.1
22.5	5.0	13	4.5	4.1	-	16.8	4.3	2.8	3.8	2.3	15	8.0	8.1	-	-	5.4	3.2	4.0	2.4	14	5.0	4.9	-	-	1.9	3.2	3.2	2.4
45	0.0	8	0.0	4.6	-	13.1	2.5[4]	4.0	5.8	4.2	10	0.5	-	-	27.9	4.8	3.3	3.5	3.0	12	1.25	5.1	-	18.6	1.8	2.7	3.2	3.0
45	2.5	22	2.3	4.5	-	13.3	4.6[4]	2.5	4.0	2.5	23	2.0	11.9	-	29.3	4.0	-	-	-	24	2.0	4.3	-	-	(5)	-	-	-
45	5.0	7	5.9	2.7	-	15.7	1.1	3.0	4.0	4.0	9	3.8	7.6	-	27.0	6.6	3.0	3.3	2.3	11	2.5	5.8	-	13.8	4.3	-	-	-

NOTES:

1) Measured over 25 inches.

2) Measured over 31 inches.

3) Stability factor equals depth of penetration in sand media divided by total deviation from normal path.

4) Came out of catcher, actual stability factor lower than shown.

5) Missed first velocity grid.

more sand in the box the projectile probably would have deviated more. Finally, the maximum crater dimensions are presented for the entrance hole, the throat and the exit hole for each test for which this data was obtained.

A perusal of Table 3 provides insights into the significance of the test data. The copper ball deformation is equatable to peak deceleration "g's". For the ogive shape tip these forces are relatively independent of obliquity or angle of attack except for the zero-zero case. Conversely, the SST loads are highest for the zero-zero case and appear to be somewhat alleviated by obliquity and angle of attack. In all instances the SST loads are higher than the ogive loads for the same test conditions. The conical tip loads tend to increase somewhat with obliquity, to be independent of angle of attack, to be less than the SST values for all tests and comparable to the ogive values for most tests.

The velocity loss factor seems to be independent of depth for the data available. As might be expected, the higher loaded SST configuration loses velocity fastest. Obliquity seems to reduce velocity loss for all three configurations. The SST trajectory is the most stable and the cone the least stable. The conical tip EP model deviated so much from the normal path on Tests 18, 21 and 24 that the first velocity grid in the sand media was missed and no in-depth velocity data obtained. The conical stability factors are lower than the SST values in all cases and comparable to the ogive values. It should be noted, however, that no ogive EP model deviated so much as to miss the in-depth velocity grids completely.

The crater data showed the following trends. The entrance hole was generally smaller than the exit hole with the throat diameter generally smaller than both. The crater size tended to increase with obliquity. The ogive crater sizes were generally equal to or larger than the SST or cone EP model produced craters.

In summary, it can be stated that the SST EP models experienced the highest peak deceleration loads and the highest velocity loss rates through the sand media while exhibiting the most stable trajectory performance. The cone tip EP models exhibited the least stable trajectory performance. Both the ogive and cone peak deceleration "g" loads were comparable and substantially lower than the SST loads.

It is recommended that the test results be used to refine currently available EP trajectory predictive techniques both as a method of further explaining the observed EP model performance and increasing the ability of predicting the performance of future EP designs.

REFERENCES

1. DeVost, V. F., NOL Copper-Ball Accelerometers, NOLTR-63-279, dated 31 October 1965.
2. DeVost, V. F., "Shock Spectra Measurements Using Multiple Mechanical Gages," NOLTR 67-151, dated 20 September 1967.

DISTRIBUTION LIST

DEPARTMENT OF DEFENSE

Director
Defense Advanced Rsch. Proj. Agency
ATTN: Technical Library
ATTN: NMRO

Director
Defense Civil Preparedness Agency
Assistant Director for Research
ATTN: Admin. Officer

Defense Documentation Center
Cameron Station
12cy ATTN: TC

Director
Defense Intelligence Agency
ATTN: Charles A. Fowler
ATTN: DI-7E
ATTN: DB-4C, Edward O'Farrell
ATTN: DT-2, Wpns. & Sys. Div.
ATTN: Technical Library

Director
Defense Nuclear Agency
ATTN: DDST
ATTN: TISI, Archives
ATTN: SPAS
3cy ATTN: TITL, Tech. Library
5cy ATTN: SPSS

Dir. of Defense Rsch. & Engineering
ATTN: S&SS(OS)

Commander
Field Command
Defense Nuclear Agency
ATTN: FCPR

Director
Interservice Nuclear Weapons School
ATTN: Document Control

Director
Joint Strat. Tgt. Planning Staff, JCS
ATTN: STINFO Library

Chief
Livermore Division, Fld. Command, DNA
Lawrence Livermore Laboratory
ATTN: FCPRL

DEPARTMENT OF THE ARMY

Dep. Chief of Staff for Rsch. Dev. & Acq.
ATTN: DAMA(CS), MAJ A. Gleim
ATTN: DAMA-CSM-N, LTC G. Ogden
ATTN: Technical Library

Chief of Engineers
2cy ATTN: DAEN-RDM
2cy ATTN: DAEN-MCE-D

DEPARTMENT OF THE ARMY (Continued)

Deputy Chief of Staff for Ops. & Plans
ATTN: Dir. of Chem. & Nuc. Ops.
ATTN: Technical Library

Chief
Engineer Strategic Studies Group
ATTN: DAEN-FES

Commander
Frankford Arsenal
ATTN: L. Baldini

Project Manager
Gator Mine Program
ATTN: E. J. Linddsey

Commander
Harry Diamond Laboratories
ATTN: DRXDO-RBH, James H. Gwaltney
ATTN: DRXDO-NP

Commander
Picatinny Arsenal
ATTN: Paul Harris
ATTN: SMUPA-AD-D-M
ATTN: Technical Library
ATTN: P. Angelloti
ATTN: SMUPA-AD-D-A
ATTN: Ray Moesner
ATTN: DR-DAR-L-C-FA
ATTN: Jerry Pental
ATTN: Marty Margolin
ATTN: SMUPA-AD-D-A-7
ATTN: Ernie Zimpo

Commander
Redstone Scientific Information Ctr.
U.S. Army Missile Command
ATTN: Chief, Documents

Commander
U.S. Army Armament Command
ATTN: Tech. Lib.

Director
U.S. Army Ballistic Research Labs.
ATTN: G. Roecker
ATTN: G. Grabarek
ATTN: DRXBR-X
ATTN: J. W. Apgar
ATTN: DRXBR-TB
ATTN: A. Ricchiazzi
ATTN: DRDAR-BLE, J. H. Keefer
2cy ATTN: Tech. Lib., Edward Baicy

Commander and Director
U.S. Army Cold Region Res. Engr. Lab.
ATTN: G. Swinzow

Commander
U.S. Army Engineer Center
ATTN: ATSEN-SY-L

DEPARTMENT OF THE ARMY (Continued)

Commander
U.S. Army Comb. Arms Combat Dev. Acty.
ATTN: LTC Pullen
ATTN: LTC G. Steger

Division Engineer
U.S. Army Engineer Div., Huntsville
ATTN: HNDED-SR

Division Engineer
U.S. Army Engineer Div., Missouri Rvr.
ATTN: Tech. Library

Commandant
U.S. Army Engineer School
ATTN: ATSE-TEA-AD
ATTN: ATSE-CTD-CS

Director
U.S. Army Engr. Waterways Exper. Sta.
ATTN: P. Hadala
ATTN: D. K. Butler
ATTN: Guy Jackson
ATTN: John N. Strange
ATTN: Behzad Rohani
ATTN: Leo Ingram
ATTN: Technical Library
ATTN: William Flathau

Commander
U.S. Army Mat. & Mechanics Rsch. Ctr.
ATTN: Technical Library

Commander
U.S.Army Materiel Dev. & Readiness Cmd.
ATTN: Technical Library

Director
U.S. Army Materiel Sys. Analysis Acty.
ATTN: Joseph Sperazza

Commander
U.S. Army Missile Command
ATTN: W. Jann
ATTN: F. Fleming
ATTN: J. Hogan

Commander
U.S. Army Mobility Equip. R&D Ctr.
ATTN: STSFB-XS
ATTN: STSFB-MW
ATTN: Technical Library

Commander
U.S. Army Nuclear Agency
ATTN: MONA-SA
ATTN: MONA-WE

Commander
U.S. Army Training and Doctrine Comd.
ATTN: LTC Auveduti, COL Enger
ATTN: LTC J. Foss

DEPARTMENT OF THE ARMY (Continued)

Commandant
U.S. Army War College
ATTN: Library

U.S. Army Mat. Cmd. Proj. Mngr. for Nuc. Munitions
ATTN: DRCPM-NUC

DEPARTMENT OF THE NAVY

Chief of Naval Operations
ATTN: Op 982, LCDR Smith
ATTN: Op 982, CAPT Toole
ATTN: Op 982, LTC Dubac
ATTN: Code 604C3, Robert Piacesi

Chief of Naval Research
ATTN: Technical Library

Officer-In-Charge
Civil Engineering Laboratory
Naval Construction Battalion Center
ATTN: R. J. O'Dello
ATTN: Technical Library

Commandant of the Marine Corps.
ATTN: POM

Commanding General
Development Center
Fire Support Branch
MCDEC
ATTN: LTC Gapenski
ATTN: CAPT Hartneady

Commander
Naval Air Systems Command
Headquarters
ATTN: F. Marquardt

Commanding Officer
Naval Explosive Ord. Disposal Fac.
ATTN: Code 504, Jim Petrousky

Commander
Naval Facilities Engineering Command
Headquarters
ATTN: Technical Library

Superintendent, (Code 1424)
Naval Postgraduate School
ATTN: Code 2124, Tech. Rpts. Librarian

Director
Naval Research Laboratory
ATTN: Code 2600, Tech. Lib.

Commander
Naval Sea Systems Command
ATTN: SEA-9931G
ATTN: ORD-033

DEPARTMENT OF THE NAVY (Continued)

Commander
Naval Surface Weapons Center
ATTN: M. Kleinerman
ATTN: Code WX21, Tech. Lib.
ATTN: Code WA501, Navy Nuc. Prgms. Off.

Commander
Naval Surface Weapons Center
Dahlgren Laboratory
ATTN: Technical Library

Commander
Naval Weapons Center
ATTN: Carl Austin
ATTN: Code 533, Tech. Lib.

Commanding Officer
Naval Weapons Evaluation Facility
ATTN: Technical Library

Director
Strategic Systems Project Office
ATTN: NSP-43, Tech. Lib.

DEPARTMENT OF THE AIR FORCE

AF Armament Laboratory, AFSC
ATTN: Masey Valentine
3cy ATTN: John Collins, AFATL/DLYV

AF Institute of Technology, AU
ATTN: Library, AFIT Bldg. 640, Area B

AF Weapons Laboratory, AFSC
ATTN: SUL

Headquarters
Air Force Systems Command
ATTN: Technical Library

Commander
Armament Development & Test Center
ATTN: Tech. Library

Assistant Secretary of the Air Force
Research and Development
Headquarters, U.S. Air Force
ATTN: Col R. E. Steere

Deputy Chief of Staff
Research and Development
Headquarters, U.S. Air Force
ATTN: Col J. L. Gilbert

Commander
Foreign Technology Division, AFSC
ATTN: NICD, Library

Headquarters, USAF/IN
ATTN: INATA

DEPARTMENT OF THE AIR FORCE (Continued)

Headquarters, USAF/RD
ATTN: RDPM
ATTN: RDQSM
ATTN: RDPS
ATTN: RDQRM

Oklahoma State University
Fld. Off. for Wpns. Effectiveness
ATTN: Edward Jackett

Commander
Rome Air Development Center, AFSC
ATTN: EMTLD, Doc. Library

SAMSO/RS
ATTN: RSS

ENERGY RESEARCH & DEVELOPMENT ADMINISTRATION

Division of Military Application
ATTN: Doc. Control for Test Office

University of California
Lawrence Livermore Laboratory
ATTN: Jerry Goudreau
ATTN: Mark Wilkins, L-504
ATTN: Tech. Info. Dept., L-3
ATTN: M. Fernandez

Los Alamos Scientific Laboratory
ATTN: Doc. Control for Reports Lib.
ATTN: Doc. Control for Tom Dowler

Sandia Laboratories
Livermore Laboratory
ATTN: Doc. Control for Tech. Library

Sandia Laboratories
ATTN: Doc. Con. for John Colp
ATTN: Doc. Con. for W. Altsmeirer
ATTN: Doc. Con. for John Keizur
ATTN: Doc. Con. for 3141, Sandia Rpt. Coll.
ATTN: Doc. Con. for Walter Herrmann
ATTN: Doc. Con. for William Caudle
ATTN: Doc. Con. for William Patterson

U.S. Energy Rsch. & Dev. Admin.
Albuquerque Operations Office
ATTN: Doc. Con. for Tech. Library

U.S. Energy Rsch. & Dev. Admin.
Division of Headquarters Services
ATTN: Doc. Con. for Class. Tech. Lib.

U.S. Energy Rsch. & Dev. Admin.
Nevada Operations Office
ATTN: Doc. Con. for Tech. Lib.

OTHER GOVERNMENT AGENCIES

NASA
Ames Research Center
ATTN: Robert W. Jackson

Office of Nuclear Reactor Regulation
Nuclear Regulatory Commission
ATTN: Robert Heineman
ATTN: Lawrence Shao

DEPARTMENT OF DEFENSE CONTRACTORS

Aerospace Corporation
ATTN: Tech. Info. Services

Agbabian Associates
ATTN: M. Agbabian

Applied Theory, Inc.
2cy ATTN: John G. Trulio

Avco Research & Systems Group
ATTN: Research Lib., A830, Rm. 7201
ATTN: David Henderson
ATTN: William Broding
ATTN: P. S. Soderstrom

Battelle Memorial Institute
ATTN: Technical Library

The BDM Corporation
ATTN: Technical Library

The Boeing Company
ATTN: Aerospace Library

California Research & Technology, Inc.
ATTN: Technical Library
ATTN: Ken Kreyenhagen

Civil/Nuclear Systems Corp.
ATTN: Robert Crawford

EG&G, Inc.
Albuquerque Division
ATTN: Technical Library

Engineering Societies Library
ATTN: Ann Mott

General Dynamics Corp.
Pomona Division
ATTN: Keith Anderson

General Electric Company
TEMPO-Center for Advanced Studies
ATTN: DASIAC

Georgia Institute of Technology
Georgia Tech. Research Institute
ATTN: L. W. Rehfield
ATTN: S. V. Hanagud

DEPARTMENT OF DEFENSE CONTRACTORS (Continued)

Honeywell, Incorporated
Defense Systems Division
ATTN: T. N. Helvig

Institute for Defense Analyses
ATTN: IDA, Librarian, Ruth S. Smith

Kaman AviDyne
Division of Kaman Sciences Corp.
ATTN: Technical Library

Kaman Sciences Corporation
ATTN: Library

Lockheed Missiles & Space Co., Inc.
ATTN: M. Culp
ATTN: Technical Library

Lockheed Missiles and Space Co., Inc.
ATTN: Tech. Info. Ctr., D/Coll.

Martin Marietta Aerospace
Orlando Division
ATTN: W. Hurt
ATTN: L. Kinnaird
ATTN: J. Rickey

Merritt Cases, Incorporated
ATTN: Technical Library
ATTN: J. L. Merritt

University of New Mexico
Dept. of Campus Security and Police
ATTN: G. E. Triandafalidis

Nathan M. Newmark
Consulting Engineering Services
ATTN: Nathan M. Newmark

Pacifica Technology
ATTN: R. Bjork
ATTN: G. Kent

Physics International Company
ATTN: Doc. Con. for Dennis Orphal
ATTN: Doc. Con. for Tech. Lib.
ATTN: Doc. Con. for Larry A. Behrmann
ATTN: Doc. Con. for Charles Godfrey

R & D Associates
ATTN: J. G. Lewis
ATTN: Cyrus P. Knowles
ATTN: Arlen Fields
ATTN: William B. Wright, Jr.
ATTN: Paul Rausch
ATTN: Harold L. Brode
ATTN: Henry Cooper
ATTN: Technical Library

The Rand Corporation
ATTN: Technical Library

DEPARTMENT OF DEFENSE CONTRACTORS (Continued)

Science Applications, Inc.
ATTN: Technical Library

Stanford Research Institute
ATTN: George R. Abrahamson
ATTN: J. D. Colton

Systems, Science and Software, Inc.
ATTN: Robert Sedgewick
ATTN: Technical Library

TRW Defense & Space Sys. Group
ATTN: Peter K. Dai, R1/2170
ATTN: Tech. Info. Center/S-1930

DEPARTMENT OF DEFENSE CONTRACTORS (Continued)

Terra Tek, Inc.
ATTN: Technical Library

TRW Defense & Space Sys. Group
San Bernardino Operations
ATTN: E. Y. Wong, 527/712

Weidlinger Assoc. Consulting Engineers
ATTN: J. M. McCormick
ATTN: Melvin L. Baron

Weidlinger Assoc. Consulting Engineers
ATTN: J. Isenberg